CYCLODEXTRIN-BASED BIODEGRADABLE POLYMER STARS: SYNTHESIS, DEGRADATION AND FLUORESCENCE STUDIES

A Thesis

Submitted to the Graduate Faculty

in Partial Fulfilment of the Requirements

for the Degree of Master of Science

Molecular and Macromolecular Sciences

Department of Chemistry

Faculty of Science

University of Prince Edward Island

Gayan K. Tennekone

Charlottetown, Prince Edward Island

April 2013

CONDITIONS FOR THE USE OF THE THESIS

PERMISSION TO USE POSTGRADUATE THESIS

Title of thesis: Cyclodextrin-based biodegradable polymer stars: synthesis, degradation and fluorescence studies

Name of Author: Gayan Tennekone

Department: Chemistry

Degree: MSc Year: 2013

In presenting this thesis in partial fulfillment of the requirements for a postgraduate degree from the University of Prince Edward Island, I agree that the Libraries of this University may make it freely available for inspection. I further agree that permission for extensive copying of this thesis for scholarly purposes may be granted by the professor or professors who supervised my thesis work, or, in their absence, by the Chair of the Department or the Dean of the Faculty in which my thesis work was done. It is understood any copying or publication or use of this thesis or parts thereof for financial gain shall not be allowed without my written permission. It is also understood that due recognition shall be given to me and to the University of Prince Edward Island in any scholarly use which may be made of any material in my thesis.

Signature: _____

Date: _____

University of Prince Edward Island

Faculty of Science

Charlottetown

CERTIFICATION OF THESIS WORK

We, the undersigned, certify that Gayan Tennekone, BSc, candidate for the degree of Master of Science has presented a thesis with the following title: "Cyclodextrin-based biodegradable polymer stars: synthesis, degradation and fluorescence studies", that the thesis is acceptable in form and content, and that a satisfactory knowledge of the field covered by the thesis was demonstrated by the candidate through an oral examination held on April 17, 2013.

Examiners: Dr Michael Shaver _____

Dr Brian Wagner _____

Dr Barry Linkletter _____

Dr Nola Etkin _____

Dr Glen Briand _____

Dr James Polson – Chair _____

Date _____

Table of Contents

List of Figures

List of Tables

List of Schemes

List of Equations

Glossary of Abbreviations

CD: cyclodextrin

7-MC: 7-methoxycoumarin

K: binding constant

H: host

G: guest

A: absorption of light

F: fluorescence

P: phosphorescence

IC: internal conversion

ISC: intersystem crossing

VR: vibrational relaxation

K_{in}: rate of entrance into the host cavity

K_{out}: rate of exit out of the host cavity

S_0: ground electronic state

S_1: first excited electronic state

T_1: triplet state

λ_{max} : wavelength of maximum intensity

cps: counts per second

βBL: beta-butyrolactone

PLA: poly(lactic acid)

PLGA: poly(lactic-*co*-glycolic acid)

PHB: poly(3-hydroxybutyrate)

PCL: poly(caprolactone)

PGA: poly(glycolic acid)

rac: racemic

ROP: ring-opening polymerization

CRP: controlled radical polymerization

ATRP: atom-transfer radical polymerization

RAFT: reversible addition-fragmentation chain-transfer polymerization

NMP: nitroxide mediated radical polymerization

CuAAC: copper-catalyzed azide-alkyne cycloaddition

PDI: polydispersity index

M_n: number average molecular weight

M_w: weight average molecular weight

$Sn(Oct)_2$: tin(II) ethylhexanoate

^{tBU}[Salen]: N,N'-bis(3,5-di-*tert*-butylsalicylidene)-1,3-propanediamine

NMR: nuclear magnetic resonance

^{1}H NMR: hydrogen-1 nuclear magnetic resonance

GPC: gel permeation chromatography

UV-Vis: ultraviolet-visible spectroscopy

IR: infrared spectroscopy

DSC: differential scanning calorimtery

TGA: thermogravimetric analysis

T_g: glass transition temperature

T_m: melting temperature

ΔH_m: melting enthalpy

T_{max}: temperature of maximum decomposition

$CDCl_3$: deuterated chloroform

CD_3SOCD_3: deuterated dimethyl sulfoxide

TBD: triazabicyclo[4.4.0]dec-5-ene

Ph_3P: triphenylphosphine

DMF: dimethylformamide

MeOH: methanol

EtOH: ethanol

δ: chemical shift in ppm

ppm: parts per million

s: singlet

d: doublet

t: triplet

m: multiplet

br: broad

Acknowledgements

I would first of all like to thank Dr. Michael Shaver and Dr. Brian Wagner for providing me with the opportunity to work on this project. I am forever grateful for the knowledge and skill they have provided me with. Without their guidance and persistent help, this project would not have been possible. I would also like to thank my committee members, Dr. Nola Etkin, Dr. Barry Linkletter and Dr. Glen Briand for their help along the way and examining this dissertation.

I would like to thank all the members of both the Shaver and Wagner lab groups. A special thank you to Dr. Laura Allan for her guidance and knowledge over the years. I cannot imagine doing research without the vast amount of knowledge that she provided me with. Many thanks to Donnie Cameron, Mitch Perry and Edward Cross who all inspired me to pursue this degree. I am forever grateful for all of the excellent students I've had the chance to work with at UPEI. Not only were they great colleagues, but some of the most special friends that I've had the honour of having.

A big thanks to UPEI Chemistry including the students and faculty. I believe that the people that I've met here at UPEI are what truly have made my time here special. As I commence a new stage of my life, I will always commemorate all of the people that I shared my experience with.

Finally I would like to thank my family and friends. My parents, Thilak and Hema and my brother, Jayoda, have always been there for me and have supported me through this journey. As new journeys await, I know they will always be there for me.

Abstract

In controlled release, each patient's body displays different pharmacokinetics for the degradation of the drug delivery system affecting the release of the bioactive compound. The proposed research aims to develop polymeric systems based on a host/guest core capable of indicating controlled release by fluorescence. Specifically, this involves the development of a prototype material based on a cyclodextrin molecule that serves as a framework for biodegradable polymer arms.

Binding constant and correlation studies were successfully conducted with β-cyclodextrin and heptakis(2,6-di-O-methyl)-β-cyclodextrin with 7-methoxycoumarin using solvent systems of water and methanol and pure water. Studies on β-CD in H_2O gave a binding constant of 238 M^{-1} and an R^2 value of 0.9580. Stronger binding and a better correlation was obtained with heptakis(2,6-di-O-methyl)-β-CD in H_2O with a binding constant of 306 M^{-1} and R^2 value of 0.998. Binding in H_2O/MeOH was also tested with heptakis(2,6-di-O-methyl)-β-CD resulting in a weaker binding constant of 120 M^{-1} and lower correlation value of 0.986 due to the decrease in solution polarity.

Polymer stars were synthesized based on core- and arm-first methods. For core-first synthesis, stars based on a heptakis(2,6-di-O-methyl)-β-cyclodextrin core that supports 7 polymer arms of poly(lactic acid) (PLA), poly(3-hydroxybutyrate) (PHB) or poly(lactic-*co*-glycolic acid) (PLGA) were synthesized by ring-opening polymerization with variation in both the polymer microstructure and arm length. Use of $Sn(Oct)_2$ as a catalyst yielded polymers with high PDI values and poor molecular weight correlation. Switching to the Al[salen] system yielded polymers with excellent PDI values but low molecular weight correlation.

For arm-first synthesis, copper-catalyzed azide-alkyne cycloaddition was used to synthesize 7 arm stars based on a β-CD-$(N_3)_7$ and acetylene terminated polymers of PLA, PHB, PCL and PLGA. Excellent levels of control and good molecular weight correlation was obtained from arm-first synthesis. However, isolation of these stars was challenging, resulting in low yields.

Analysis of these polymers by ^{1}H NMR spectroscopy revealed the polymer composition whilst differential scanning calorimetry gave glass, melt and crystallization temperatures. Decomposition temperatures were also investigated by thermogravimetric analysis. Molecular weights and polydispersities of these polymers were determined by using gel permeation chromatography coupled with light scattering detectors as well as ^{1}H NMR spectroscopy.

A 7-methoxycoumarin fluorophore was used to demonstrate the controlled release characteristics of these novel materials by fluorescence spectroscopy by uncatalyzed and enzyme catalyzed degradations, showing that they have potential as controlled release vectors.

Chapter One

1 Introduction

1.1 Controlled Drug Delivery Systems

In 1966 Judah Folkman, MD, circulated rabbit blood inside a silicone rubber arterio-venous shunt and discovered that if the tubing was exposed to anaesthetic gases on the outside, the rabbits would fall asleep. This led to the proposal that short, sealed segments of silicone tubing could be implanted and, if the dimension and composition were kept constant, the implant would become a constant rate drug delivery device.[1] Folkman was also able to show that the rate of release decreased as the tubing size increased, which was the first suggestion of a zero order controlled drug delivery system. Alejandro Zafforini, a synthetic chemist and entrepreneur, expanded Folkman's idea of a zero order controlled drug delivery system. His company, Alza, developed the first controlled drug delivery systems which were macroscopic in scale.[2] One system released

an anti-glaucoma drug, pilocaprine, at a constant rate in the eye, while another released the contraceptive steroid, progesterone, at a constant rate in the uterine cavity. These first-generation drug delivery systems were based on poly(ethylene-*co*-vinyl acetate) materials and were used as rate controlling membranes.[1] It was the development of these early systems that laid the foundation for the field of controlled drug delivery.

In the 1960s and 1970s, biodegradable polymers of poly(hydroxyl acid)s were developed for biomedical sutures.[1] This technology was then applied to the development of drug delivery systems.[3] Biodegradable polymers as drug delivery systems were of particular interest due to the ability of these polymers to be broken down into non-toxic products and reabsorbed by the body, alleviating the need to remove the drug delivery device.[3] The use of these new materials developed macroscopic zero order systems of the 1970s and 1980s into sustained release macro/microscopic biodegradable systems that were applied in clinical trials during the mid to late 1980s.[1,4] Materials such as poly(glycolic acid) (PGA), poly(lactic-*co*-glycolic acid) (PLGA) and poly(lactic acid) (PLA) were then adopted as materials to be used in drug delivery due to their biodegradability and renewability. These polymers became the most widely studied polyesters and, similar to other poly(hydroxyl acid)s, were also initially investigated as biodegradable sutures in the early 1970s. It was found that varying the composition of the material by altering monomer ratios and changing the processing conditions, the polymeric materials could exhibit drug release timeframes of months or even years.[5] The rate of degradation was found to depend on various properties of the materials including crystallinity. Materials that were more crystalline resulted in extended degradation timeframes because of ordered regions in the polymeric material. These materials were

prepared as films, microparticles and rods, as well as other forms that encapsulate the drug and release it at controlled rates for relatively long periods of time.[3,5]

During the 1980s and 1990s there was a drive to improve drug delivery systems while minimizing toxic side effects.[6] While early nanoparticle and microparticle systems were developed using poly(alkylcyanoacrylate), the promise of these initial systems was hampered by the size limitations of particles able to cross the intestinal barriers into the lymphatic system following oral delivery[7] and limitations to the therapeutic effects of drugs at high loading as the particles were cleared rapidly by phagocytosis after intravenous administration.[7]

There has been vast evolution in the field of controlled drug delivery systems over the past 50 years as new novel polymers are becoming a driving force for the evolution of drug delivery in the medical field.[8] The advancement of these systems has helped to improve the efficiency of drug delivery and will likely enable the creation of entirely new therapeutic vectors. The field of controlled drug delivery remains optimistic given the wide array of innovative materials and technologies that are now available.

1.2 Biodegradable Polymers

Over the past three decades there has been a shift from biostable biomaterials to biodegradable materials that are capable of hydrolytic and/or enzymatic degradation for medical and related applications.[9] Over the next decade, it is predicted that many permanent prosthetic devices will be replaced by biodegradable devices that will help the body repair and regenerate damaged tissues.[10] The main driving force for the development of these new materials is the long-term biocompatibility issue with many of

the existing permanent implants, and many levels of ethical and technical issues associated with revision surgeries.[10]

The biomedical application of enzymatically degradable natural polymers dates back thousands of years with the use of natural biomaterials derived from plant and animals such as chitin and collagen.[11] The application of synthetic biodegradable polymers started only in the latter half of the 1960s.[12] Rapid advancement over the last 30 years lead to the development of a new generation of synthetic biodegradable polymers specifically for biomedical applications.[12] The emergence of new biomedical technologies such as tissue engineering, regenerative medicine, gene therapy, controlled drug delivery and bionanotechnology have all aided in the growth of synthetic biodegradable polymer research.[8,9]

Biodegradation of polymeric biomaterials involves the hydrolytic or enzymatic cleavage of labile bonds leading to polymer degradation. Synthetic biomaterials tend to be biologically inert as they have predictable properties and batch-to-batch uniformity. Tailored properties give them profiles for specified applications as well as controlled degradation timeframes, without the disadvantages that natural polymers have such as purification issues.[13] The success of the first synthetic poly(glycolic acid) based suture system in the 1960s paved the way for a new generation of biodegradable polymers used as implants for medical applications.[14] Since then, the field of synthetic biodegradable polymers has expanded into many different classes with the two largest classes being poly(hydroxyalkanoate)s, of which poly(3-hydroxybutyrate) is the most common,[15] and aliphatic polyesters.

Polyesters are thermoplastic polymers that can be cleaved hydrolytically or enzymatically, leading to polymer degradation.[15] All polyesters are theoretically degradable, however only aliphatic polyesters with short chains between the ester bonds can degrade over a time period suitable for biomedical applications.[9,15] The uniqueness of this group of synthetic biodegradable polymers lies in the immense diversity of monomers available as well as synthetic versatility. Polyesters can be synthesized via ring opening or condensation polymerization from a variety of different catalytic systems.[16] In addition to chemical synthesis, polyesters can also be synthesized by bacterial bioprocesses.[16] Among these chemically synthesized polyesters, the most extensively investigated are poly(hydroxyl acid)s (Figure 1.1), which include poly(glycolic acid) and the stereoisomeric forms of poly(lactic acid).

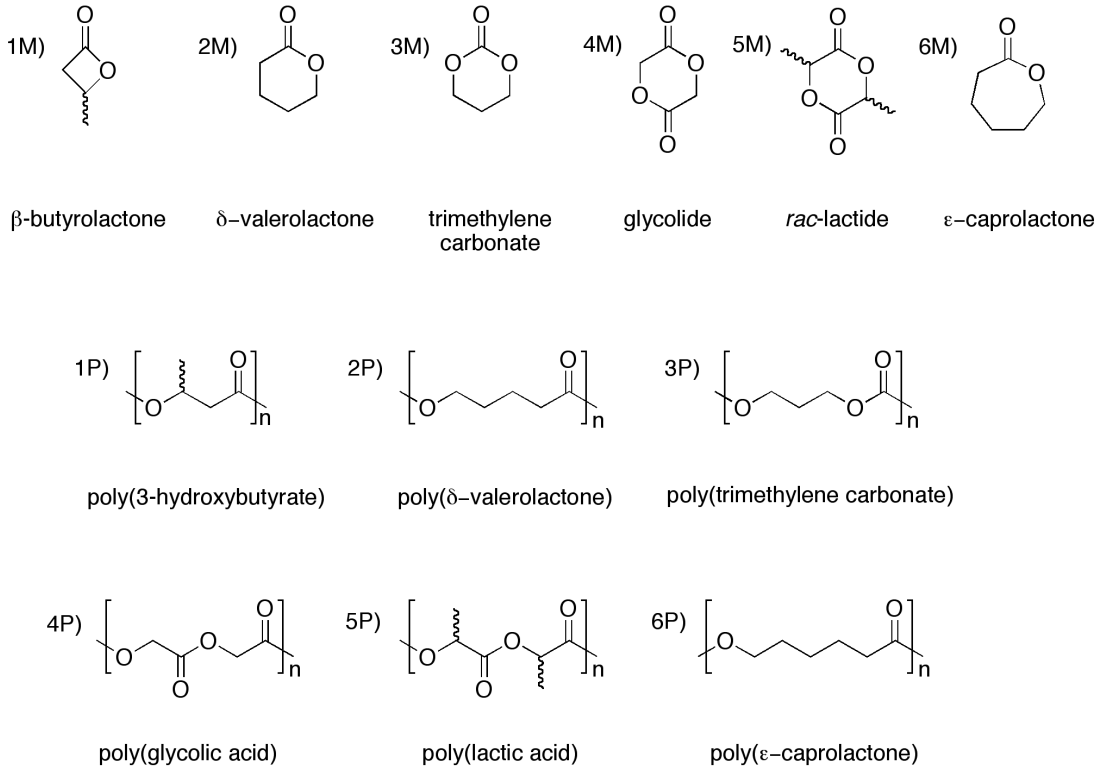

Figure 1.1. Monomers and biodegradable polyesters.

Polyesters can be synthesized via two routes, the first of which uses polycondensation of difunctional monomers such as hydroxyl acids, diacids with diols, diacid chlorides with diols or by the ester interchange reaction.[17] It is difficult to obtain high molecular weights or uniform molecular weight distributions using polycondensation routes, which has limited its use in the development of biomaterials.[17] The second method, and by far the most prevalent, is the ring-opening polymerization (ROP) of cyclic lactones. The advantages of ROP over the polycondensation method include milder reaction conditions, shorter reaction times, fewer byproducts and versatility towards different sizes of lactones. ROP also allows the production of high molecular weight polymers by varying reaction conditions and timeframes, as well as by altering the catalyst and initiator.[18] Further biocompatibility of these systems is achieved by the development of solvent-free ROP reactions.[16,19] A variety of cyclic lactones have been studied in ROP. However, the most extensively studied for biomedical applications are lactide, glycolide and ε-caprolactone monomers.[20]

The ROP mechanism involves the use of catalysts to activate monomer polymerization.[21,22] Six-membered rings such as lactide traditionally wouldn't be expected to have high ring strain, however, the ester linkages align in a planar fashion, which results in the ring adopting a unique skew-boat conformation in which the methine protons are positioned on the axial positions and the methyl groups on the equatorial positions.[23] This unusual ester linkage geometry increases the bonds strain.

ROP is typically used to achieve living characteristics. A living polymerization can be defined as polymerization in which chain transfer and chain termination are absent.[24] The control of these reactions is achieved through fast initiation followed by

slow propagation of the polymer chain, giving polymers with narrow molecular weight distributions (M_n and M_w), resulting in a low polydispersity index (PDI) that is ideally equal to 1 (Equation 1).

$$M_n = \frac{\sum_i N_i M_i}{\sum_i N_i} \qquad M_w = \frac{\sum_i N_i M_i^2}{\sum_i N_i M_i} \qquad PDI = \frac{M_w}{M_n}$$

Equation 1. Mathematical representation of M_n, M_w and PDI.

Most polyesters are synthesized via a living metal-mediated ROP process that proceeds through a coordination insertion mechanism **(**Scheme 1.1**).**[25] The first step involves the coordination of lactide to the metal center through a Lewis acid-base bond between the metal center (M) and the carbonyl oxygen (**1**). The second step is the insertion of the monomer into the metal-alkoxide bond generating a secondary alkoxide species (**2**). Acyl bond cleavage then follows (**3**), opening the ring and generating the polymer chain with the alcohol group on one end and the metal complex on the other end (**4**). The chain will continue to propagate until the reaction is terminated by hydrolytic cleavage of the metal species or until the monomer is consumed.[25,26]

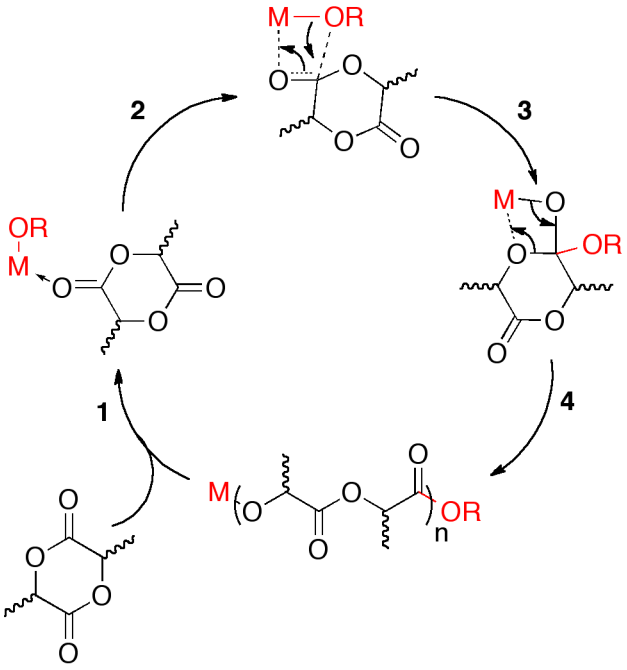

Scheme 1.1. General coordination insertion mechanism of lactide polymerization in the presence of a metal catalyst.

1.2.1 Poly(lactic acid)

Poly(lactic acid) is the most extensively studied biodegradable and renewable thermoplastic polyester.[27] PLA technologies have emerged and continue to develop with the potential to have properties that are superior or equivalent to most of today's conventional polymers.[27] This progression of PLA research has made it a possible material to replace commodity plastics.[28] Converting starch or sugar obtained from renewable feedstocks such as corn, wheat or rice can produce lactic acid, the monomeric building block of PLA.[28] Lactic acid (2-hydroxy propionic acid) is the simplest hydroxy acid with an asymmetric carbon atom and exists as two optically active isomers: L-lactic acid and D-lactic acid.[29] Polymerization of lactic acid to PLA can be achieved directly through a condensation process, however the most prevalent method requires an initial conversion of lactic acid to a cyclic dimer intermediate, lactide. Lactide can exist in three different stereoisomers: D-lactide, L-lactide and *meso*-lactide. The lactide monomer can

then undergo ROP to produce PLA, in which the stereochemical composition of the lactide isomers determine the final properties of the polymer.

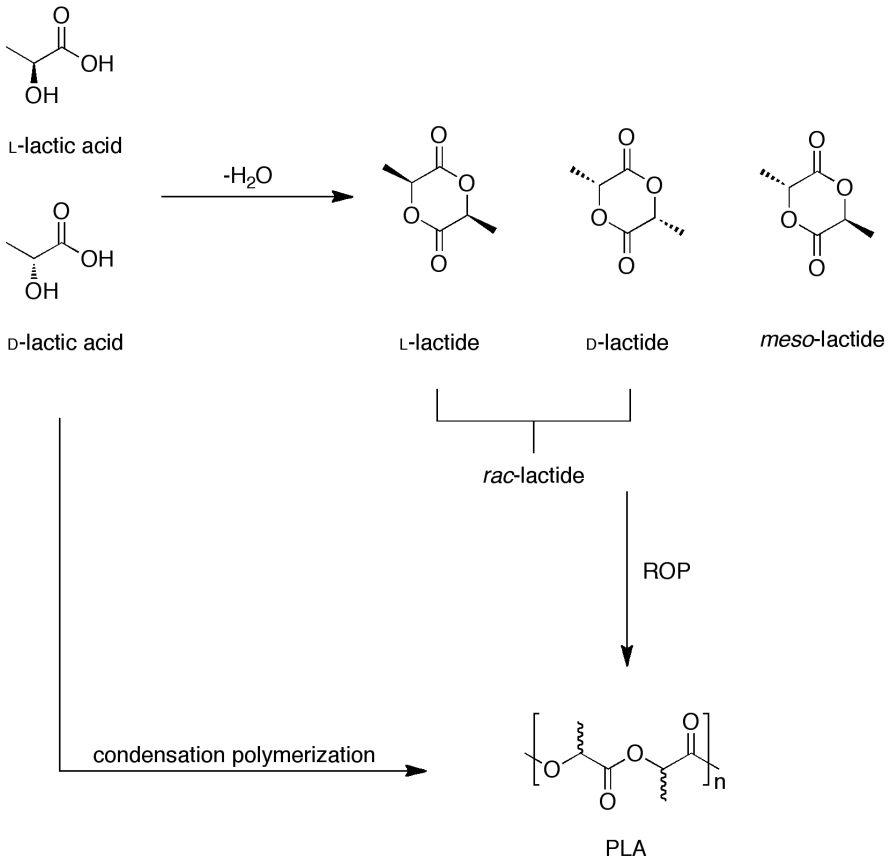

Scheme 1.2. Synthesis of PLA from lactic acid and lactide.

One of the important features of PLA is the ability to obtain different microstructures or tacticities in the polymer chain. Through variation of the microstructure, the properties of the polymer chain can be varied. Stereocontrolled ROP of *meso*-lactide can result in either syndiotactic PLA (alternating S and R stereocenters) or heterotactic PLA in which the stereocenters doubly alternate. *Rac*-lactide can also lead to heterotactic PLA by alternating insertion of D- and L-lactide enantiomers. *Rac*-lactide can also produce atactic PLA, in which there is a random arrangement of stereocenters and isotactic PLA, in which all of the stereocenters in the PLA chain are identical.[30]

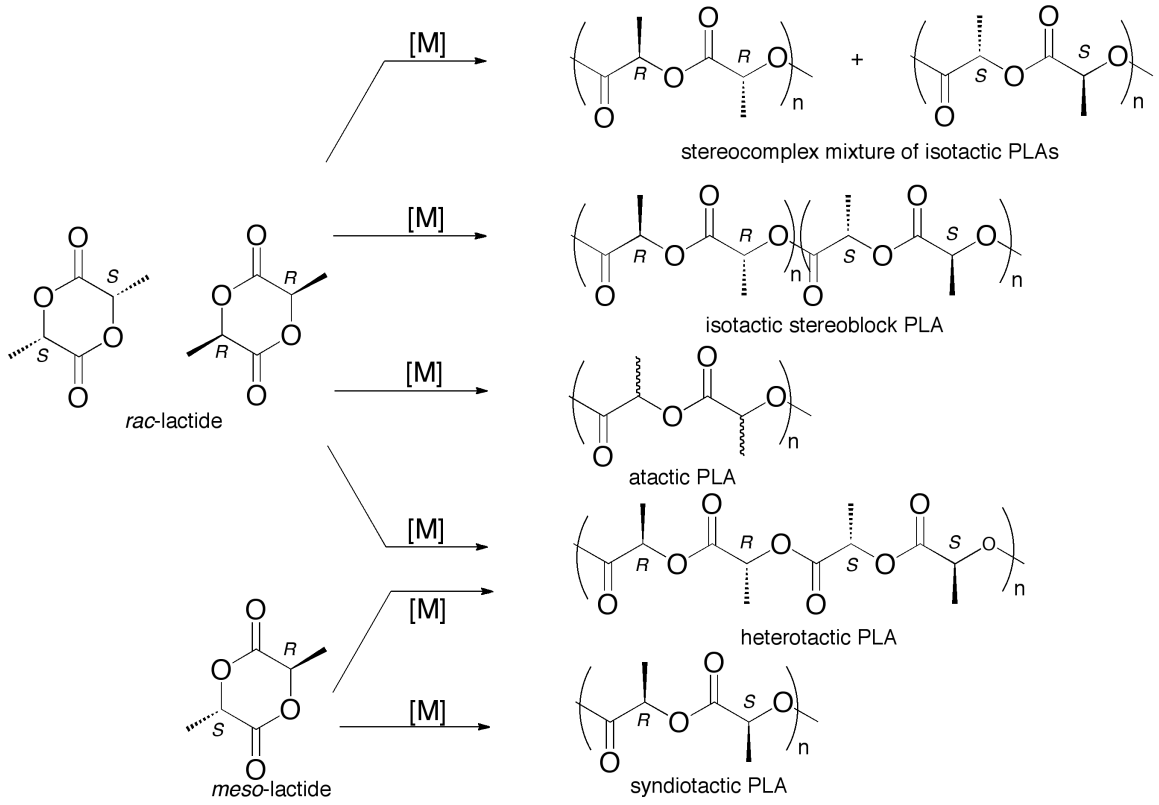

Scheme 1.3. PLA microstructures from the stereocontrolled ROP of lactide.[30]

Currently the largest producer of PLA is NatureWorks of Cargill Dow, which sells PLA under the branded name Ingeo™. Lactic acid is obtained from dextrose (D-glucose), which is extracted from corn and then fermented. NatureWorks claim their materials are the first greenhouse-gas neutral polymers ever produced on a commercial scale, with the process utilizing 68% less fossil fuel energy than traditional plastics.[31]

The progress of PLA research has made it a prominent material in the field of synthetic polyesters. However, other derivatives of PLA, such as its copolymer PLGA in which lactide and glycolide are copolymerized, are important fields of interest as well.[32] In addition, different cyclic lactones such as β-butyrolactone and ε-caprolactone have

received significant attention in recent literature[33] and will be discussed in further sections.

1.2.2 Poly(lactic-*co*-glycolic acid)

A considerable amount of research into drug delivery using biodegradable polymers has been carried out over the past 30 years due to their potential to be used in bioresorbable surgical devices.[34] Poly(lactic-*co*-glycolic acid) (PLGA) is an FDA-approved material that has strong physical properties and is highly biocompatible, making it a leader in the development of new materials for drug delivery systems and scaffolds for tissue engineering.[32,35] It has been extensively studied for the delivery of drugs,[36] proteins[37] and other macromolecules such as DNA,[38] RNA[39] and peptides.[40] In addition, PLGA has displayed favourable degradation properties, making it a candidate for sustained drug release by implantation without invasive surgical procedures.[9]

Both L- and D-lactide have been used for copolymerization with glycolide for the synthesis of PLGA (Scheme 1.4). PLGA with the composition range of 25-75% lactide results in amorphous polymers.[41] Miller *et al.* showed that a 50/50 PLGA is very hydrolytically unstable and degrades in the range of 1-2 months.[42] Other compositions displayed higher levels of hydrolytic stability with 75/25 degrading in 4-5 months and 85/15 in 5-6 months.[9] PLGA undergoes bulk erosion through hydrolysis of the ester bonds and the rate of degradation depends on a variety of parameters, including the lactide:glycolide ratio, molecular weight and the shape and structure of the matrix.[43] The multiple tunable properties of PLGA, in addition to its FDA approval to be used in humans, make it an ideal material to be used in sutures and drug delivery systems.

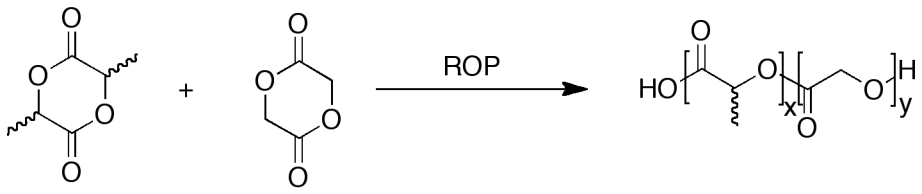

Scheme 1.4. PLGA synthesis.

1.2.3 Poly(3-hydroxybutyrate)

Polyhydroxyalkanoates (PHAs) are a family of biopolymers that are synthesized by microorganisms under conditions of nutrient stress, to use as energy storage materials.[44] PHAs have properties that are similar to many petroleum-based conventional plastics, but are also biodegradable, with significant potential to be used as replacements for commodity bulk plastics in the development of sustainable materials. Amongst the diverse family of PHAs, poly(3-hydroxybutyrate) (PHB), which accumulates in bacteria such as *Alcaligenes eutrophus* and *Azotobacter vinelandii*, is the most popular and widely researched material.[45] PHB that is naturally synthesized by bacteria tends to be isotactic in nature, as well as being highly crystalline and thermoplastic.[44,46]

There is also growing interest in the use of β-lactones, specifically β-butyrolactone (βBL) (Figure 1.1), to synthesize PHB.[47] Advancements in the ROP of βBL have allowed high degrees of control over properties of the polymer, such as the molecular weights and PDI, as well as the microstructures leading to high levels of stereocontrol.[48] Much attention has been focused on the ROP of racemic β-butyrolactone (*rac*-βBL), the simplest chiral β-lactone, to prepare syndiotactic PHB.[49] It is important to note that much like PLA, ROP of βBL allows for a range of stereocenters by homo- or copolymerization yielding a wide variety of materials with different properties.

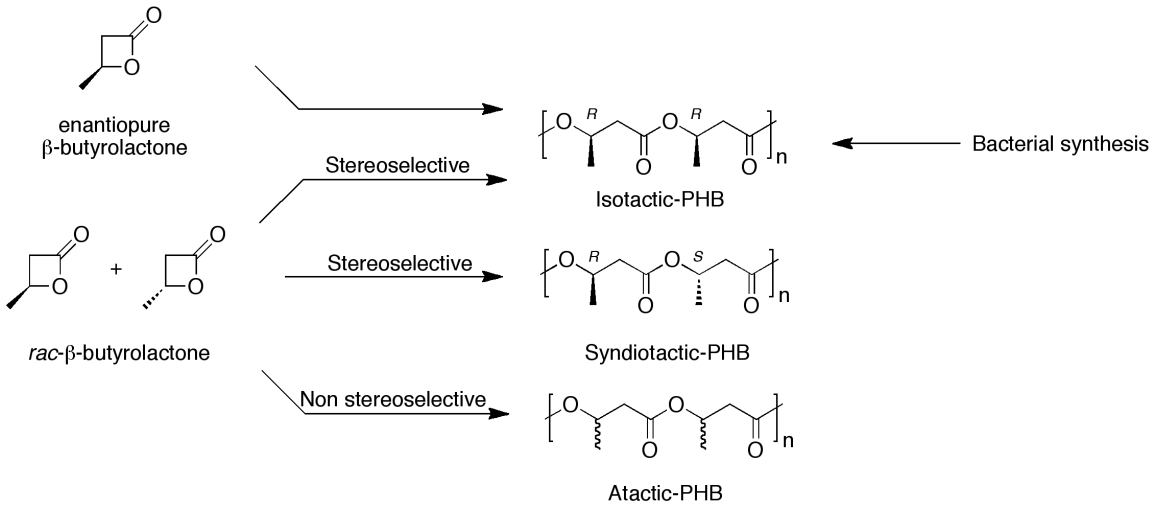

Scheme 1.5. PHB microstructures accessible by ROP and bacterial synthesis using βBL.[49]

1.2.4 Poly(ε-caprolactone)

Poly(ε-caprolactone) (PCL) is an aliphatic polyester composed of hexanoate repeat units derived from the monomer ε-caprolactone. It is a polyester of great interest, particularly due to the commercial availability of ε-caprolactone. PCL is semi-crystalline in nature and the physical and thermal properties of PCL depend on its molecular weight and degree of crystallinity.[50] At room temperature, PCL is soluble in a wide array of organic solvents[51] as well as displaying the rare property of being miscible in other polymers such as poly(vinyl chloride), poly(styrene-acrylonitrile) and poly(bisphenol-A).[9,52] In addition to its high solubility, PCL is mechanically compatible with other polymers such as polyethylene, polypropylene, natural rubber, poly(vinyl acetate) and poly(ethylene-propylene) making composite materials readily accessible.[9,50]

PCL copolymers undergo hydrolytic degradation due to the presence of hydrolytically labile ester linkages in the polymer chain. However, the rate of degradation is slow with timeframes ranging from 2-3 years, although this timeframe can vary based

on the crystallinity of the polymer and the conditions of degradation.[53] The amorphous phase tends to degrade first, which results in an increase in the degree of crystallinity while the molecular weight remains constant. This is followed by the cleavage of ester bonds that results in mass loss.[51] Due to the slow degradation timeframe, high permeability to many drugs and non-toxicity, PCL has been investigated as long-term drug delivery vehicles.[54] In addition to drug delivery, PCL has also been investigated in areas such as tissue engineering,[55] microelectronics,[56] adhesives[57] and packaging.[58] Studies have been conducted to potentially increase the degradation rate of PCL through copolymerization. Copolymers of ε-caprolactone and lactide have shown more rapid degradation rates,[59] while copolymers with glycolide were found to be less rigid compared to the PCL homopolymer, resulting in increased degradation rates.[9]

Unlike many other cyclic esters that are obtained from renewable feedstock resources, ε-caprolactone is derived from petrochemical sources. It is important to note that PCL is not truly a "green" material in source but is still degradable. A number of microorganisms oxidize cyclohexanol into adipic acid in which both ε-caprolactone and 6-hydroxy-hexanoic acid are intermediary products (Scheme 1.6). Industrially, ε-caprolactone is prepared by the oxidation of the cyclohexanone by peracetic acid (Scheme 1.7).[50]

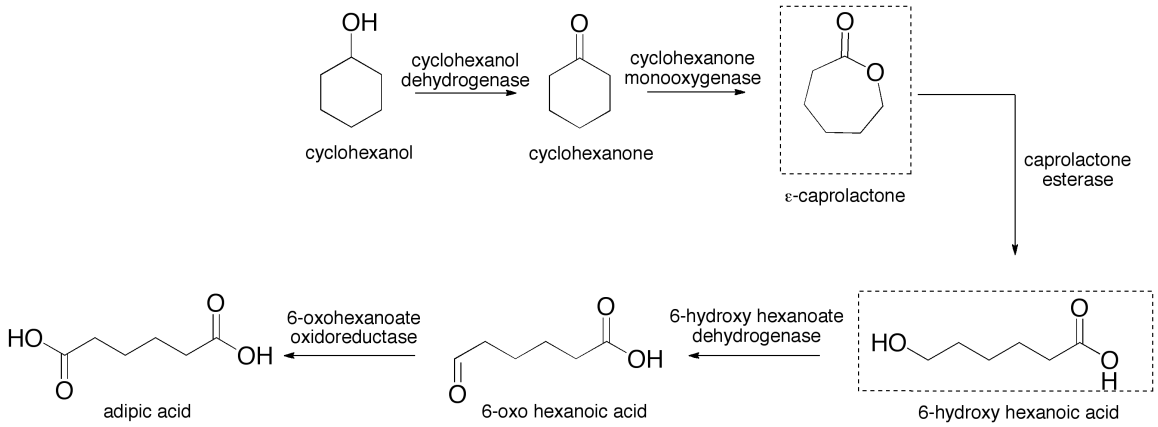

Scheme 1.6. Oxidation of cyclohexanol to adipic acid in microorganisms.[50]

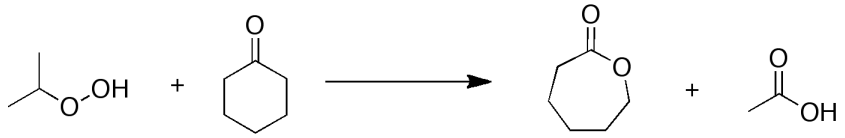

Scheme 1.7. Industrial production of ε-caprolactone from cyclohexanone and peracetic acid.[50]

1.2.5 Metal Catalysts for ROP of Lactones

The catalyst plays an essential role in controlling the molecular weights and molecular weight distributions of the polymerization. In addition, the catalyst can impose different levels of stereocontrol in the polymer, ultimately determining the physical properties of the materials. Since ROP by the coordination-insertion mechanism has become the most widely accepted method for the synthesis of controlled polyesters, a large number of studies have been conducted on synthesizing metal-based catalysts and understanding their activity. The first generation of metal-based catalysts were simple homoleptic metal complexes, specifically, tin(II) 2-ethylhexanoate ($Sn(Oct)_2$), zinc(II) lactate and aluminum(III) isopropoxide ($AlO\textit{i}Pr_3$) (Figure 1.2).[22,60] These first generation systems are still studied today and used as standards of comparison, industrial catalysts and in biomedical applications. In addition they have also helped understand the

mechanism of coordination-insertion. For example, Dittrich and Schulz were the first to define the coordination-insertion mechanism using ROP of L-lactide in 1971.[61] Kricheldorf *et al.* and Teyssie *et al.* further investigated and supported the coordination-insertion mechanism through the use of the Al*O*i*Pr*$_3$ system and various lactones.[62,63]

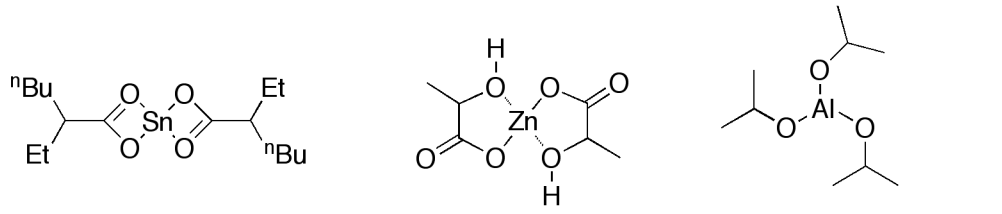

tin(II) 2-ethylhexanoate zinc lactate aluminum(III) isopropoxide

Figure 1.2. First generation metal catalysts for ROP via coordination-insertion

$Sn(Oct)_2$ remains the preferred catalyst in industry for the synthesis of polyesters.[64] Tin-based systems, specifically $Sn(Oct)_2$, have successfully polymerized many cyclic lactones.[64] One topic of interest is the mechanism by which these tin systems polymerize cyclic esters, as it differs from the traditional ROP coordination-insertion mechanism that was discussed earlier. Penczek described the mechanism through the polymerization of lactide, with two chains propagating from the metal center (Scheme 1.8).[65] In living polymerization, this changes the catalyst:initiator ratio to 0.5:1 in contrast to a 1:1 ratio for the coordination-insertion initiation mechanism described earlier. Unfortunately these tin systems cause side reactions such as transesterification,[66] ultimately leading to higher PDI values. A number of attempts have been made to overcome these side reactions by modifying the catalyst. Catalysts based on bis- and trisaryl tin(IV) alkoxides ($Ph_2Sn(OR)_2$ and $Ph_3Sn(OR)$),[67] tin(IV) amides ($Ph_2Sn(NMe_2)_2$)[66] and cyclic tin(IV) bisalkoxides ($Bu_2Sn(-OCH_2CH_2O-$)[68] have all been

synthesized with hopes to alleviate the side reactions. However, it was found that these systems were still limited because of issues with hydrolysis resistance and slow polymerization rates.

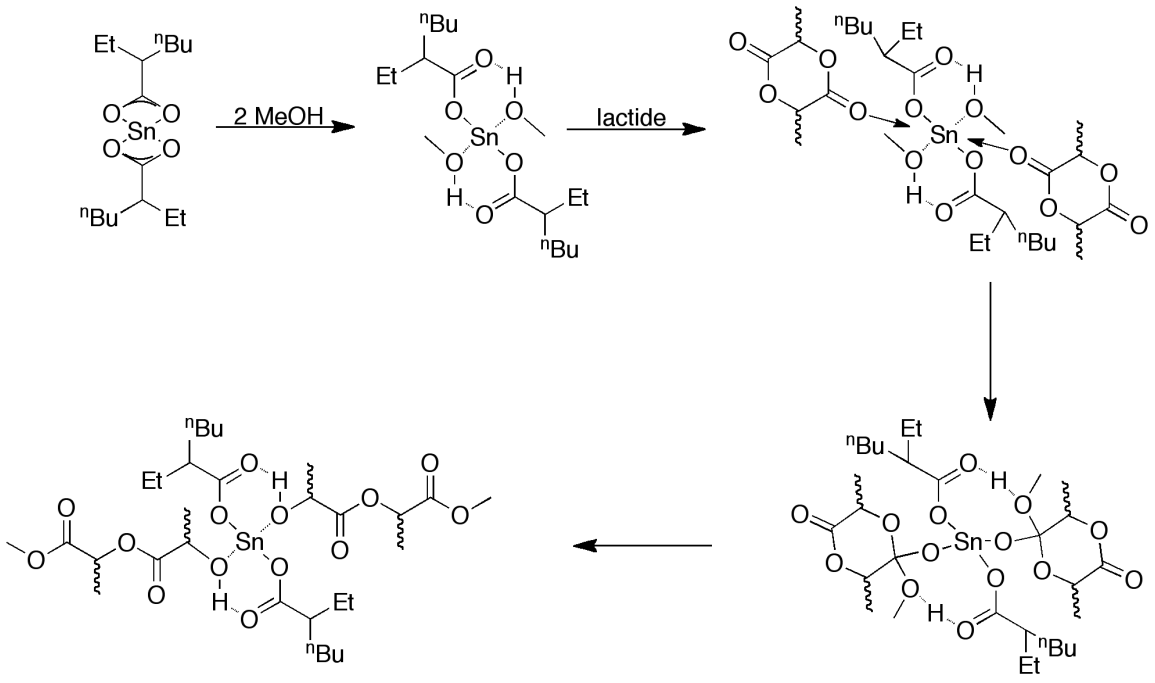

Scheme 1.8. Initiation of lactide by $Sn(Oct)_2$.

Several limitations were found in these first-generation systems. Complicated equilibrium mechanisms as well as multiple nucleophilic species have resulted in deviation in levels of control. The tendency of these metal systems to promote side reactions at higher temperatures, including intramolecular and intermolecular transesterification reactions (Scheme 1.9), in which the polymer chains cleave and reform, results in a broad molecular weight distribution and high PDI values.[22] Intramolecular transesterification occurs via a back-biting mechanism which results in the formation of a shortened linear chain and cyclic polymer. Intermolecular

transesterification results when the polymer chain ends of two closely associated chains undergo a random exchange process that produces two new chains.

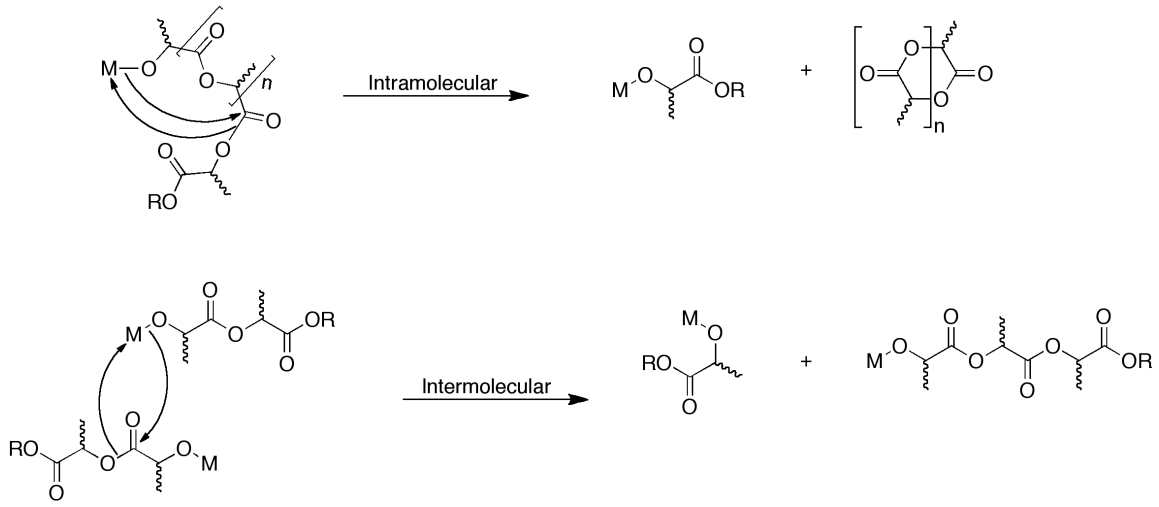

Scheme 1.9. Intramolecular and intermolecular transesterification mechanisms.

In addition to a lack of control, these first-generation catalysts offered no option of stereocontrol in lactones with chiral centers, limiting the full potential of these novel materials. Recent studies have addressed these problems and attempted to overcome the obstacles observed in the first generation systems. The main focus in these next generation systems involves fine tuning the ligands to control factors such as control over molecular weight distributions, activity and the ability to impose stereochemistry.[22] Some of the most successful second-generation catalyst systems are the aluminum salen and salan systems, which have the potential to overcome all liabilities of the first-generation systems.

1.2.6 Aluminum Salen and Salan Catalysts.

Over the past two decades there has been significant development of catalytic systems used in the ROP of cyclic esters to overcome the limitations observed in the first

generation systems. There has been a tremendous movement towards the development of single site catalysts that have the general formula of L_nMR where M is the central metal surrounded by the ancillary ligand L_n. Variation in the steric and electronic properties of the ligand can influence the activity and stereoselectivity of the catalyst. R, the initiating group, can also have a strong influence on the activity of the complexes. It was found that variation of the metal-ligand framework allowed precise control over the polymerization rate, molecular weight, PDI and stereochemistry. Some of the most significant developments have been made using aluminum systems, specifically the Al(salen) and Al(salan) complexes, in which the general structures are highlighted in Figure 1.3. These complexes have been thoroughly studied in the literature, demonstrating excellent control in the polymerization of lactide,[69] β-butyrolactone[70] and ε-caprolactone[70,71] In addition to high levels of control, these catalyst systems have also been found to impose high levels of stereocontrol in the polymerization of lactide.[30,70]

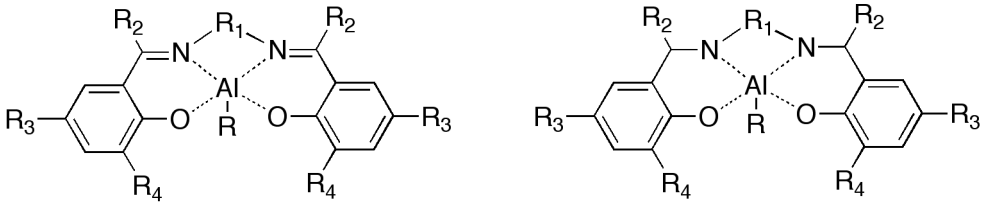

Figure 1.3. Aluminum salen and salan general structures.

Table 1.1. Substituents for aluminum salen catalysts

Entry	R	R_1	R_2	R_3	R_4
1[72]	OMe	C_2H_4	H	H	H
2[72]	OMe	C_2H_4	H	Cl	H
3[73]	OMe	C_2H_4	Me	H	H
4[74]	OMe	$C_{20}H_{12}$	H	H	H
5[74]	O^{i}Pr	$C_{20}H_{12}$	H	H	H
6[75]	O^{i}Pr	C_6H_{10}	H	^{t}Bu	^{t}Bu
7[76]	Et	$(CH_2)_2$	H	H	H
8[76]	Et	$(CH_2)_2$	H	Me	Me
9[76]	Et	$(CH_2)_2$	H	H	^{i}Pr
10[76]	Et	$(CH_2)_2$	H	H	Ph
11[76]	Et	$(CH_2)_2$	H	^{t}Bu	^{t}Bu
12[76]	Et	$(CH_2)_3$	H	H	H
13[76]	Et	$(CH_2)_3$	H	Me	Me
14[76]	Et	$(CH_2)_3$	H	H	^{i}Pr
15[76]	Et	$(CH_2)_3$	H	H	Ph
16[76]	Et	$(CH_2)_3$	H	^{t}Bu	^{t}Bu
17[77]	Et	C_5H_{10}	H	^{t}Bu	^{t}Bu
18[78]	Me	C_2H_4	H	H	H
19[78]	Me	C_2H_4	H	Cl	H
20[78]	Me	C_2H_4	H	Cl	Cl
21[78]	Me	C_2H_4	H	^{t}Bu	^{t}Bu
22[78]	Me	C_3H_6	H	H	H
23[78]	Me	C_3H_6	H	Cl	Cl

24[78]	Me	C_3H_6	H	^{t}Bu	^{t}Bu
25[70]	Me	C_2H_4	H	Me	Ad

Various substituents on the aluminum salen catalyst system, which is used in this project, are summarized in Table 1.1. With regard to the activity of these aluminum systems, appending electron-withdrawing substituents to the phenoxide donor enhances the rate of polymerization.[79] Enhanced activities have also been observed by using a salicylketimine derivative containing neither bulky nor electron-withdrawing substituents on the phenoxide donor.[80] A study conducted by Gibson *et al.* revealed several important factors influencing the ROP of *rac*-lactide by Al(salen) initiators. First, flexible 3-carbon linkers between the imino nitrogen donors enhanced activities. Second, activities were suppressed by large *ortho*-phenoxy substituents. Third, the stereoselectivity is favoured by a combination of a flexible aliphatic C_3 linker and sterically demanding *ortho*-phenoxy groups.[78]

1.3 Aliphatic Polyester Polymer Stars.

Polymers may be synthesized in a variety of different architectures. Star polymers are branched, multi-armed polymers that radiate from a central core. In contrast to traditional linear polymers, star polymers exhibit rheological, mechanical and biomedical properties that are not prevalent in their linear counterparts.[81] This has made these systems attractive in different fields of biomedicine including drug delivery systems. In addition, they also have increased functional end groups, improving control over solubility and hydrodynamic volumes.

Three methods are currently used for the synthesis of polymer stars (Scheme 1.10). The core-first method involves the polymerization of a monomer in the presence of a multi-functional initiator and polymer chains radiate out from the core. The arm-first method involves grafting of previously synthesized end-functionalized polymer arms onto a functionalized core through a coupling reaction, or termination of a living polymerization by a multi-functional agent.[81]

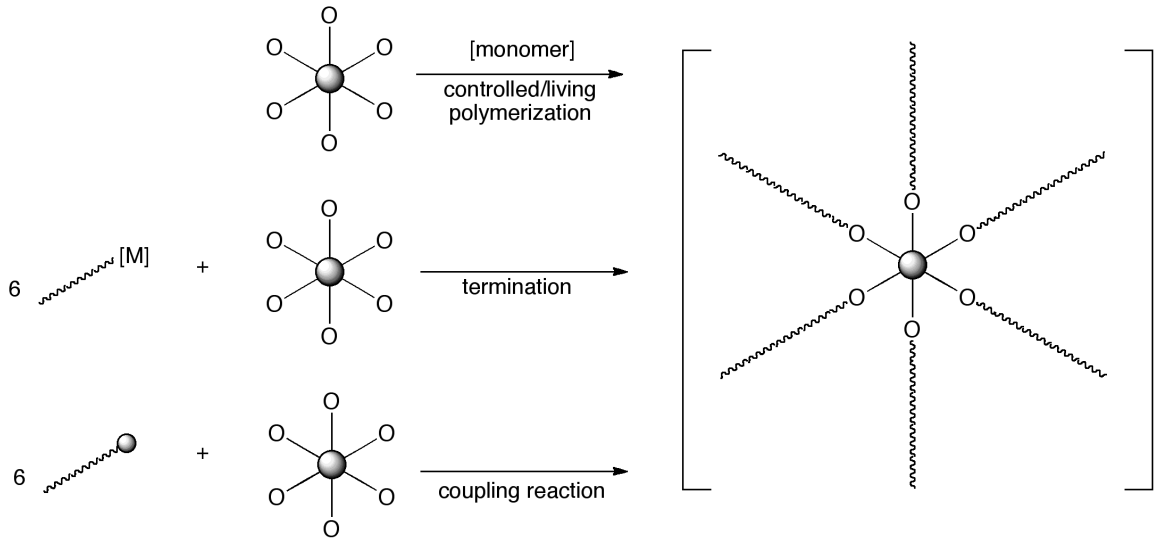

Scheme 1.10. Synthetic routes to polymer stars.

A topic of great interest is the synthesis of polymer stars based on aliphatic polyesters.[81] This is due to the variety of different polyesters accessible as homopolymers as well as copolymers. In addition, multi-functional alcohol based molecules such as cyclodextrins can act as initiators for polymer star synthesis in ROP. For coupling reactions, addition of a terminal functionality to the linear polymer can be used to graft the polymer chains onto a functionalized core, resulting in the formation of a star. A variety of different stars have been synthesized using aliphatic polyesters such as PLA, PCL and βBL, reported in a recent review article.[81] Cyclodextrin-based polymer stars are

of particular appeal in drug delivery, as they offer the biodegradable properties of polyesters, as well as loading capacities of cyclodextrins.

1.4 Cyclodextrins as Hosts: Guest Inclusion

Supramolecular chemistry can be defined as "chemistry beyond the molecule".[82] Supramolecular chemistry traditionally encompasses the formation of complex molecular systems from the association of two or more chemical species held together by intermolecular forces, in contrast to the breaking and forming of bonds in molecular chemistry.[82] These intermolecular forces include electrostatic interactions, van der Waals interactions, hydrophobic interactions and hydrogen bonding.[83] Therefore, instead of focusing on single molecules and their individual properties, the interaction between the constituents of the supramolecular structure becomes important as the properties of these supramolecular complexes differ from their constituent molecules.[84] The unique properties of supramolecular systems have made them applicable in fields such as molecular recognition, molecular sensors, molecular transport, catalysis and molecular devices.[85]

Supramolecular host-guest inclusion complexes form via the inclusion of smaller substrates within the internal cavity of a larger host molecule as shown in Scheme 1.11. The simplest and most common example of these systems involves the inclusion of a single guest inside a single host and is collectively referred to as a 1:1 complex.[86] This complex represents the simplest form of a supramolecular structure as it involves the minimum of two interacting molecules. However, higher order systems can also form, involving two or more guests and/or two more hosts that form due to size variances in the host and the guest.[87]

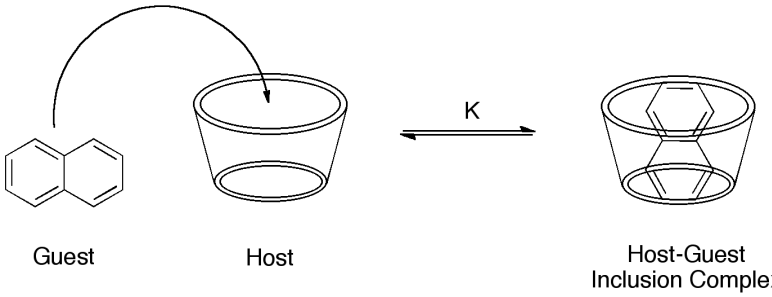

Scheme 1.11. Host-guest inclusion complex formation.

The guest can essentially be any molecule, as long as it is of sufficient size and geometry to enter the host cavity. In contrast, there are fewer examples of host molecules due to the requirement of a well-defined internal cavity.[88] These hosts traditionally tend to be large macrocyclic organic molecules, however, there have been reports of inorganic hosts as well.[89] Examples of organic hosts include cyclodextrins,[90] calixarenes,[91] cucurbiturils,[92] crown ethers,[93] cyclophanes,[94] cavitands[95] and carcerands.[96] Of these compounds, cyclodextrins are the most commonly used and studied[97] and will be the focus of the work presented in this thesis.

Cyclodextrins (CDs) are cyclic oligosaccharides consisting of repeating glycopyranose units.[98,99,100,101] Cyclodextrins were first discovered by Villiers in 1891, with the first detailed synthesis and isolation procedures described by Shardinger in 1903.[102] Early synthetic methods involved the treatment of starch with a group of amylases called cyclodextrinases that resulted in hydrolyzation of the starch helix and the formation of α-1,4 linkages between the ends of the starch molecules.[103,104] There are three major sizes of cyclodextrins, referred to as α-cyclodextrin, β-cyclodextrin and γ-cyclodextrin, consisting of six, seven and eight glycopyranose units respectively, as shown in Figure 1.4.[105,106]

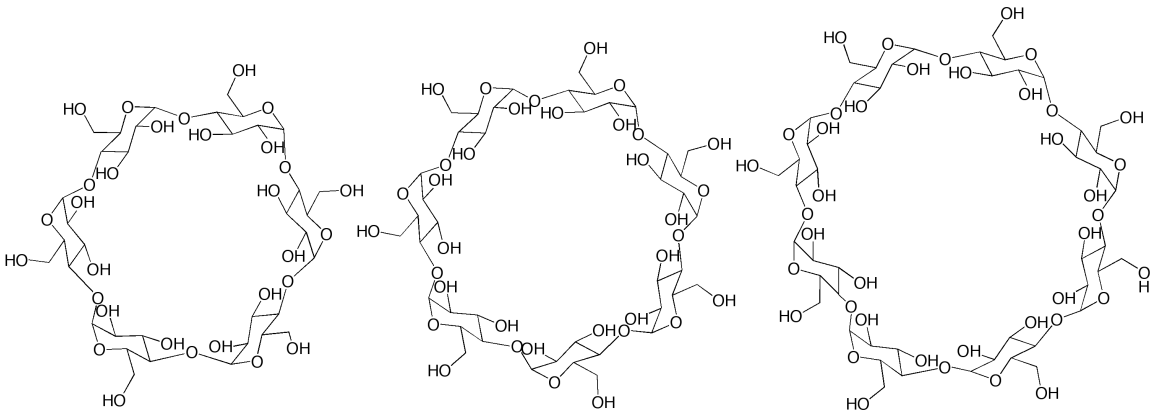

Figure 1.4. Three major cyclodextrins: α-cyclodextrin, β-cyclodextrin and γ-cyclodextrin.

Due to the cyclic nature of cyclodextrins, the primary and secondary hydroxyl groups line the rim of the molecular structure. These hydroxyl groups are of particular importance due to hydrogen bonding with water that allows improved solubility of these large molecules, whilst intramolecular hydrogen bonding is important in establishing their truncated cone shape in solution.[107] The resulting structure resembles a bucket, as the inner region of the cyclodextrin contains a nano-cavity. As the number of glycopyranose units in α-, β- and γ-cyclodextrins varies from 6 to 8, the nano-cavity can also varies in size. It is this nano-cavity that causes cyclodextrins to be studied so thoroughly, as cyclodextrins have an extraordinary ability to form inclusion complexes with a wide range of organic guest molecules in solution. This is the result of two unique properties of the cyclodextrin molecule. First, the cavity becomes filled with high-energy water molecules that hydrogen bond with the hydroxyl groups of the cyclodextrin, resulting in the formation of a truncated cone shape, as mentioned above. Secondly, since the inside of the cavity is highly nonpolar compared to the surrounding environment, hydrophobic guest molecules will show a preference for the environment inside the cavity in aqueous solution.[97] The result of this is the inclusion of the organic guest molecule inside the cyclodextrin cavity by the expelling of the previously included water

molecules. In addition to the ability to form host-guest inclusion complexes, cyclodextrins are optically transparent above 300 nm, which makes them ideal host molecules for studying the photochemistry and spectroscopy of a wide range of guest molecules.

The ability of cyclodextrins to form host-guest complexes has allowed them to be applied in a number of different fields including the cosmetics, foods, adhesives, coatings, agricultural and chemical industries, as well as pharmaceuticals in the field of drug delivery as described in this work.[108] There are many different applications for cyclodextrins in the pharmaceutical industry. For example, addition of cyclodextrins to substances that have poor water-solubility improves their bioavailability and increases their pharmacological effect, allowing a reduction in drug dosage.[108] Formation of an inclusion complex can also facilitate the handling of volatile products, leading to different methods of drug administration, such as in the form of tablets. Cyclodextrins may also be used to improve the stability of substances to increase their resistance to hydrolysis, oxidation, heat, light and metal salts.[108] The inclusion of irritating bioactive molecules in cyclodextrin cavities can be used to protect the gastric mucosa for oral consumption or prevent skin damage for dermal intake.[108]

Cyclodextrins are highly resistant to starch degrading enzymes, although they can be degraded at slow rates by α-amylases and absorbed by the body, making them ideal biodegradable and bioassimilable compounds for drug delivery. Degradation of these compounds is not performed by saliva or pancreas amylases, but α-amylases from microorganisms in the colon. Absorption studies revealed that only 2-4% of cyclodextrins were absorbed in the small intestines and the remainder were degraded and taken up as

glucose.[108] This can explain the low toxicity found upon the oral administration of cyclodextrins.

1.5 Cyclodextrin-based Polymer Stars.

New opportunities arise from the synthesis of polymer stars based on supramolecular systems such as cyclodextrins. A variety of different techniques have been used to develop cyclodextrins polymer stars based on core- and arm-first methods. Controlled radical polymerization (CRP) techniques including atom transfer radical polymerization (ATRP),[109] reversible addition-fragmentation chain-transfer polymerization (RAFT)[110] and a combination of ATRP with nitroxide mediated radical polymerization (NMP)[111] have all been used to synthesize polymer stars based on cyclodextrins.

The most commonly used technique to synthesize cyclodextrin polymers is ATRP. The use of cyclodextrins as a macroinitiator by ATRP was first reported by Haddleton and co-workers using β-cyclodextrin.[109] Since then macroinitiators based on β- and α-cyclodextrin have been used; γ-cyclodextrin, however, has not yet been investigated.[112] These macroinitiators were synthesized by reacting a cyclodextrin with 2-bromoisobutyryl bromide/chloride, 2-bromoisobutyric anhydride, or 2-bromopropionyl bromide.[113] By using α-cyclodextrin, 18 arm stars can be synthesized; similarly 21 arm stars can be synthesized from β-cyclodextrin. However, four arm polymer stars were synthesized when β-cyclodextrin was treated with four equivalents of 2-bromoisobutyryl bromide.[114] A 20 arm star was synthesized by using nitroxide-capped polystyrene arms followed by functionalization with 2-bromoisobutyric acid.[115] Although bromine-based initiators are the most common, there have been reports of iodine-based initiators used in

conjunction with [$FeCp(CO)_2I$] and CDs.[113] The bromine based initiators are most commonly used with a copper(I) bromide catalyst system with various ligands. Cyclodextrin-based polymer stars have been synthesized using styrene,[116] N-isopropylacrylamide[117] and (meth)acrylate derivatives using ATRP.[109]

Other techniques for cyclodextrin-based stars have also been used. ROP of lactide,[118] ε-caprolactone[119] and 2-ethyl-2-oxazoline[118] have been reported using cyclodextrins as initiators. $Sn(Oct)_2$ was initially used as a catalyst in these polymerizations with temperatures exceeding 100°C. Alternative methods were then attempted by using sodium hydride for anionic ROP. It was shown that this alternative method works, however it resulted in polymers with broad PDI values due to transesterification reactions.[120]

NMP and RAFT have also been used for the synthesis of novel stars. 2,2,6,6-Tetra-methyl-1-piperidinyl-N-oxy (TEMPO)-modified cyclodextrin was used to polymerize styrene by NMP.[115] This was found to be an inefficient process as trimodal molecular weight distributions were observed, with both linear and star components forming during the polymerization. For RAFT, Stenzel and Davis reported the synthesis of a heptafunctional trithiocarbonyl RAFT agent for the polymerization of styrene.[121] The RAFT agent was anchored to the CD core, leading to the absence of star coupling products. It was observed that the molecular weight increase of each arm slowed down at higher conversions, indicating shielding of the RAFT agent. Limitations associated with the core-first method include the number of well-defined arms and initiation of all functionalities, have led to exploration of other polymer star synthetic methods such as arm-first synthesis.

The highly efficient copper(I)-catalyzed azide-alkyne cycloaddition (CuAAC), better known as "click chemistry" (Scheme 1.12), is considered to be one of the most suitable approaches for synthesizing arm-first polymer stars. Click chemistry is highly favourable because of the high yields, simple reaction conditions, fast reaction times and high regioselectivity.[122] The strategy for star synthesis is as follows: 1) azide functionalization of the cyclodextrins, 2) synthesis of alkyne-terminated polymer arms and 3) click reaction to form 1,2,3-triazole.[122]

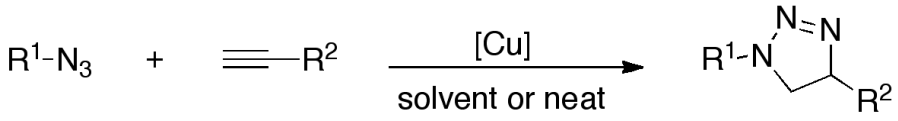

Scheme 1.12. Copper(I)-catalyzed azide-alkyne cycloaddation to form a 1,2,3-triazole.

Using the described method, alkyne-terminated poly(*N*-isopropylacrylamide) was prepared by ATRP using propargyl 2-bromoisobutyrate as an initiator with a CuCl/Me_6TREN complex. Click reaction with azide modified β-cyclodextrin yielded polymer stars with narrow molecular weight distributions.[123] Using the same strategy, ROP of ε-caprolactone was carried out in the presence of 5-hexyn-1-ol with $Sn(Oct)_2$. Microwave irradiation was then used to click the PCL arm on in the presence of $CuSO_4$ and sodium ascorbate. The reaction yielded PCL polymer stars with good levels of molecular weight control and excellent PDI values.[124]

So far, the development of polymer stars based on cyclodextrin cores has been promising using both core-first and arm-first methods. With both aliphatic polymers and cyclodextrins being used in drug delivery, conjugation of these two systems offer a new efficient strategy in controlled drug delivery to develop systems with tunable properties

as well as personalized treatment protocols. As each patient displays different pharmacokinetics for the degradation of drug delivery systems and release of bioactive compounds, cyclodextrin stars with fluorophore inclusion would offer new opportunities for the individualized and optimized treatment regimens.

1.6 Molecular Fluorescence and Effects of Inclusion

Luminescence can be defined as the emission of light from an electronically excited molecule upon the transition from a higher energy state to a lower one.[125] In order for luminescence to occur there must be an initial electronic excitation by electrical discharge, absorption of light (A), or a chemical reaction. Luminescence can be divided into two different processes, fluorescence (F) and phosphorescence (P).[126] Fluorescence is characterized by luminescence emitted by a molecule during an electronic transition between states of the same multiplicity, therefore the transition is spin allowed and the fluorescence is very fast. Fluorescence usually involves the transition of a molecule from the first excited singlet state S_1 to the ground singlet state S_0.[126] Phosphorescence is defined as the luminescence emitted by a molecule during an electronic transition between states of different spin multiplicity, which is a forbidden transition, and therefore a weak and slow process. This generally involves the transition from the first triplet state T_1 to the ground singlet state S_0.[126] The emission rate of fluorescence is typically 10^8 s^{-1} which results in a timeframe of approximately 10 nanoseconds. In contrast, phosphorescence rates are much slower resulting in timeframes of milliseconds to seconds.[127] The lifetime of a fluorophore (τ) is defined as the time it takes for the excited population to decrease to 1/e of the initial excited population.[127] Due to the short lifetime

of fluorescence, the measurement of time-resolved emission requires complex optics and electronics. [127]

Fluorescence and phosphorescence are referred to as radiative transitions as the excess energy of the excited state is released as photons.[128] In contrast, a nonradiative transition can also occur in which the excess energy is emitted as heat instead of photons.[126] The two main types of nonradiative transitions are internal conversion (*IC*) and intersystem crossing (*ISC*). Internal conversions are transitions between states with the same spin multiplicities, e.g. from S_1 to S_0, whereas intersystem crossing occurs between states with different spin multiplicities, e.g. from S_1 to T_1.[126] Another type of non-radiative relaxation process is vibrational relaxation (*VR*) in which a molecule can be excited into a higher vibrational level of an electronic state, e.g. S_1, followed by rapid relaxation to the lowest vibrational level of that state. All of these transitions can be summarized in a Jablonski diagram (Figure 1.5).[126]

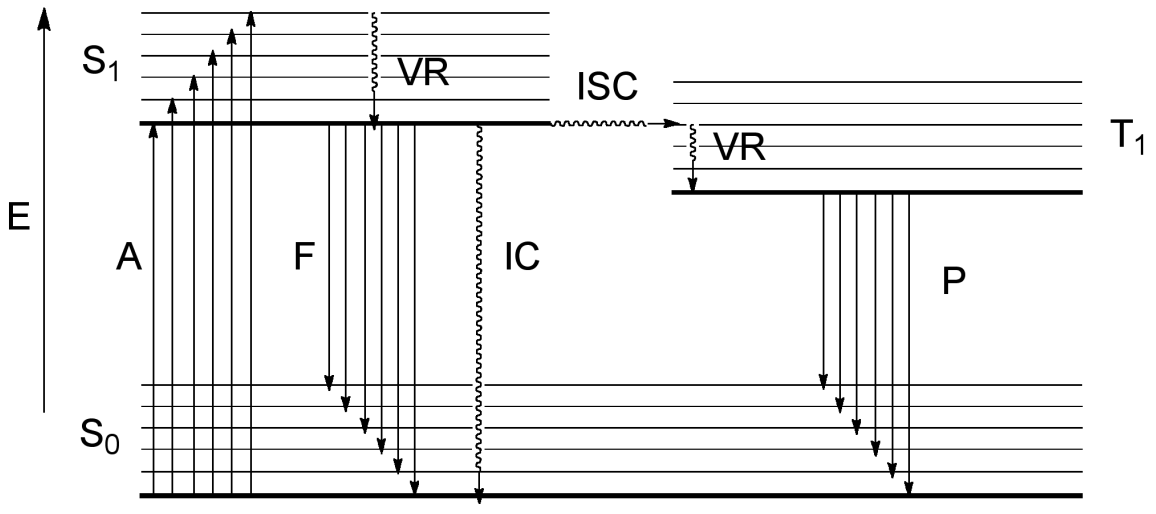

Figure 1.5. Jablonski diagram of the lowest electronic states and the radiative and nonradiative transitions that occur between them.

Molecular fluorescence associated with host-guest systems has become a vastly studied field in supramolecular chemistry since fluorescence is an extremely sensitive technique and requires only small amounts of fluorescent species, making it a powerful tool for studying the phenomenon of host-guest inclusion systems.[129] The majority of host-guest systems, including those with cyclodextrins, involve the inclusion of a fluorescent guest inside the cavity of a non-fluorescent host. For cyclodextrins and other hosts, inclusion of a guest fluorophore will result in significant changes to the fluorescent properties of the guest, including the wavelength of maximum fluorescence emission, quantum yield and lifetime.[129] The measurement of these properties of the fluorescent guest in the presence of a host can yield a great deal of information about the inclusion process, such as the binding constant K or the correlation of host to guest. The quantum yield will increase or decrease upon inclusion resulting in significant enhancement or loss of fluorescence intensity depending on the fluorophore used.[130] Likewise, the fluorescence lifetime may also increase or decrease. In addition, the wavelength of maximum fluorescence intensity may also change, usually by a blueshift as the first excited electronic state S_1 is more polar than the than the ground state S_0. Thus, the S_1 state will be much more destabilized in a non-polar medium than the S_0 state.[131] Changes to the fluorescence of the guest upon inclusion are a result of the following factors:[131] 1) The polarity of the host cavity is different to that of the bulk medium, 2) Intramolecular rotation is reduced due to the confined space of the cavity and 3) The guest is protected from quenchers such as O_2.

Most studies involving molecular fluorescence are conducted in aqueous media, meaning that the free guest molecule will be present in a very polar medium. In contrast,

the inside of the cyclodextrin cavity is relatively nonpolar. Thus, if the guest is a polarity sensitive probe it will exhibit significant changes to its fluorescence properties upon inclusion into the cyclodextrin cavity.[132] In most cases, the quantum yield and the lifetime will increase and the wavelength of maximum emission will blueshift. This is attributed to the first electronic excited state S_1 being more polar than the ground state S_0, as depicted in Figure 1.6.[127] There is a differential destabilization that results in the S_1- S_0 energy gap, $\Delta E(S_1- S_0)$ being larger in the non-polar environment (inside of a host cavity) when compared to the polar aqueous solution. This has two very important effects on the fluorescence properties. First, the increased energy gap means that the molecule will fluoresce at higher energy, or a shorter wavelength. Secondly, the increased energy gap results in a decreased rate of internal conversion.[133] This relationship is described by the energy-gap law of radiationless decay, which states that the rate constant for a nonradiative decay process is inversely related to the exponential of the energy gap ΔE between the initial and final steps.[133] In other words, internal conversion does not compete as effectively due to the larger energy gap, resulting in a fluorescence enhancement. Enhancement does not occur with all fluorophores as some exhibit what is known as fluorescence suppression upon encapsulation into a cavity. The polarity dependence of the specific suppression fluorophore 7-methoxycoumarin (7-MC), which is used in this work, is as follows. In a nonpolar medium, the energy of the S_1 state is very similar to a nearby upper triplet state. This results in a very efficient intersystem crossing transition, which depopulates the S_1 state and therefore competes with fluorescence, resulting in a relatively low fluorescence quantum yield.[131] However, in a polar medium the energy of this triplet state is increased above that of the S_1 state so intersystem

crossing transition becomes much less efficient due to a significant energy gap. Upon inclusion of the fluorophore into the host cavity, the decrease in polarity will decrease the quantum yield through an increase in intersystem crossing and hence a decrease in fluorescence or fluorescence suppression.[131]

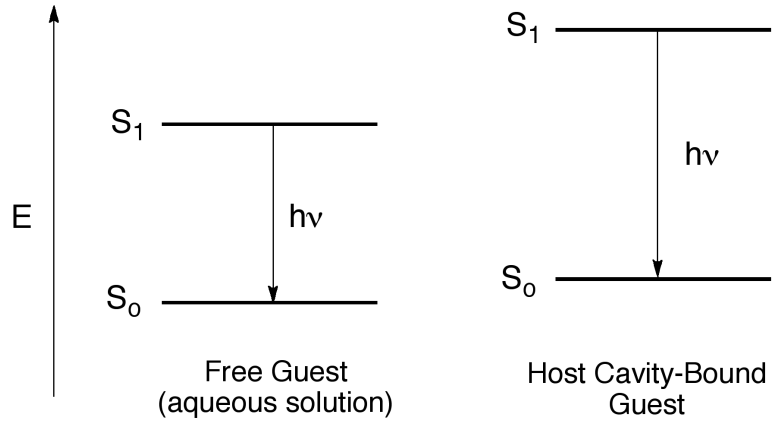

Figure 1.6. Spacing of S_0 and S_1 states of polarity sensitive probes in polar and non-polar environments.

The capability of these fluorophores to exhibit changes in their fluorescence can be exploited in different fields such as drug delivery. Cyclodextrins have already been used in pharmaceuticals for the delivery of drugs for different medicinal purposes. The use of fluorescence guests with cyclodextrin hosts for drug delivery potentially offers a method to create new types of drug delivery systems that are able to indicate treatment regimens of the drug through molecular fluorescence.

1.7 Mandate of research

This thesis is focused on the development of polymer stars based on cyclodextrin cores. It is expected that developing stars with cyclodextrin cores will lead to promising materials for use in the field of controlled drug delivery. As both cyclodextrins and aliphatic polyesters have previously been applied in biomedical sciences, conjugation of

these systems would lead to ideal characteristics for biomedical applications as both molecules can be broken down in the body. In order to understand the binding properties of these cores, binding constant and correlation studies are proposed using β-cyclodextrin and heptakis(2,6-di-O-methyl)-β-cyclodextrin with a 7-methoxycoumarin fluorophore due to the good binding reported in literature.[131] Polymer stars based on β-cyclodextrin derivatives and PLA, PLGA, PHB and PCL arms will be prepared, with the synthesis of these stars being carried out using both core-first and arm-first methods. In addition to the polymer star synthesis, inclusion of a fluorophore into the polymer network, followed by degradation under catalytic and non-catalytic conditions will be studied to in order to understand the controlled release properties of these materials.

For the core-first method, polymer stars based on a heptakis(2,6-di-O-methyl)-β-cyclodextrin multi-functional initiator will be prepared using two different catalyst systems: 1) $Sn(Oct)_2$ and 2) ^{t}Bu[salen]AlMe. The main goal of this method is to synthesize materials of controlled molecular weights and narrow PDI values (≈ 1). Thermal analysis of these materials will evaluate their morphologies as well as their degradation temperatures. Inclusion of the fluorophore will be achieved by heating the polymer above its glass transition temperature (T_g) in the presence of excess fluorophore to include the fluorophore in the network. Degradation studies of this material with both catalyzed and uncatalyzed methods will reveal if it possesses controlled release properties and potentially the location of the fluorophore in the polymer star (arms or core).

For the arm-first stars, copper(I)-catalyzed azide-alkyne cycloaddition (CuAAc) will be used. In order to use CuAAc, an azide-modified cyclodextrin, heptakis-azido-β-cyclodextrin will be prepared. In addition, linear alkyne-terminated polymers based on

PLA, PLGA, PHB and PCL will be prepared using 5-hexyn-1-ol as the initiator. Click reactions will then be carried out using $CuSO_4$ and sodium ascorbate as they have yielded well-defined polymer stars in literature.[124] Similar fluorophore inclusion to the core-first stars will be conducted in conjunction with degradation studies to examine the controlled release properties of these novel materials.

Chapter Two

2 Host-Guest Inclusion Studies Based on β-Cyclodextrin and Heptakis(2,6-di-O-methyl)-β-Cyclodextrin with 7-Methoxycoumarin

2.1 Host-Guest Inclusion Studies with 7-Methoxycoumarin and β-Cyclodextrins

Host-guest inclusion studies are important because they provide an understanding of how a host and guest will interact in solution. They can be used to determine how strongly the guest will bind to the host and they indicate the binding of host to guest. CDs have the ability to form host-guest inclusion complexes, and if the guest is a polarity-sensitive fluorescent probe, CD inclusion will significantly affect the measured fluorescence intensity. In most cases, polarity sensitive probes are more fluorescent in a non-polar medium, so the formation of an inclusion complex results in an enhancement

of fluorescence. However in the case of 7-methoxycoumarin (7-MC, shown in Figure 2.1), the probe is more fluorescent in the polar medium, therefore inclusion into the CD results in a decrease in fluorescence intensity. By embedding the fluorophore into the polymeric network, controlled release of the drug delivery vector would be indicated by an increase in fluorescence as 7-MC is released into the polar environment as the polymer star degrades. Cyclodextrins that were used for this study were standard β-cyclodextrin and a modified heptakis(2,6-di-O-methyl)-β-cyclodextrin (Figure 2.2).

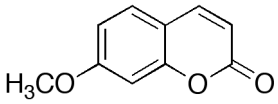

Figure 2.1. Structure of 7-methoxycoumarin.

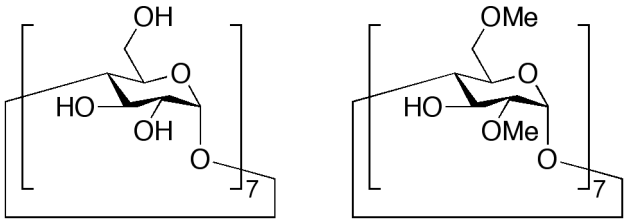

Figure 2.2. Structure of β-cyclodextrin and heptakis(2,6-di-O-methyl)-β-cyclodextrin.

Due to the absence of covalent binding between the host and guest, complexation is a dynamic phenomenon and an equilibrium is established in solution between the complex and the free host and guest. From this equilibrium it is possible to obtain the binding constant, K, which is a measurable property of the host-guest complex, and its magnitude is indicative of the total driving forces for inclusion in terms of the Gibbs energy change for the inclusion, ΔG ($K = e^{-\Delta G/RT}$), from a thermodynamic perspective. From a kinetic perspective, K is equal to the ratio of the rate constant of entrance into the cavity (K_{in}) to the rate constant for exit from the cavity (K_{out}), i.e. $K = K_{in}/K_{out}$.[134] In order

to obtain a significant concentration of host-guest complex, the rate of entrance into the cavity (K_{in}) must be larger than the rate of exit (K_{out}).[134]

$$K = \frac{K_{in}}{K_{out}} = \frac{[CD:7MC]}{[7MC][CD]}$$

Equation 2. Equation for binding constant, K.

In order to obtain the binding constant for β-CD and 7-MC a 3.0×10^{-5} M solution of 7-MC was prepared in water. The solution was shaken vigorously and sonicated to ensure that the 7-MC was dissolved. The solution was then monitored by ultraviolet-visible spectroscopy (UV-Vis) at 320 nm to obtain the absorbance at the excitation wavelength. 320 nm was chosen because it is near the maximum absorbance of the 7-MC absorption peak, thus making it an ideal excitation wavelength for the fluorescence titration experiments. The absorbance at 320 nm was observed to be 0.32, which is ideal. It is important for the fluorescence measurement for the absorbance not to exceed 0.40 because the excitation light could then be absorbed by the solution at the front of fluorescence cuvette, and a decreased signal would be observed.

To determine the association constants of the host cyclodextrins and 7-MC, fluorescence titration experiments were performed. 3 mL of the 7-MC water solution were added to nine separate vials containing 1-9 mM of β-CD. The solutions became cloudy white suspensions as the 7-MC solution was added, indicating that the β-CD was not highly soluble in water. The presence of particulates in the samples would cause the light to scatter and give inaccurate fluorescence measurements and so, the samples were

sonicated for 15 minutes. Once removed from the sonicator, the samples were clear, indicating the cyclodextrins had dissolved.

3 mL of the stock 7-MC solution was then placed into a 1 cm^2 glass cuvette and the fluorescence emission of the solution was measured from 330-630 nm. The monochromator slits on the fluorimeter were adjusted so that the counts per second did not exceed 2×10^6 to prevent damage to the photomultiplier tube. For the 7-MC standard solution it was observed that the fluorescence peak ranged from 350-490 nm with the wavelength of maximum intensity (λ_{max}) located at 385 nm (Figure 2.3). The total area under the peak is equivalent to the total fluorescence emitted and is referred to as F_o.

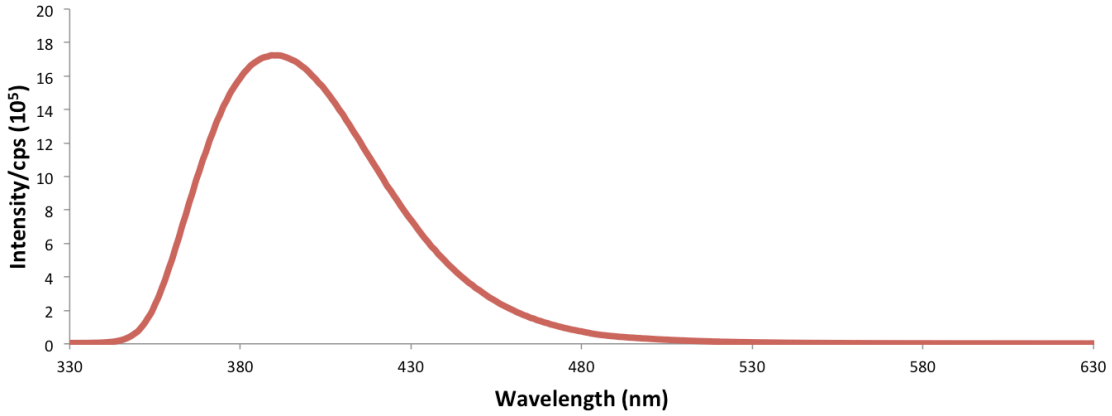

Figure 2.3. Emission spectrum of 7-MC in H_2O.

Using the same method the samples containing cyclodextrins were analyzed and as expected, an increase in the CD concentration resulted in a decrease in the fluorescence intensity (F). In addition, a solvent blank consisting of fresh deionized water was run, to ensure that no impurities were affecting the fluorescence spectra. Once the fluorescence was determined for each sample, the total peak area of the solvent blank was subtracted from each value. In addition, each F value was divided by F_o, the total area of the 7-MC solution, in order to determine the F/F_o ratio, which represents the effect the

CD has on the fluorescence emitted. In this case, the F_o value was higher than all of the F values, which is indicative of fluorescence suppression.

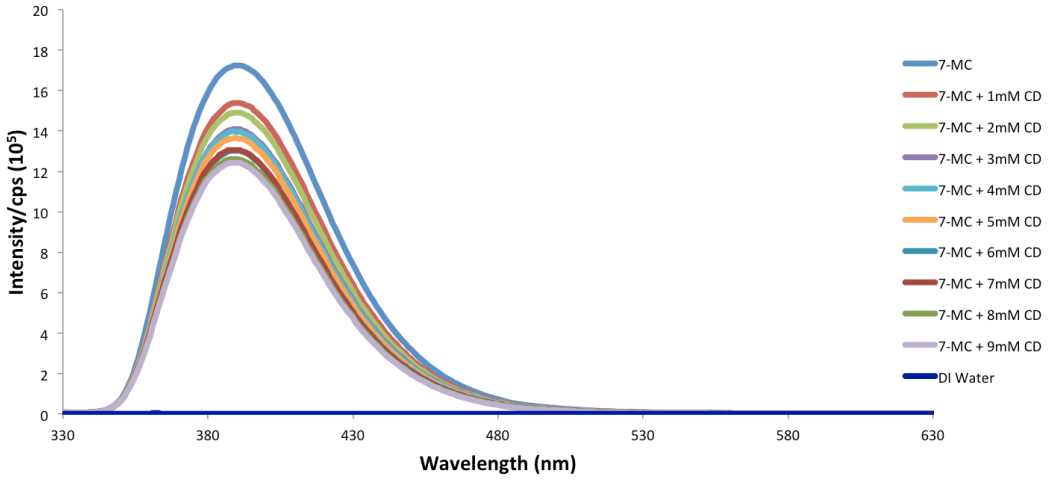

Figure 2.4. Fluorescence titration spectra of 7-MC and β-cyclodextrin.

The data were then plotted as the F/F_o ratio as a function of the concentration of cyclodextrin in order to observe the decrease in fluorescence as the concentration of cyclodextrin increased. In order to obtain the binding constant, K, methods reported by Peña et al were used.[135] If there is a 1:1 host guest formation in this study the relationship can be expressed as:

$$\frac{F}{F_o} = 1 + \frac{\left(\frac{F_\infty}{F_o} - 1\right) K[H]_o}{1 + K[H]}$$

Equation 3. F/F_o equation used to obtain the binding constant, K.

This ratio is of significant importance as it permits independence from experimental conditions such as probe concentration, monochromator slit width and light intensity. In addition the ratio ensures easy reproducibility from trial to trial. It is possible

to obtain a double reciprocal plot of $1/(F/F_o-1)$ versus $1/[H]_o$ where $[H]_o$ is the host concentration.[135] A linear relationship in a double reciprocal plot is indicative of a 1:1 complex formation. In contrast, if a 2:1 complex is formed, the double reciprocal plot will adopt a concave curvature.[136] By using Equation 3 it is possible to obtain the binding constant, K, by computer analysis using a non-linear least-squares method.

Fluorescence titration experiments were performed three times to ensure consistency of the results. The F/F_o values, K and R^2 from the double reciprocal plot are reported in Table 2.1 and Table 2.2. As expected there was a decrease observed in the F/F_o values as the CD concentration was increased, due to the fluorescence suppression. The K values were found to vary during the trials. This was attributed to moderate solubility of β-CD, as even after sonication of the solution it is likely that some CD did not fully dissolve therefore causing small deviations in the K for each trial. Similarly, the range of the R^2 values (0.91-0.98) indicates deviations from the trials possibly due to formation of a small amount of higher order complexes.

Table 2.1. F/F_o for 7-MC and β-CD fluorescence titrations in H_2O.

[CD] (mM)	F/F_o (Trial 1)	F/F_o (Trial 2)	F/F_o (Trial 3)	F/F_o (Average)
1	0.8839	0.8518	0.9144	0.8834
2	0.8438	0.8160	0.8722	0.8441
3	0.8129	0.7970	0.8323	0.8140
4	0.7524	0.7750	0.7884	0.7720
5	0.7240	0.7374	0.7631	0.7415
6	0.7099	0.7170	0.7377	0.7215
7	0.6890	0.7010	0.7110	0.7000
8	0.6741	0.6817	0.6907	0.6822
9	0.6681	0.6757	0.6868	0.6765

Table 2.2. K and R^2 values for 7-MC and β-CD fluorescence titrations in H_2O.

	Trial 1	Trial 2	Trial 3	Average
K (M^{-1})	249	305	158	238 ± 60
R^2	0.958	0.909	0.986	0.958

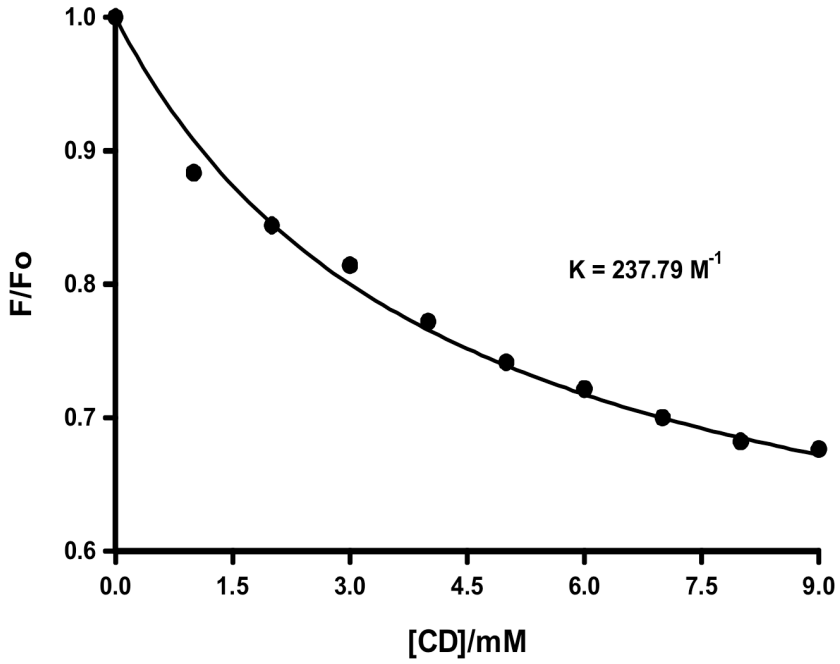

Figure 2.5. F/F_o vs [CD] plot of β-CD and 7-MC in H_2O.

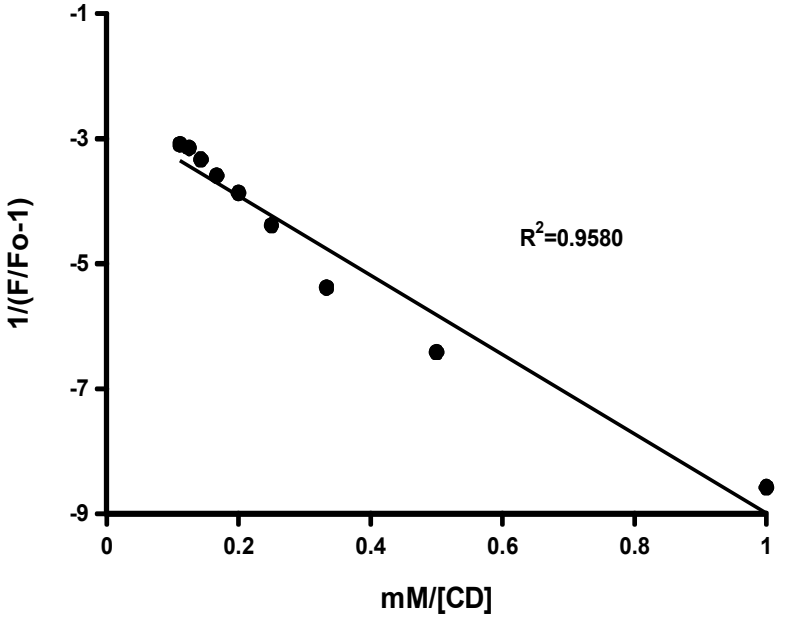

Figure 2.6. Double reciprocal plot of β-CD and 7-MC in H_2O.

The average F/F_o values of the three trials were obtained and then plotted using the same non-linear least-squares method to give an average K value of 238 ± 60 K^{-1} and a R^2 value of 0.9580 (Figure 2.5 and Figure 2.6). This result was found to differ from the value reported in the literature of β-CD and 7-MC which was 128 ± 32 K^{-1}.[131] A possible explanations for this is the variable percentage of water weight per cyclodextrin sample, as tests showed 11.8% water content in β-CD after heating at 180 °C under vacuum for 4 hours. The β-CD was not dried prior to use, however the calculated CD concentrations were corrected using the water content values. Despite determining the average percentage of the β-CD, this may differ from sample to sample, therefore affecting the actual concentrations of the CD and resulting in variation in K values for separate trials. In order to address this, it was proposed that a high purity chemically modified derivative, heptakis(2.6-di-O-methyl)-β-cyclodextrin, would potentially offer more reliable associations with 7-MC.

2.2 Host-Guest Inclusion Studies with 7-Methoxycoumarin and Heptakis(2,6-di-O-methyl)-β-Cyclodextrin

Heptakis(2,6-di-O-methyl)-β-cyclodextrin is a chemically modified derivative of β-cyclodextrin. The hydrogen atoms of the secondary hydroxyl group at the 2 position and the primary hydroxyl group at the 6 position are substituted for methyl groups (Figure 2.2). Similar binding constant studies to those described in Section 2.1 were performed using heptakis(2,6-di-O-methyl)-β-CD. As expected, this derivative was much more soluble than unmodified β-CD due to decreased intermolecular bonding, and thus higher concentrations of heptakis(2,6-di-O-methyl)-β-CD (1-15 mM) could be used in the fluorescence titrations.

Table 2.3. F/F_o for 7-MC and heptakis(2,6-di-O-methyl)-β-CD fluorescence titrations in H_2O.

[CD] (mM)	F/F_o (Trial 1)	F/F_o (Trial 2)	F/F_o (Trial 3)	F/F_o (Average)
1	0.8431	0.8269	0.8418	0.8373
2	0.7499	0.7416	0.7615	0.7510
3	0.6858	0.6884	0.7051	0.6931
4	0.6475	0.6329	0.6642	0.6482
5	0.6229	0.6052	0.6224	0.6168
6	0.5954	0.5820	0.5996	0.5923
8	0.5469	0.5355	0.5699	0.5508
10	0.4980	0.5042	0.5368	0.5130
12	0.4849	0.4823	0.5105	0.4926
15	0.4563	0.4639	0.4886	0.4696

Table 2.4. K and R^2 values for 7-MC and heptakis(2,6-di-O-methyl)-β-CD fluorescence titrations in H_2O.

	Trial 1	Trial 2	Trial 3	Average
K (M^{-1})	283	326	313	306 ± 31
R^2	0.999	0.998	0.998	0.998

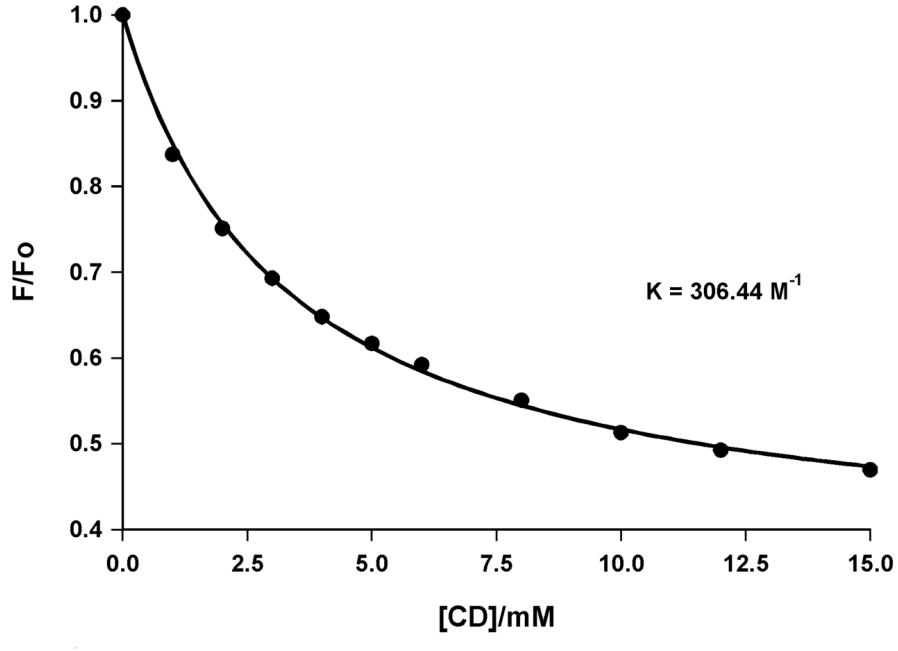

Figure 2.7. F/F_o vs [CD] plot of heptakis(2,6-di-O-methyl)-β-CD and 7-MC in H_2O.

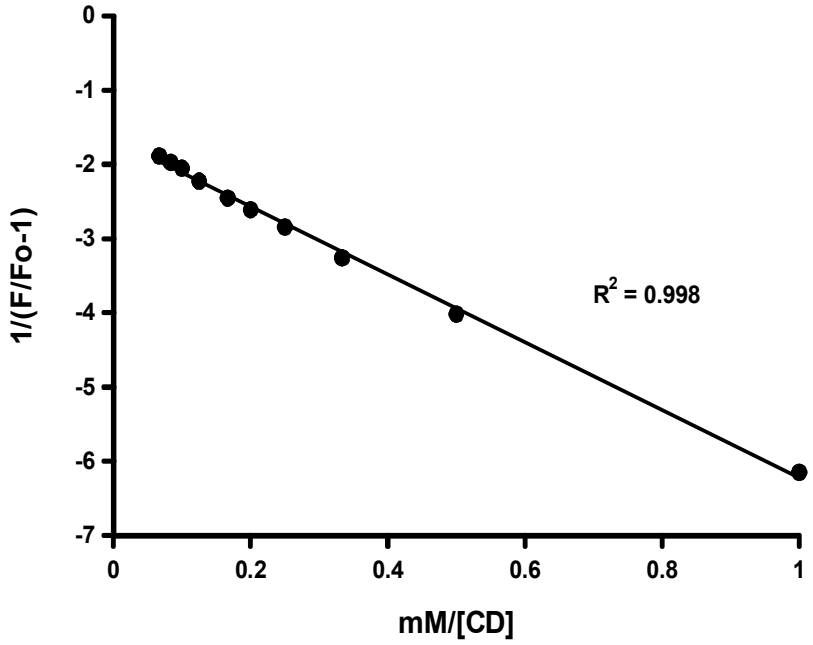

Figure 2.8. Double reciprocal plot of heptakis(2,6-di-O-methyl)-β-CD and 7-MC in H_2O.

The results obtained with heptakis(2,6-di-O-methyl)-β-CD were found to be much more consistent over the course of three trials when compared to that of the parent β-CD. F/F_o values followed the same trend, as increased CD concentrations resulted in fluorescence suppression (Table 2.3). The heptakis(2,6-di-O-methyl)-β-CD was found to have higher solubility than that of parent β-CD and as a result these trials were carried out without sonication of the solutions. K and R^2 values showed less variation in comparison to β-CD, with the F/F_o vs. [CD] plot showing excellent correlation between data points and theoretical fit (Figure 2.7), as well as the double reciprocal plot exhibiting excellent correlation with an R^2 of 0.9980 (Figure 2.8).

There are two possible modes of inclusion of 7-MC into the CD for a 1:1 host-guest complex, with insertion of either the carbonyl or methoxy group first. It is difficult to establish which of these insertions would be preferred and it is expected that significant interaction between the hydroxyl groups on the upper rim of the CD and the oxygen atoms on either end of the 7-MC molecule will occur.[131] Replacement of the hydroxyl hydrogens with methyl groups is anticipated to extend the size of the CD cavity and reduce the cavity polarity.[137] We therefore expected that heptakis(2,6-di-O-methyl)-β-CD will give greater fluorescence suppression compared to β-CD. An average K value of 306 ± 31 K^{-1} was obtained after computational analysis. This indicated that stronger binding of 7-MC occurred with the methylated CD, agreeing with literature reports that modified CDs affect fluorescence intensity more than their parent CDs.[138,139]

The excellent binding results obtained using heptakis(2,6-di-O-methyl)-β-CD prompted the use of different solvent systems in the host-guest studies. This is an attractive prospect because the degradation of polymers proceeds faster in more alkaline

environments.[31] Methanol, ethanol and dimethylformamide were chosen as candidates for fluorescence studies due to the variances in polarity. However, initial fluorescence studies revealed that, in comparison to water, organic solvents exhibited poor 7-MC fluorescence emissions, orders of magnitude lower than that of 7-MC in water. Both ethanol and methanol exhibited fluorescence intensities about 9× less than that of water, whereas 7-MC in DMF displayed virtually no fluorescence (Figure 2.9). This indicated that in the absence of water 7-MC displayed very poor fluorescence emission and it was not viable to perform the binding studies in relatively less-polar solvents.

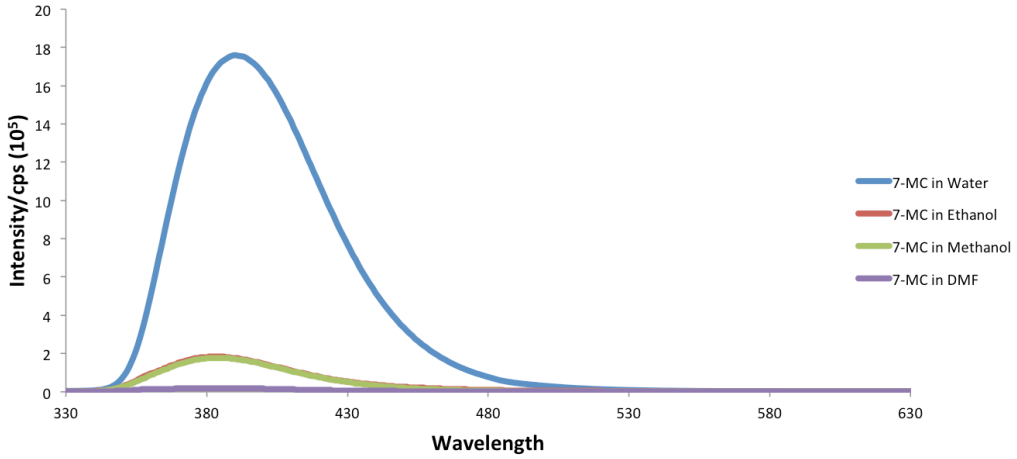

Figure 2.9. Fluorescence intensities of 7-MC: H_2O (blue), EtOH (red), MeOH (green) and DMF (purple).

In order to overcome the limitations of fluorescence imposed by solely using organic solvents, a mixture of methanol with water was investigated. This allowed binding constants to be obtained, as the fluorescence spectra were well defined. The mixture of water and methanol also provided a more alkaline environment in which the polymer stars could degrade, thus allowing for a faster controlled release profile to be observed. A 50:50 mixture of water and methanol was chosen. Similar to the previous

two studies, three trials were performed to obtain F/F_o, K, and R^2 values (Table 2.5 and Table 2.6).

Table 2.5. F/F_o for 7-MC and heptakis(2,6-di-O-methyl)-β-CD fluorescence titrations in a 50:50 mixture of H_2O and MeOH.

[CD] (mM)	F/F_o (Trial 1)	F/F_o (Trial 2)	F/F_o (Trial 3)	F/F_o (Average)
1	0.9534	0.9211	0.9696	0.9479
2	0.9226	0.9087	0.9314	0.9209
3	0.8990	0.8777	0.8942	0.8903
4	0.8610	0.8589	0.8674	0.8624
5	0.8520	0.8511	0.8597	0.8543
6	0.8486	0.8410	0.8513	0.8470
8	0.8175	0.8121	0.8270	0.8202
10	0.7829	0.8040	0.8035	0.7968
12	0.7530	0.7717	0.7781	0.7676
15	0.7129	0.7133	0.7663	0.7308

Table 2.6. K and R^2 values for 7-MC and heptakis(2,6-di-O-methyl)-β-CD fluorescence titrations in a 50:50 mixture of H_2O and MeOH.

	Trial 1	Trial 2	Trial 3	Average
K (M^{-1})	82	152	127	121 ± 36
R^2	0.996	0.941	0.991	0.976

As expected, much less fluorescence suppression occurred in the water/methanol mixture, with the F/F_o values ranging from 0.9-0.7 in comparison to 0.8-0.4 for the study in pure water. This can be attributed to a significant decrease in the polarity of the bulk solution in the presence of methanol. This results in fewer guests entering the cavity due

to the smaller difference in polarity between the cavity and bulk solution, resulting in less suppression. Nonetheless, good correlation values were obtained, with an overall K value of 121 ± 36 M^{-1}. As expected, the binding was significantly less in water/methanol due to the decreased polarity of the bulk solution resulting in fewer inclusion complexes forming. However, there was still moderately good correlation between the experimental data and the theoretical fit on the F/F_o vs. [CD] plot. In addition an R^2 value of 0.986 was obtained on the double reciprocal plot, indicating that a 1:1 host-guest complex still forms in 50:50 water-methanol mixture.

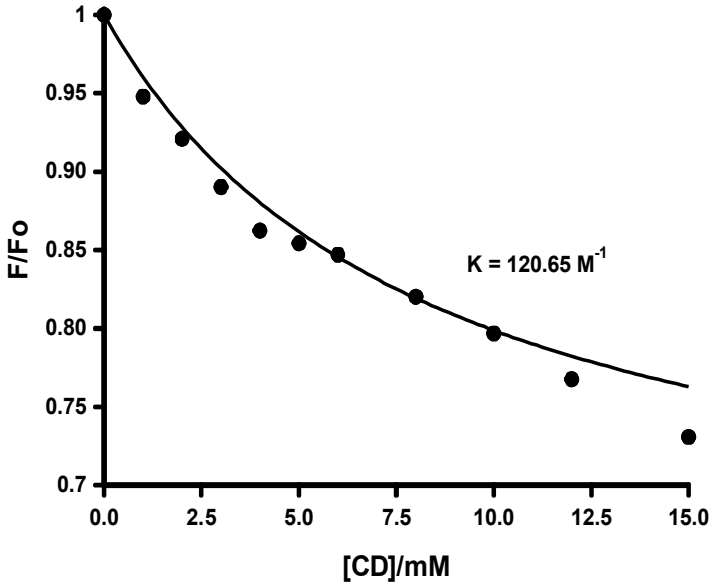

Figure 2.10. F/F_o vs [CD] plot of heptakis(2,6-di-O-methyl)-β-CD and 7-MC in a 50:50 mixture of H_2O and MeOH.

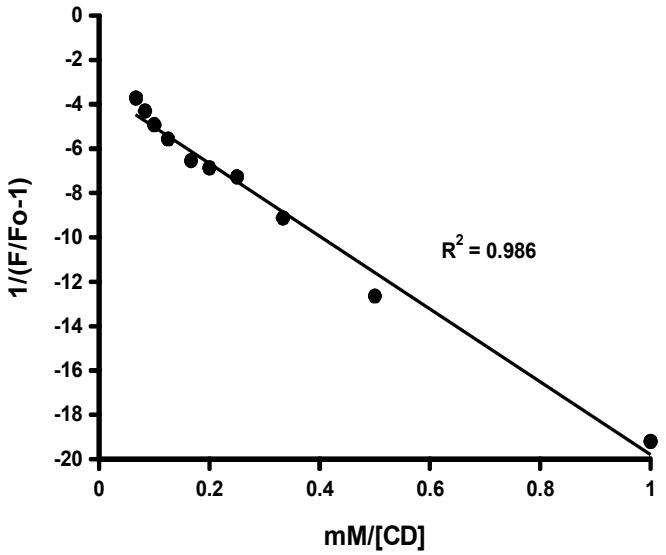

Figure 2.11. Double reciprocal plot of of heptakis(2,6-di-O-methyl)-β-CD and 7-MC in H_2O in a 50:50 mixture of H_2O and MeOH.

In light of the results obtained with β-CD and heptakis(2,6-di-O-methyl)-β-CD for the binding effect of 7-MC binding studies, both were chosen as macroinitiators for core-first polymerization studies for the synthesis of cyclodextrin-based polymer stars.

Chapter Three

3 Core-First Polymer Stars: Synthesis and Degradation Studies

3.1 Attempted Synthesis of Polymer Stars using β-CD.

Initial core-first polymerizations were attempted with β-CD pre- dried at 100 °C in a vacuum oven. This core was used as an initiator for the polymerization of *rac*- and L-lactide in the presence of $Sn(Oct)_2$ (Figure 3.1) at 70 °C in toluene. After 3 hours the reaction was quenched and precipitated with pentane. However, GPC analysis showed that there was no polymer present, indicating that no productive polymerization had occurred, potentially due to poor initiation. Higher temperatures of 120 °C in toluene and neat conditions were then investigated. Reactions were carried out for 1, 3, 6 and 9 hours, but all reactions were unproductive. A possible explanation for poor initiation was the high insolubility of β-CD in the reaction medium, which remained a suspension at

elevated temperatures. In addition, β-CD has a high water content and even after drying for 24 hours, some water may still have been present leading to catalyst death during the polymerization.

3.2 Synthesis of Polymer Stars based on Heptakis(2,6-di-O-methyl)-β-CD.

In light of the unsuccessful initiation with β-CD, polymer star synthesis based on a heptakis(2,6-di-O-methyl)-β-CD core and catalyst systems of $Sn(Oct)_2$ and ^{tBu}[salen]AlMe were proposed. Heptakis(2,6-di-O-methyl)-β-CD cyclodextrin was investigated because of its commercial availability, excellent binding with 7-MC and increased solubility in organic media compared to an unmodified β-cyclodextrin. The core contains seven alcohol functionalities on the 3′ carbon, which were used as macroinitiators for the ring-opening polymerization of lactide, β-butyrolactone and glycolide.

$Sn(Oct)_2$ (**1**) and ^{tBu}[salen]AlMe (**2**) (Figure 3.1) were chosen as catalysts because of their excellent control over the synthesis of linear PLA polymer chains as well as star polymers.[81] Aluminum salen tetradentate catalysts have been reported to have excellent control over both molecular weight distribution and the microstructure of PLA.[78] In contrast, catalyst **1** is the most widely used industrial catalyst for PLA synthesis and yields atactic polymer with narrow molecular weight distributions. This allowed for the exploration of the effects of tacticity in the degradation of these polymer stars.[48]

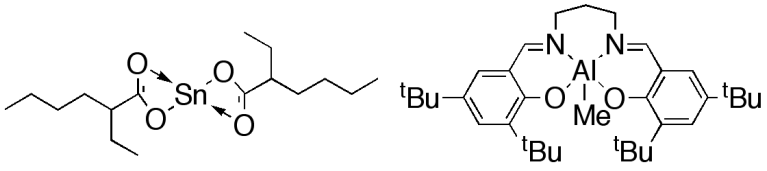

Figure 3.1. Catalyst systems $Sn(Oct)_2$ (**1**) and ^{tBu}[salen]AlMe (**2**).

Initially, synthesis of the cyclodextrin polymer stars was carried out using standard reaction conditions reported for the synthesis of PLA polymer stars based on dipentaerythritol cores.[140] A catalyst:alcohol functionality ratio of 1:0.5 was used for catalyst **1**, as one metal center can initiate two alcohol functionalities. In contrast, a ratio of 1:1 was used for catalyst **2**, since only 1 chain per metal center will grow. The monomer:initiator ratios were varied from 10-50:1 or 0.5 in order to provide seven-armed stars with 10-50 monomer units per arm. By varying the monomer equivalents a library of PLA stars were synthesized.

The first polymerization studies were carried out with *rac*-lactide and **1** at 70 °C in toluene for 3 hours. However, the isolated material showed no polymer by GPC and ^{1}H NMR spectroscopic analysis, which was attributed to inefficient initiation of the cyclodextrin core at this temperature. The temperature was increased to 120 °C and the isolated products showed poly(lactic acid) with monomodal GPC traces, indicating that successful initiation was achieved. In a representative reaction shown in Scheme 3.1, *rac*-lactide, 1 equivalent of CD, 0.5 equivalents of **1** and 2 mL of toluene were added to an ampule under an N_2 atmosphere. The ampule was sealed and heated at 120 °C in order to initiate the polymerization. After the set time period, the reactions were exposed to the

atmosphere and quenched with a 10:1 mixture of DCM and MeOH and then precipitated, filtered and dried *in vacuo* for 24 hours prior to analysis.

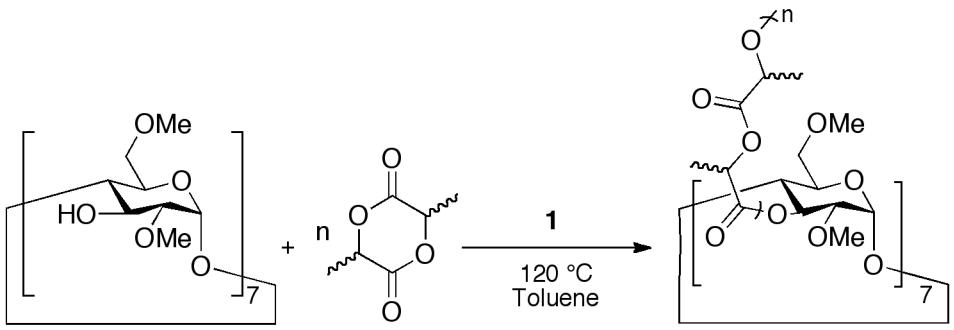

Scheme 3.1. CD poly(lactic acid) polymer stars based on *rac*-lactide and $Sn(Oct)_2$ (**1**).

Table 3.1. Polymerization data for CD poly(lactic acid) polymer stars based on *rac*-lactide and $Sn(Oct)_2$ (**1**).

[M]:[C]:[I]	% Conv.[a]	$M_{n,th}$[b]	$M_{n,\ GPC}$[c]	$M_{n,\ NMR}$[d]	PDI[c]	PDI_{arm}[e]
70:0.5:1	57	7082	29310	17209	1.25	3.11
140:0.5:1	60	13438	37900	25702	1.37	3.78
210:0.5:1	72	23307	54150	49071	1.28	3.35
280:0.5:1	70	29581	70790	52587	1.35	3.54
350:0.5:1	78	40679	87040	71327	1.41	3.96

Polymerizations were conducted in 2 mL of toluene with 0.01 mmol of $Sn(Oct)_2$ at 120 °C for 3 hours, using heptakis(2,6-di-O-methyl)-β-CD as an initiator. [a] % Conv. determined by gravimetric analysis. [b] $M_{n,th}$ = [M](per arm) × 7(Initiating Groups) × MW(Lactide) × (% conv.) + MW(core) [c] Determined by GPC using refractive index coupled with light scattering detectors. [d] M_n from ^1H NMR spectroscopy. [e] Calculated from the Szymanski method.

The polymers were analyzed using ^1H NMR spectroscopy and GPC analysis. Characteristic resonances in the ^1H NMR spectra were located at δ 3.63 and 3.39 ppm, corresponding to the methoxy groups of the cyclodextrin core located on the 2′ and 6′ carbons, as shown in Figure 3.2. The integration of these signals with respect to the methyl and methine protons of the PLA chains allowed for calculation of the molecular weights and yield information about the PLA arms of the star.

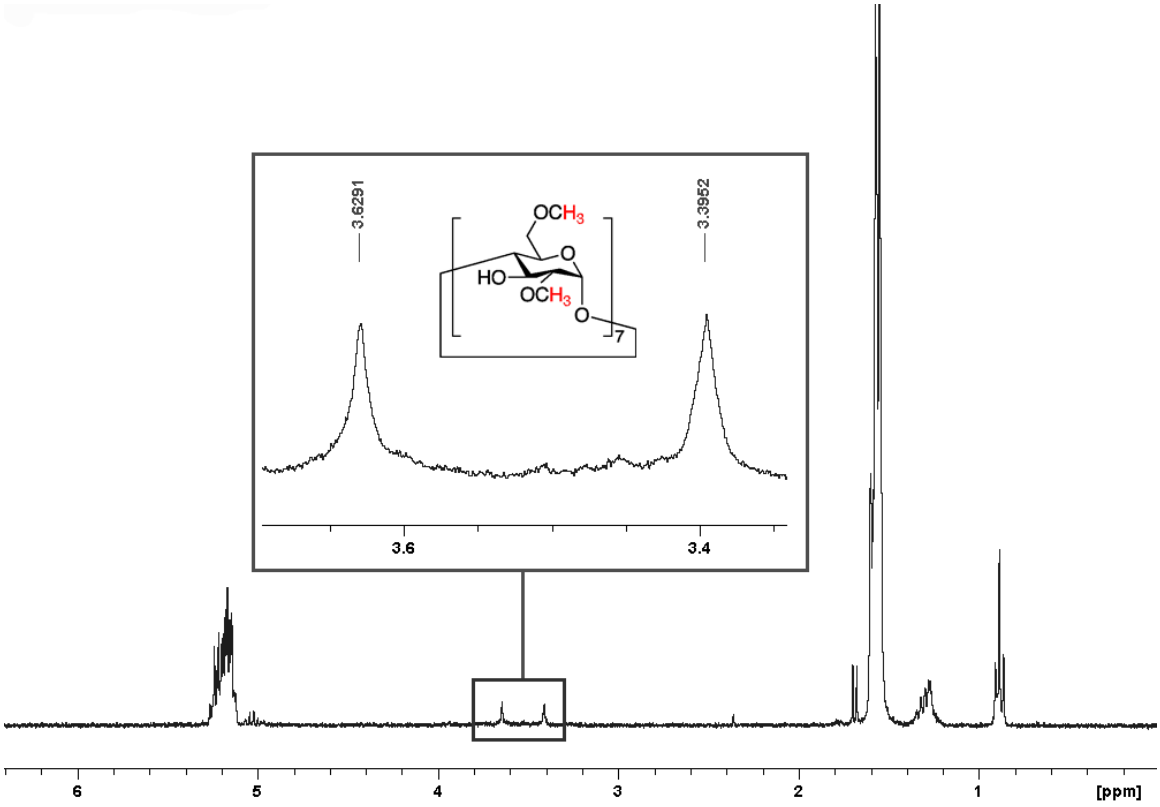

Figure 3.2. OCH_3 diagnostic resonances for CD polymer stars.

Monomer conversion was determined gravimetrically and the theoretical molecular weights ($M_{n,th}$) were determined from monomer conversion. Molecular weights obtained from GPC were significantly higher than the $M_{n,th}$ values for all entries. Molecular weights were also determined by ^1H NMR and showed significant deviation from the theoretical molecular weights. This indicated that the polymerizations were not proceeding in the desired controlled fashion and molecular weights were likely affected by the absence of uniform arm length on individual stars and inefficient initiation of the hydroxyl groups on the core. This was also confirmed by the broad molecular weight distributions obtained which, although monomodal, gave PDIs >1.25. The PDI of the arms (PDI_{arm}) was calculated using the Szymanski method as shown in Equation 4 and is often used in the analysis of dendritic and hyperbranched polymers, with this measure of

arm uniformity recognized as being broader than traditional PDI values. *Rac*-PLA stars from **1** show PDI_{arm} values of < 4, indicating moderate levels of control over distribution of arm lengths, as values less than four are typically considered controlled.[141]

$$PDI_{star} = 1 + \left(\frac{PDI_{arm} - 1}{f}\right) \times \left(\frac{M_{nstar} - M_{core}}{M_{nstar}}\right)^2$$

Equation 4. Formula for PDI of polymer star arm (PDI_{arm}) from PDI of star (PDI_{star}), number of arms (f), molecular weight of star (M_n, star) and molar mass of core (M_{core}).

Similar trends were observed when the modified CD core was used to initiate L-lactide as shown in Table 3.2. A better agreement between the experimental and theoretical molecular weight is observed from these isotactic derivatives, (Table 3.2**)** indicating better molecular weight control, however larger deviations for 280 and 350 monomer eq. are noted for these high M_n derivatives, potentially due to the insolubility of these crystalline polymers in organic media.[142] Molecular weights obtained from GPC show that as the monomer ratio is increased the molecular weights do not increase in the expected linear fashion. One explanation for this is the low solubility of these highly crystalline isotactic polymer stars in THF, which could result in only lower molecular weight fractions being analyzed by GPC as a result of incomplete dissolution. As the length of the arms increase, the crystallinity may also increases and thus the polymers become more insoluble. Molecular weights obtained by GPC for 280 and 350 monomer eq. could be attributed to a small fraction of low molecular weight polymer that does dissolve in THF and is not representative of the bulk sample. In an attempt to overcome this insolubility, the polymer was stirred in THF for 24 hours, however no significant changes in molecular weight and PDI were observed after filtering and analyzing by GPC.

In contrast, molecular weights obtained by ^{1}H NMR spectroscopy showed a linear increase in molecular weights as monomer concentration was increased and a better correlation of theoretical molecular weights with experimental values at higher molecular weights due to the higher solubility of these polymers in $CDCl_3$ when compared to THF. Regardless of initiator, reaction conditions or characterization technique, $Sn(Oct)_2$, **1**, offered poor control over the synthesis of β-CD polymer stars.

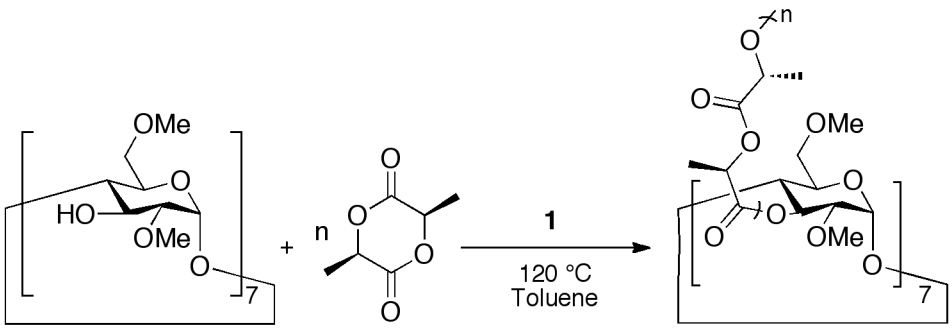

Scheme 3.2. CD poly(lactic acid) polymer stars based on L-lactide and $Sn(Oct)_2$ (**1**).

Table 3.2. Polymerization data for CD poly(lactic acid) polymer stars based on L-lactide and $Sn(Oct)_2$ (**1**).

[M]:[C]:[I]	% Conv.[a]	$M_{n,th}$[b]	$M_{n,\ GPC}$[c]	$M_{n,\ NMR}$[d]	PDI[c]	PDI_{arm}[e]
70:0.5:1	50	7082	19630	13883	1.27	3.31
140:0.5:1	60	13438	19270	25127	1.29	3.34
210:0.5:1	64	20702	14900	34880	1.41	4.46
280:0.5:1	68	28774	16080	41760	1.40	4.33
350:0.5:1	80	41688	16130	44676	1.31	3.59

Polymerizations were conducted in 2 mL of toluene with 0.01 mmol of $Sn(Oct)_2$ at 120 °C for 3 hours, using heptakis(2,6-di-O-methyl)-β-CD as an initiator. [a] % Conv. determined by gravimetric analysis. [b] $M_{n,th}$ = [M](per arm) × 7(Initiating Groups) × MW(Lactide) × (% conv.) + MW(core) [c] Determined by GPC using refractive index coupled with light scattering detectors. [d] M_n from ^{1}H NMR spectroscopy. [e] Calculated from the Szymanski method.

Due to the disappointing control observed with **1**, catalyst **2** was investigated. Polymerizations were performed under the optimized conditions of 120 °C in toluene for

3 hours, however, only *rac*-lactide was used as Al-salen systems induce isospecificity to form crystalline PLAs from the racemic mixture of lactides, while still providing excellent control over the molecular weights and PDIs.[143] Results obtained from **2** are summarized in Table 3.3. Although significant deviations between theoretical molecular weight and M_n values obtained from both GPC and ^{1}H NMR spectroscopy are still observed, control over the polymerization is excellent with PDIs of <1.15 and PDI_{arm} values <1.60, as well as the expected linear increase in the M_n values with increased monomer:initiator ratios. The deviations in molecular weights, especially in light of the experimental levels of control, are suggestive of inaccuracies in the determination of conversions, with loss of material upon workup. This problem would be somewhat alleviated for higher molecular weight polymer due to easier isolation of the bulk material. Another possibility is that not all CD cores are initiating possibly due to solubility of the core in organic media. Once activated, the core becomes much more soluble and polymer chains propagate, therefore any uninitiated cores result in lower conversions and higher molecular weight deviations would be observed.

Table 3.3. Polymerization data for CD poly(lactic acid) polymer stars based on *rac*-lactide and ^{tBu}[salen]AlMe (**2**).

[M]:[C]:[I]	% Conv.[a]	$M_{n,th}$[b]	$M_{n,\ GPC}$[c]	$M_{n,\ NMR}$[d]	PDI[d]	PDI_{arm}[e]
70:1:1	62	7081	24490	13883	1.06	1.47
140:1:1	59	12691	28890	25127	1.07	1.53
210:1:1	59	18643	53340	34880	1.15	1.51
280:1:1	69	32933	55470	41760	1.07	1.53
350:1:1	65	35208	76600	44676	1.06	1.44

Polymerizations were conducted in 2 mL of toluene with 0.02 mmol of ^{tBu}[salen]AlMe at 120 °C for 3 hours, using heptakis(2,6-di-O-methyl)-β-CD as an initiator. [a] % Conv. determined by gravimetric analysis. [b] $M_{n,th}$ = [M](per arm) ×

7(Initiating Groups) × MW(Lactide) × (% conv.) + MW(core) [c] Determined by GPC using refractive index coupled with light scattering detectors. [d] M_n from ^{1}H NMR spectroscopy. [e] Calculated from the Szymanski method.

The promising results obtained with **2** and lactide led us to expand our scope by synthesizing new biodegradable polymer stars with PHB and PLGA arms (Table 3.4). Conditions used were similar to the ones optimized for lactide with reactions proceeding for 3 hours at 120 °C in toluene. The PHB stars displayed excellent control with PDIs as low as 1.01 and PDI_{arm} values <2.70, representing the best control over PHB stars thus far reported in the literature. Synthesis of larger stars with 280 and 350 monomer equivalents were attempted, however no product could be isolated due to insufficient initiation of the CD core or catalyst death, even after different timeframes of 3, 6 and 24 hours. Percent conversions for the synthesized stars were also very high, with >90 % monomer conversion determined by ^{1}H NMR spectroscopy after 3 hours. Likewise, a library of PLGA stars were synthesized using a 1:1 ratio of *rac*-lactide and glycolide with **2** at 120 °C in toluene for 3 hours. These copolymer stars displayed moderate levels of control for PLGA, with PDIs <1.31 and PDI_{arm} values <3.70. Correlation between molecular weights from GPC and ^{1}H NMR spectroscopy was also observed to be good**,** although at 350 monomer eq. a greater deviation was observed possibly due to increased crystallinity affecting the polymer solubility. Molecular weights obtained from ^{1}H NMR spectroscopy however, showed good correlation for this star, indicating that poor solubility in THF likely affected the molecular weight obtained from GPC. Percent conversions, which were determined by gravimetric analysis, were moderate to high. The synthesis of these stars highlights the versatility of both CD cores and aluminum salen complexes to initiate polymer and copolymer synthesis.

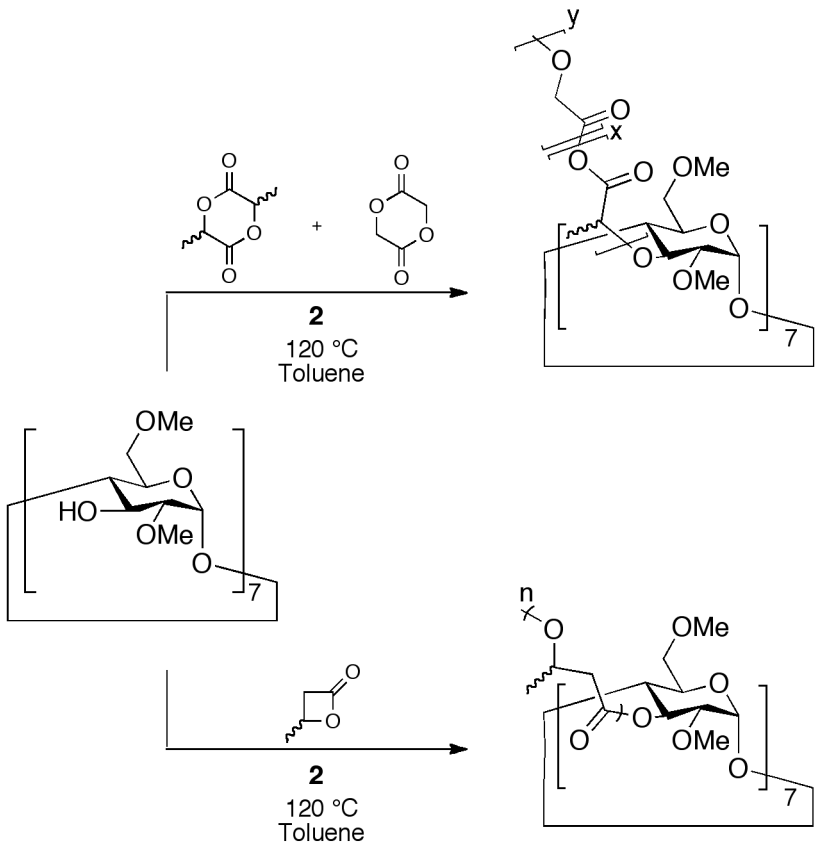

Scheme 3.3. PHB and PLGA polymer star synthesis using ^{tBu}[salen]AlMe (**2**).

Table 3.4. Polymerization data for CD poly(3-hydroxybutyrate) and poly(lactic-*co*-glycolic acid) polymer stars based on ^{tBu}[salen]AlMe (**2**).

Polymer	[M]:[C]:[I]	% Conv. [a]	$M_{n,th}$ [b]	$M_{n,\ GPC}$ [c]	$M_{n,\ NMR}$ [d]	PDI [c]	PDI_{arm} [e]
PHB	70:1:1	98	7211	15310	12126	1.19	2.60
PHB	140:1:1	96	12902	29440	22984	1.09	1.69
PHB	210:1:1	94	19410	28710	24896	1.01	1.07
PLGA	70:1:1	68	7096	10760	8320	1.17	2.55
PLGA	140:1:1	81	15827	18750	21060	1.31	3.51
PLGA	210:1:1	41	19410	18360	20269	1.30	3.44
PLGA	280:1:1	45	16987	21760	26487	1.18	2.43
PLGA	350:1:1	69	31411	24530	28999	1.16	2.25

Polymerizations were conducted in 2 mL of toluene with 0.02 mmol of ^{tBu}[salen]AlMe at 120 °C for 3 hours, using heptakis(2,6-di-O-methyl)-β-CD as an initiator. [a] % Conv. determined by gravimetric analysis. [b] $M_{n,th}$ = [M](per arm) × 7(Initiating Groups) × MW(Monomer) × (% conv.) + MW(core) [c] Determined by GPC using refractive index coupled with light scattering detectors. [d] M_n from ^{1}H NMR spectroscopy. [e] Calculated from the Szymanski method.

3.3 Thermal Analysis of Polymer Stars

Thermal transitions of the polymer stars were analyzed by differential scanning calorimetry (DSC) and thermogravimetric analysis (TGA). The glass-transition temperatures (T_g) as well as the melting temperatures (T_m) where applicable, were obtained for these stars. As expected, the thermal transitions for the polymer stars were lower than those of the linear analogues of *rac*-PLA, L-PLA, PHB and PLGA.[144,145,146,147] Interestingly, there was no trend observed between the thermal transitions as the molecular weight increased of the PLA stars synthesized with **1**. This could be explained by inefficient initiation of the hydroxyl groups or varying arm lengths that change the overall molecular weight. Generally, T_g values of *rac*-PLA stars synthesized using **1** were lower than stars synthesized using L-LA due to the absence of crystallinity. T_g values for *rac*-PLA stars ranged from 42-53 °C, whereas, the T_g values of L-PLA stars ranged from 50-59 °C. T_m values of the L-PLA stars were similar, ranging from 166-169 °C. In addition, the melting enthalpies, ΔH_m, for the L-PLA stars were obtained from instrumental analysis and ranged from 39-48 J/g indicating very small differences in crystallinity as the size of the polymer star increased.

Table 3.5. DSC and TGA thermal transitions observed for PLA polymer stars synthesized using **1**.[a,b]

Ratio	Polymer	T_g (°C)	T_m (°C)	ΔH_m (J/g)	Onset (°C)	50% (°C)	T_{max} (°C)
70:0.5:1	*rac*-PLA	53	-	-	217	261	286
140:0.5:1	*rac*-PLA	48	-	-	229	268	292
210:0.5:1	*rac*-PLA	42	-	-	221	251	275
280:0.5:1	*rac*-PLA	53	-	-	261	285	304
350:0.5:1	*rac*-PLA	54	-	-	267	292	310
70:0.5:1	L-PLA	57	166	48	262	300	336
140:0.5:1	L-PLA	57	169	39	248	275	287
210:0.5:1	L-PLA	50	168	38	218	253	275
280:0.5:1	L-PLA	50	168	39	236	270	295
350:0.5:1	L-PLA	59	169	43	254	324	370

[a] DSC purge flow 50 mL/min N_2, heating/cooling rate 5 °C/min, heat (200 °C)/cool (0 °C) cycle employed.[b] TGA heating rate of 10 °C/min.

The thermal transitions for PLA stars synthesized with **2** are summarized in Table 3.6. T_m values were of particular interest as the increase of the molecular weight of the polymer stars results in a less defined T_m to the point where it couldn't be defined on 40 and 50 monomer arm length stars (Figure 3.3). This may be explained by the increase in stereoerrors as the length of the polymer chains increase and the concentration of the catalyst decreases giving poorer strereocontrol. As the stereoerrors increase, there will be less isotactic character present in the polymer, thus making the T_m less defined.[140] By comparing T_m values in Table 3.6, namely, the isospecific *rac*-PLA stars synthesized with **2**, to the purely isotactic L-PLA stars synthesized with **1** (Table 3.5), it can be observed the T_m of the purely L-PLA is clearly defined in comparison to the imposed tacticity of **2**.

Similarly, very little discrepancy in T_g values is observed between purely *rac*-PLA stars from **1** and isospecific PLA stars from **2**, indicating that **2** did not impose a high degree of tacticity control, which would result in errors in the polymer chain. In addition, the ΔH_m values of the isospecific stars from **2** were significantly lower than those of the purely isotactic ones from **1**, indicating less crystallinity.

Table 3.6. DSC and TGA thermal transitions observed for PLA polymer stars synthesized using **2**.[a,b]

Ratio	Polymer	T_g (°C)	T_m (°C)	ΔH_m (J/g)	Onset (°C)	50% (°C)	T_{max} (°C)
70:1:1	*rac*-PLA	52	165	9	299	341	376
140:1:1	*rac*-PLA	43	163	10	314	342	374
210:1:1	*rac*-PLA	43	160	1	297	335	371
280:1:1	*rac*-PLA	49	-	-	304	347	372
350:1:1	*rac*-PLA	47	-	-	317	352	378

[a] DSC purge flow 50 mL/min N_2, heating/cooling rate 5 °C/min, heat (200 °C)/cool (0 °C) cycle employed.[b] TGA heating rate of 10 °C/min.

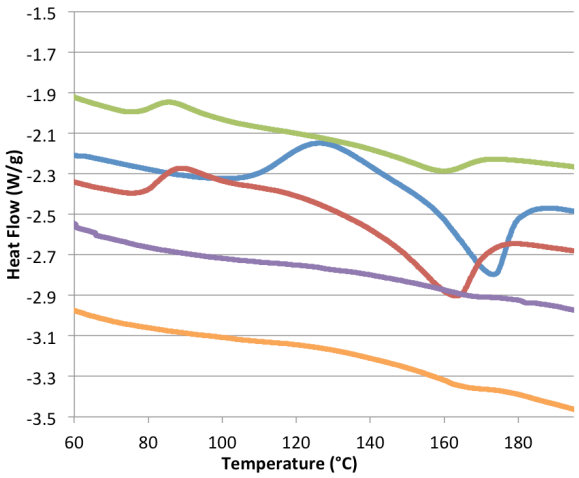

Figure 3.3. DSC overlay of T_m region for CD-PLA stars synthesized from using *rac*-lactide using **2.** Polymer star arm lengths: Blue = 10, red = 20, green = 30, purple = 40, orange = 50.

Aside from the thermal transitions, the decomposition properties of the polymer stars were investigated by thermogravimetric analysis. Generally, it would be expected that the purely atactic stars in Table 3.5 would have the lowest maximum decomposition temperature (T_{max}) due to the absence of stereoblock complex formation. However, the purely isotactic stars did not display T_{max} values that were significantly higher, and some isotactic entries were observed to have a lower T_{max} than that of their atactic counterpart. It is believed that the variation of T_{max} values between these sets of entries is associated with the lack of control observed in the formation of these polymers, where the absence of uniform molecular weight distributions is offsetting any expected trends in decomposition temperatures. This can be confirmed by the comparison of PLA stars synthesized from **2** where stereochemistry was imposed and much better control was obtained. Decomposition temperatures in Table 3.6 display consistent values throughout, with higher T_{max} values correlating with the formation of stereoblock complexes when compared to purely atactic stars.

PHB and PLGA polymer stars were also analyzed by DSC and TGA (Table 3.7). All PHB stars exhibited very similar thermal transitions with T_g values of -19 °C as well as very similar decomposition temperatures. PLGA polymer stars displayed T_g values ranging from 42-53 °C, in addition to T_m values ranging from 202-210 °C. In comparison to PLA stars synthesized from **2**, the PLGA stars did not exhibit the same trend of less defined T_m values as the star size increased. This may be explained by the crystalline characteristics obtained from PGA segments in the copolymer chain. The ΔH_m values for PLGA stars ranged from 3-22 J/g, which were generally higher than those of PLA synthesized by **2** (1-10 J/g) indicating that PLGA stars have higher crystallinity.

Table 3.7. DSC and TGA thermal transitions observed for PHB and PLGA polymer stars synthesized using **2**.[a,b]

Ratio	Polymer	T_g (°C)	T_m (°C)	ΔH_m (J/g)	Onset (°C)	50% (°C)	T_{max} (°C)
70:1:1	PHB	-19	-		283	303	318
140:1:1	PHB	-19	-		280	302	317
210:1:1	PHB	-19	-		282	305	319
70:1:1	PLGA	43	203	12	271	316	344
140:1:1	PLGA	54	210	16	294	330	374
210:1:1	PLGA	43	207	22	295	349	390
280:1:1	PLGA	43	205	10	306	360	393
350:1:1	PLGA	42	202	3	302	353	329

[a] DSC purge flow 50 mL/min N_2, heating/cooling rate 5 °C/min, heat (200 °C)/cool (0 °C) cycle employed.[b] TGA heating rate of 10 °C/min.

3.4 Polymer Star Degradation

In order to test the controlled release characteristics of these novel polymer stars, 7-methoxycoumarin required embedding into the polymer network. The polymer star with 210 eq. of lactide (~30 monomer units per arm) was chosen to test degradations due to its low PDI value. In order to embed 7-MC into the polymer network, the polymer was dissolved in CH_2Cl_2 and100 equivalents of 7-MC was added to the solution. The solution was then refluxed for 24 hours and the polymer was precipitated and washed with MeOH until a constant correlation between 7-MC and CD was obtained by ^{1}H NMR spectroscopy, confirming the removal of any surface 7-MC. The polymer was dried *in vacuo* prior to degradation. In addition to ^{1}H NMR spectroscopy, the polymer was analyzed using fluorescence spectroscopy. The polymer was dissolved in dichloromethane and then cast onto a glass plate (Figure 3.4). Fluorescence was

measured using front face emission and the presence of a fluorescence peak located at 385 nm, which corresponds to 7-MC, was indicative that the fluorophore was included in the polymer network.

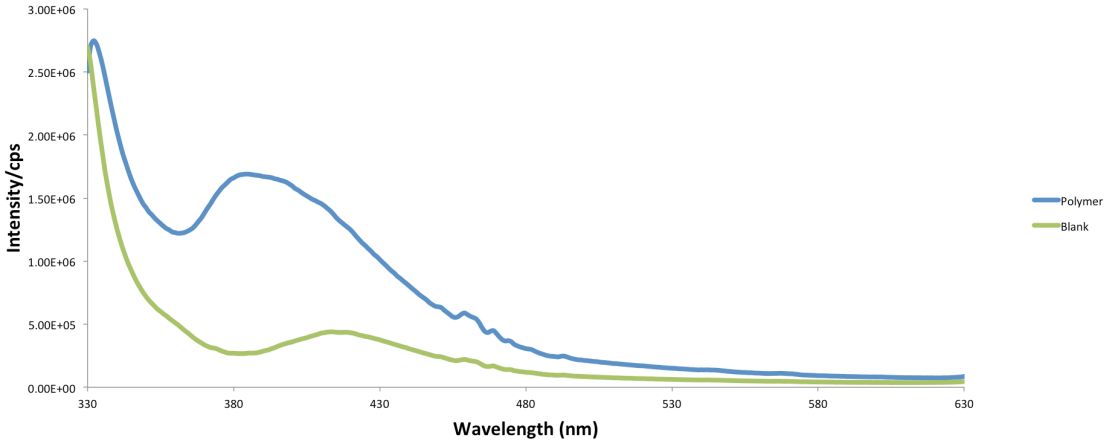

Figure 3.4. Polymer star with 7-MC included dry-cast.

For initial trials, PLA pellets were formed using a manual press and were degraded in vials containing either a 1:1 mixture of nano-pure H_2O and MeOH or nano-pure H_2O.[148] It is important to note that these degradations were carried out in the absence of acid or base, as we discovered that 7-MC is quenched in strongly alkaline or acidic environments, therefore rendering fluorescence measurements unfeasible. This is shown in Figure 3.5 with the quenching of 7-MC fluorescence in the presence of KOH over a period of 10 minutes. Similar trends were observed with the use of NaOH and 1,5,7-triaza-bicyclo[4.4.0]dec-5-ene (TBD), as well as acids such as HCl and CH_3COOH.

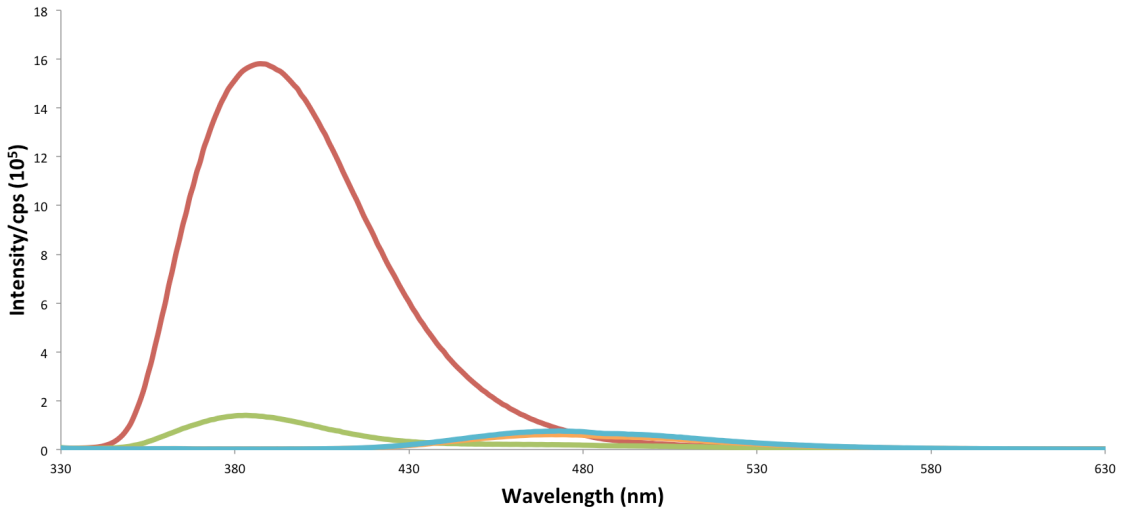

Figure 3.5. Fluorescence quenching of 7MC in the presence of KOH. Blue = Stock 7-MC solution, Green = 7-MC + KOH 0 min, Blue = 7-MC + KOH 5 min, Orange = KOH + 7-MC 10 min.

In order to measure the fluorescence, standard stock solutions of 7MC were prepared using H_2O/MeOH and H_2O of 1.5×10^{-5} and 3.0×10^{-5} M solutions respectively, to provide a fixed 7-MC concentration reference for the fluorescence intensity. Degradations were observed to proceed at a slow rate without catalysis. Aliquots of the solution in which the pellets were degrading were tested periodically over the course of 135 days in order to observe 7-MC release. The fluorescence intensity of the pellet solution increased over time and the ratio between the pellet solution and the stock solution was compared after each run using Equation 5:

$$\frac{F}{F_o} = \frac{\int I_F\, dv, HG - \int I_F\, dv, Blank}{\int I_F\, dv, G - \int I_F\, dv, Blank}$$

Equation 5. Equation for obtaining F/F_o values from fluorescence spectra.

F/F_o is the ratio between the pellet containing solution and the standard stock solution of 7-MC. By taking the integration of both signals and then dividing the area of

the signal of the pellet solution, HG, with the blank subtracted by the area of the signal of the stock solution, G, with the blank subtracted, the F/F_o value can obtained. The F/F_o values were plotted with respect to time as shown in Figures 3.6 and 3.7.

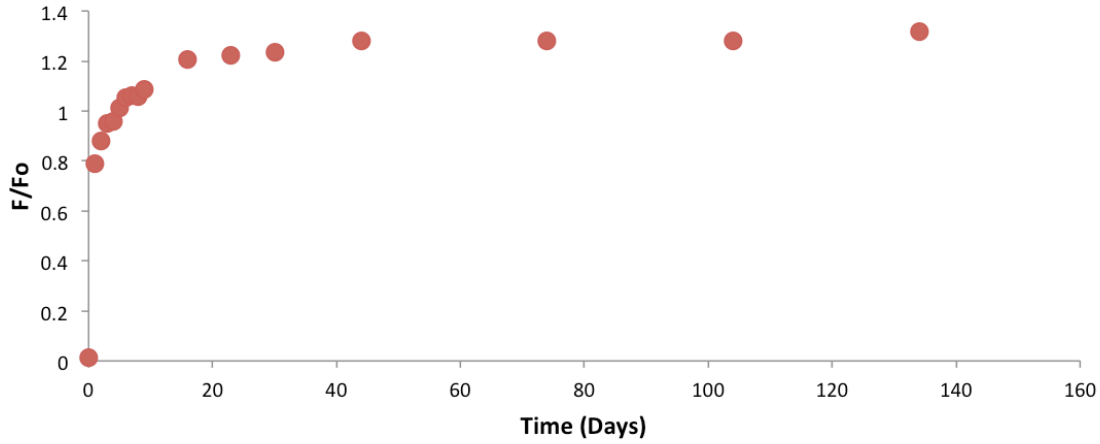

Figure 3.6. Degradation of PLA pellet in 1:1 mixture of H_2O and MeOH.

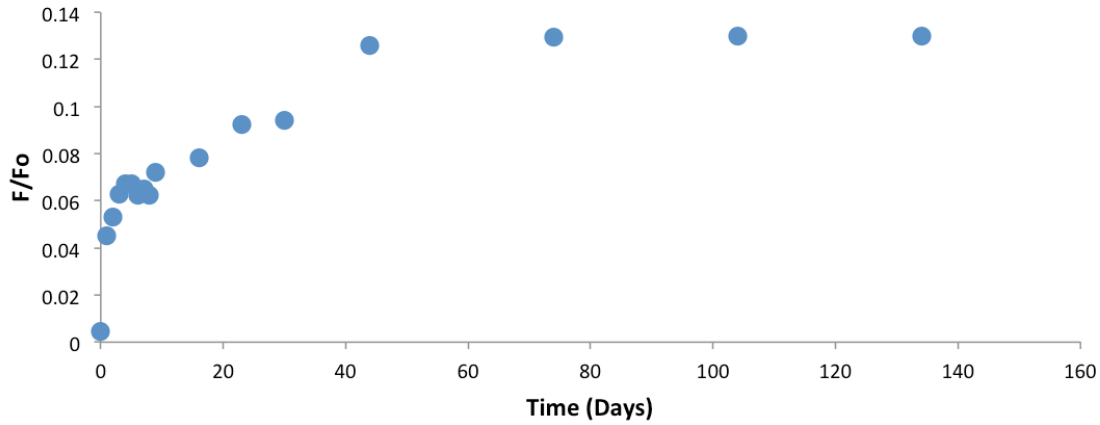

Figure 3.7. Degradation of PLA pellet in H_2O.

No fluorescence is observed immediately after the pellet was immersed in solution. However after one day there is an initial burst in fluorescence intensity due to leeching of the 7-MC into solution as the alcohol terminus of the polymer chains are soluble in in solution. It is after this burst that the controlled release is observed, with a

steady increase in the fluorescence intensity as the solution becomes more concentrated. As expected, the PLA in H_2O/MeOH degrades significantly faster than the PLA in H_2O, due to increased alkalinity provided by MeOH. By normalizing the plots by the F/F_o value in which they plateau it is possible to observe the increased degradation rate in the more alkaline environment (Figure 3.8).

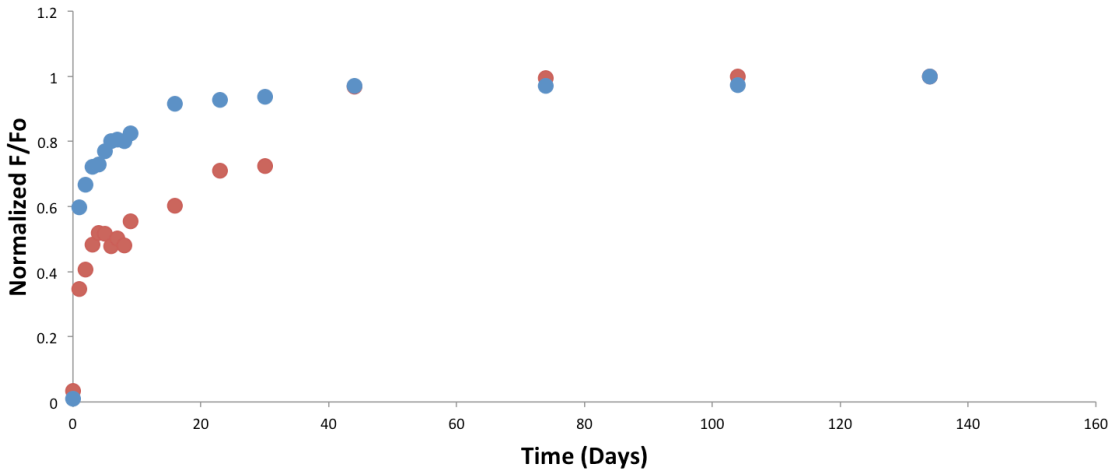

Figure 3.8. Normalized F/F_o plot for degradation in H_2O/MeOH (blue) and pure H_2O (red).

Although controlled release of fluorescence was demonstrated by these measurements, complete degradation of these PLA pellets was not demonstrated due to the extensive degradation timeframe. We wished to accelerate the degradation process and turned to enzymatic degradation by using the enzyme proteinase K. Proteinase K is a protease secreted by the fungus *Trirachium album* and has been reported to enzymatically degrade PLA.[149] The degradation of PLA using proteinase K is shown in Figure 3.9.

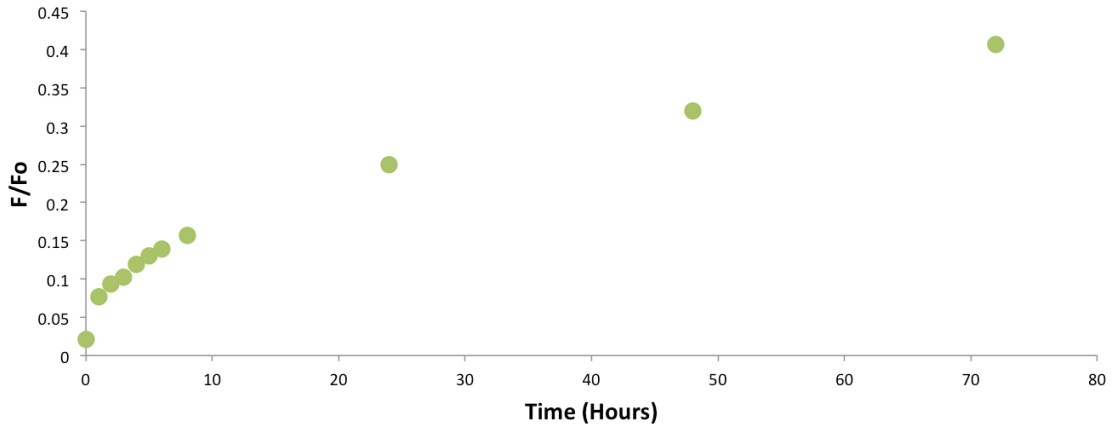

Figure 3.9. Degradation of PLA pellet in H_2O/MeOH with proteinase K.

In order to observe the accelerated release profile, an identical experiment was performed without the use of proteinase K. As expected, in the absence of proteinase K, a much slower degradation and release was observed with the increase of the F/F_o after the burst release compared to the catalyzed degradation. This provided strong indication that the enzyme had a significant effect on the release profile of the material. By normalizing the F/F_o after the initial burst release it was possible to observe the increased rate of 7-MC release with proteinase K (Figure 3.10). Degradation of the pellets did not reach completion, as significant portions of the pellet still remained long after fluorescence measurements were taken. This was an indication that the enzyme degradation was still too slow for complete degradation to occur. However, accelerated degradation in the presence of the enzyme indicates that fine tuning of the materials to specific degradation times such as the variation in arm length could lead to full degradation in the presence of enzymatic activity.

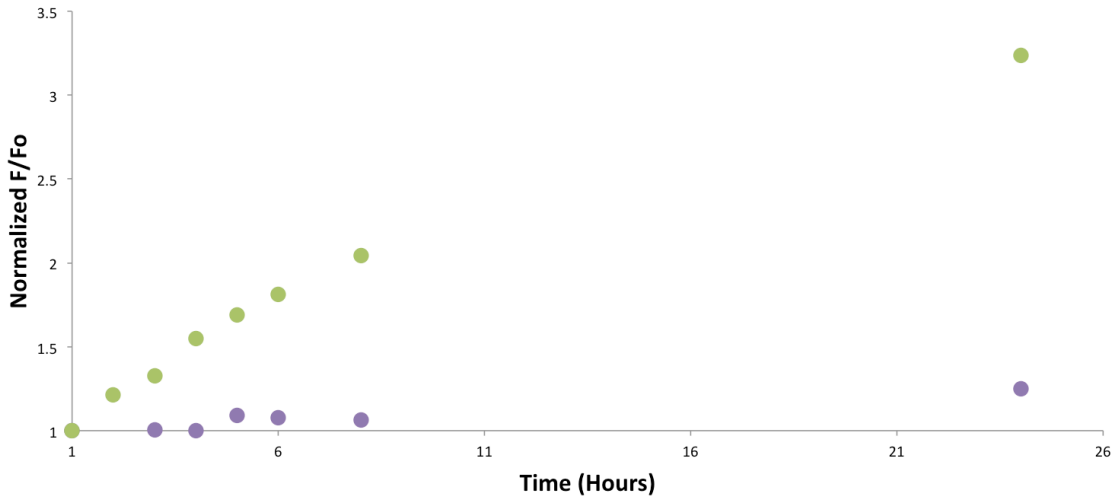

Figure 3.10. Normalized F/F_o plot for degradation in with proteinase K (green) and without (purple).

The PHB stars were not analyzed for degradation as their thermoplastic properties make them unfeasible for embedding and pellet pressing. PLGA degradation in the presence of proteinase K was however performed using polymer stars synthesized using 210 eq. of monomer (Figure 3.11). As expected, the PLGA pellets degraded faster than the PLA pellets due to the higher accessibility of ester linkages in the PLGA polymer chains.[150] The trend of controlled release was identical to that observed with the other degradations, except with a significantly larger rate of 7-MC release such that F/F_o increased from 0.06 to 0.90 over the period of 8 hours.

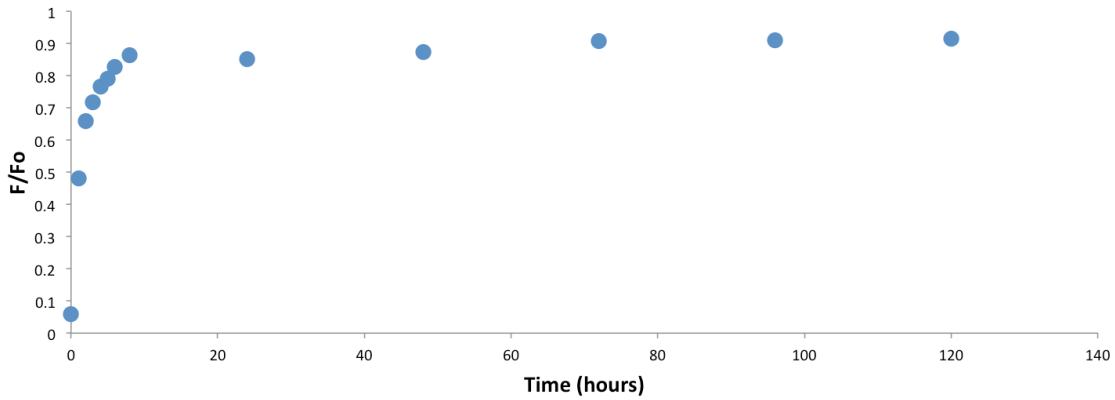

Figure 3.11. Degradation of PLGA pellet in H_2O/MeOH with proteinase K.

Controlled release by periodic monitoring of pellet degradations demonstrated that these materials could be used for controlled release and that the same trends of release could be expected upon embedding of bioactive molecules into the polymer network. The core-first technique provided a method to synthesize a library of diverse polymer stars with varying molecular weights and excellent PDI values. However molecular weight correlation was poor possibly due inaccurate conversions or poor solubility of the core resulting in inefficient initiation. In an attempt to advance the properties of these materials and fine-tune them further by having better correlation of molecular weights and PDI values, an arm-first method was proposed where acetylene terminated polymer arms could be "clicked" onto an azide-modified cyclodextrin using copper-catalyzed azide-alkyne cycloaddition (CuAAC).

Chapter Four

4 Arm-First Polymer Stars: Synthesis and Degradation Studies

4.1 Synthesis of Polymer Stars based on Heptakis-Azido-β-CD.

A prerequisite of arm-first synthesis is the requirement for the azide functionalization of a parent β-CD. The symmetric derivatization of β-CD was originally reported by Defaye and Gadelle[151] and allowed the selective replacement of all primary hydroxyl groups in the 6′ position with iodine atoms. Thus, freshly dried β-CD was treated with I_2 and PPh_3 in DMF at 70 °C for 24 hours under an inert nitrogen atmosphere (Scheme 4.1). The reaction was partially concentrated under reduced pressure and placed in an ice bath in order to aid precipitation of the intermediate. A 3.218 M solution of sodium methoxide was then added drop wise to the solution, changing the color of the solution from a dark brown to a deep red, with concomitant formation of a white

precipitate. The solution was left to stir for 1 hour and then precipitated into methanol to yield a yellow solid, which was filtered and dried *in vacuo*. To purify the iodo derivative, the CD was placed in a Soxhlet extractor and refluxed with methanol for 24 hours. After, the purified product was collected and dried. The overall yield isolated was 50%. The iodo derivative was then analyzed by ^{1}H NMR spectroscopy with the observed resonances in accordance to those reported in the literature.[152]

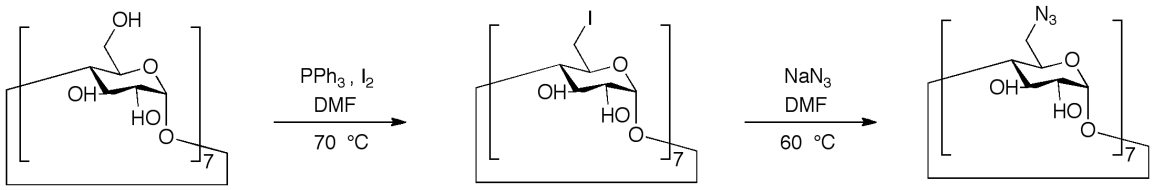

Scheme 4.1. Synthesis of the β-CD-$(N_3)_7$.

Preparation of β-CD-$(N_3)_7$ was successfully achieved by the addition of 7 eq. of NaN_3 to β-CD-$(I)_7$ in DMF in order to replace the iodine atoms with azide groups. The solution was stirred for 24 hours at 60 °C under an inert nitrogen atmosphere. The solution was cooled to room temperature and DI water was then added to the solution, which immediately turned white with the formation of azide product. The product was then filtered, dried, and analyzed by ^{1}H NMR spectroscopy. It was difficult to compare the ^{1}H NMR of the β-CD-$(N_3)_7$ to that of the β-CD-$(I)_7$, as there were no new protons in the structure. However, shifting of the methylene resonances for the protons in close proximity to the 6′ position in the region of 3.2-3.8 ppm was indicative that the 6′ group had changed from iodine to an azide. The ^{1}H NMR spectroscopic resonances of the heptakis azide product also showed good correlation with those reported in the literature.[152]

An alternative method to confirm the presence of azide functionalization of the β-CD is infrared (IR) spectroscopy. Powder samples were run of both the β-CD-$(I)_7$ and β-CD-$(N_3)_7$. It was found that both IR spectra were similar except for the presence of a large azide stretch located at 2100 cm^{-1} (Figure 4.1) for the β-CD-$(N_3)_7$. This indicated that an azide group was present on the final product and an azide-modified β-CD had successfully been synthesized. It is also important to note that while the CH_2-I stretch would be located around 650 cm^{-1}, it was difficult to assign stretches due to the presence of many different signals, making the stretch unclear.

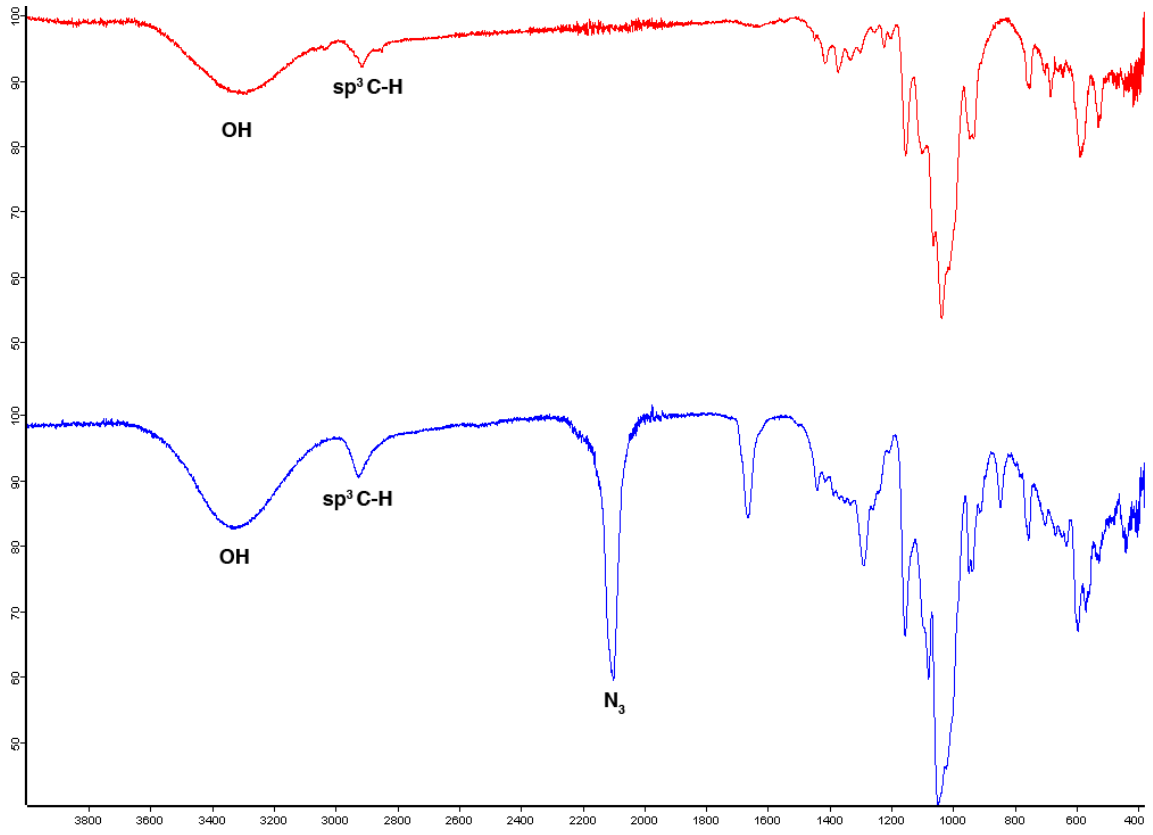

Figure 4.1. IR spectra of β-CD-$(I)_7$ (red) and β-CD-$(N_3)_7$ (blue).

4.2 Synthesis of Acetylene-Terminated Linear Polymers.

In addition to the azide-modified CD, the second component required for CuAAC click reactions were the acetylene terminated linear polymers. Most acetylene-functionalized polymers in the literature are prepared using an end-group functionalization method[153] or via the use of protected acetylenes.[154] Fréchet *et al.* reported dendronized linear polymers prepared from dendritic azides and poly(vinylacetylene) using click chemistry, with poly(vinylacetylene) prepared through 4-TMS-1-buten-3-yne from a Sonogashira reaction.[153] Opsteen reported the synthesis of polymeric building blocks containing terminal azide and alkyne functionalities prepared via ATRP and used them to synthesize block copolymers via a 1,3-dipolar cycloadditon reactions.[154]

Schubert *et al.* reported an elegant ROP method to synthesize acetylene terminated PCL, utilizing the unprotected 5-hexyn-1-ol as an initiator and $Sn(Oct)_2$ as a catalyst. Moderate levels of control over molecular weight and PDI values of 1.16 were obtained. With the success that Schubert achieved, it was proposed that this project should utilize 5-hexyn-1-ol as an initiator for the ROP of lactones including *rac*-lactide, L-lactide, βBL, glycolide and ε-caprolactone, to provide a library of linear polymers for click chemistry reactions.

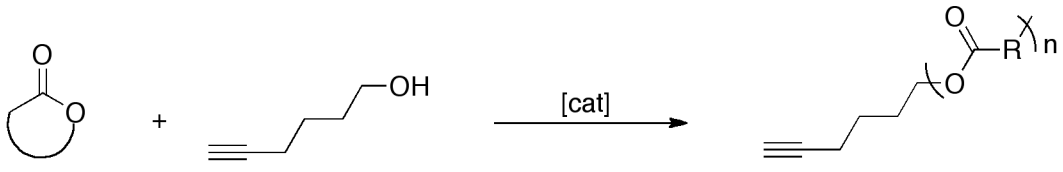

Scheme 4.2. Synthesis of acetylene terminated linear polymers.

The first attempted syntheses of acetylene-terminated polymers were carried out using *rac*-lactide (Table 4.1). Initially, reactions were performed in toluene using a 30:1 ratio of monomer:initiator at 120 °C using $Sn(Oct)_2$ (**1**) as a catalyst. It was found that high % conversions could be reached (98%), however very poor levels of control were observed at timeframes ranging from 1-48 hours. High PDI values (1.34-1.71) were indicative of inefficient initiation or the presence of intramolecular transesterification. Bulk reactions also gave high conversions, however, control was still poor, with PDI values upwards of 1.54. In an attempt to improve the control, ^{tBu}[salen]AlMe (**2**) was used at 120 °C and gave a PDI of 1.20 which was a vast improvement (Table 4.2).

Table 4.1. Polymer data for acetylene terminated *rac*-PLA from $Sn(Oct)_2$ (**1**).

[M] : [C] : [I]	Temp (°C)	Time (hours)	% Conv.[a]	$M_{n,th}$[b]	$M_{n,\ GPC}$[c]	PDI[c]
30 : 0.5 : 1	120	1	98	4249	2663	1.35
30 : 0.5 : 1	120	3	98	2692	2730	1.51
30 : 0.5 : 1	120	6	98	3254	1979	1.44
30 : 0.5 : 1	120	24	98	4206	2477	1.71
30 : 0.5 : 1	120	48	98	3557	3723	1.34
10 : 0.5 : 1	70	3	>99	833	793	1.11
20 : 0.5 : 1	70	3	>99	2635	1349	1.10
30 : 0.5 : 1	70	3	99	2433	1654	1.10
40 : 0.5 : 1	70	3	98	5748	3048	1.13
50 : 0.5 : 1	70	3	98	7161	3609	1.14

Polymerizations were conducted in 2 mL of toluene with 0.06 mmol of $Sn(Oct)_2$ at 70 °C, using 5-hexyn-1-ol as an initiator. [a] % Conv. determined by ^{1}H NMR spectroscopy. [b] $M_{n,th}$ = [M] × MW(Lactide) × (% conv.) + MW(5-hexyn-1-ol) [c] Determined by GPC using refractive index coupled with light scattering detectors.

Table 4.2. Polymer data for acetylene terminated *rac*-PLA from ^{tBu}[salen]AlMe (**2**).

[M] : [C] : [I]	Temp (°C)	Time (hours)	% Conv.[a]	$M_{n,th}$[b]	$M_{n,\ GPC}$[c]	PDI[c]
30 : 0.5 : 1	120	3	95	4122	2738	1.20

Polymerization was conducted in 2 mL of toluene with 0.12 mmol of ^{tBu}[salen]AlMe at 120 °C, using 5-hexyn-1-ol as an initiator. [a] % Conv. determined by ^{1}H NMR spectroscopy. [b] $M_{n,th}$ = [M] × MW(Lactide) × (% conv.) + MW(5-hexyn-1-ol) [c] Determined by GPC using refractive index coupled with light scattering detectors.

Different reaction conditions were then adopted by lowering the temperature to 70 °C and using **1**, which resulted in far superior levels of control, with PDI values ranging from 1.10-1.14. Lowering the temperature would likely ensure a faster more controlled initiation, thus providing a more controlled polymerization. A timeframe of 3 hours was used at 70 °C in which a high correlation between M_n and $M_{n,th}$ and an excellent conversion of 99% was obtained. Good levels of control were obtained when the monomer concentration was varied from 10-50 eq. allowing variation in the polymer star arm lengths and therefore varying the molecular weight. In addition, a linear increase in molecular weight was observed with increasing monomer equivalents. ^{1}H NMR spectroscopy was used to confirm the presence of the acetylene end group of these novel materials. The main diagnostic resonance was the proton on the sp-hybridized carbon located at δ 1.96 ppm, in addition to the CH_2-O triplet located at δ 3.75 ppm (Figure 4.2).

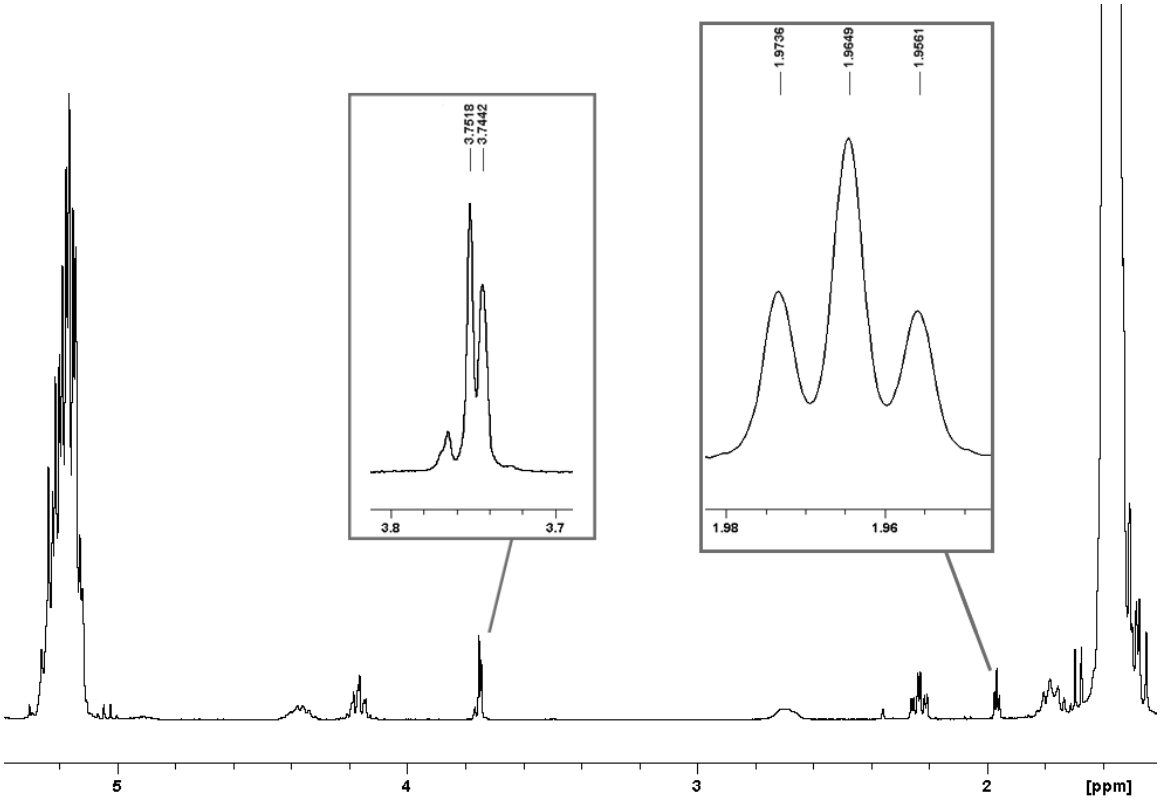

Figure 4.2. Acetylene end-group analysis by ^{1}H NMR spectroscopy.

Similar trends were observed when *rac*-lactide was substituted for L-lactide, with the best levels of control were observed a 70 °C in toluene (Table 4.3). Experiments were also performed at 120 °C, but yielded polymer with a high PDI value of 1.34. Variation of the monomer ratios from 10-50 eq. showed good levels of controls with PDIs as low as 1.05 with excellent conversions.

Table 4.3. Polymer data for acetylene terminated L-PLA from $Sn(Oct)_2$ (**1**).

[M] : [C] : [I]	Temp (°C)	% Conv.[a]	$M_{n,th}$[b]	$M_{n,\ GPC}$[c]	PDI[c]
10 : 0.5 : 1	70	>99	1539	1401	1.18
20 : 0.5 : 1	70	>99	2391	2390	1.15
30 : 0.5 : 1	120	99	4280	6411	1.34
30 : 0.5 : 1	70	99	4422	2657	1.08
40 : 0.5 : 1	70	98	5748	3934	1.04
50 : 0.5 : 1	70	98	7088	3956	1.05

Polymerizations were conducted in 2 of mL toluene with 0.06 mmol of $Sn(Oct)_2$ at 70 or 120 °C for 3 hours, using 5-hexyn-1-ol as an initiator. [a] % Conv. determined by ^{1}H NMR spectroscopy. [b] $M_{n,th}$ = [M] × MW(Lactide) × (% conv.) + MW(5-hexyn-1-ol) [c] Determined by GPC using refractive index coupled with light scattering detectors

The success achieved with *rac*-PLA and L-PLA prompted the exploration of other acetylene-terminated polymers. Initial trails with βBL yielded no polymer at timeframes of 1-24 hours, implying that $Sn(Oct)_2$ is not an effective catalyst for βBL. Thus an alternative strategy was employed with the use of ^{tBu}[salen]AlMe. Salen systems are of particular interest in the polymerization of βBL, due to the high levels of control which have been recently reported in literature.[70] The ^{tBu}[salen]AlMe system yielded acetylene-terminated PHB with excellent levels of control over molecular weights and PDI values as low as 1.04. In addition, excellent conversions were obtained, with all trials reaching >99% at 3 hours (Table 4.4). Excellent correlation between M_n and $M_{n,th}$ was observed for 10-30 eq. of monomer, although greater deviation occurred at 40 and 50 eq. indicating possible transesterification reactions.

Table 4.4. Polymer data for acetylene terminated PHB from ^{tBu}[salen]AlMe (**2**).

[M] : [C] : [I]	% Conv.[a]	$M_{n,th}$[b]	$M_{n,\ GPC}$[c]	PDI[c]
10 : 1 : 1	>99	1539	1401	1.18
20 : 1 : 1	>99	2391	2390	1.15
30 : 1 : 1	>99	2680	1907	1.04
40 : 1 : 1	>99	5748	3934	1.04
50 : 1 : 1	>99	7088	3956	1.05

Polymerizations were conducted in 2 mL of toluene with 0.12 mmol of ^{tBu}[salen]AlMe at 70 °C for 3 hours, using 5-hexyn-1-ol as an initiator. [a] % Conv. determined by ^{1}H NMR spectroscopy. [b] $M_{n,th}$ = [M] × MW(βBL) × (% conv.) + MW(5-hexyn-1-ol) [c] Determined by GPC using refractive index coupled with light scattering detectors.

Schubert previously reported the synthesis of acetylene-terminated PCL using 5-hexyn-1-ol and $Sn(Oct)_2$ at 110 °C with PDI values around 1.16.[124] Using the modified method that was successful for PLA and PHB synthesis, superior molecular weight distributions of <1.10 were obtained by lowering the temperature to 70 °C and using $Sn(Oct)_2$. Attempts to replicate the experiments reported in literature were unsuccessful as performing the polymerization at elevated temperatures of 120 °C and 110 °C gave consistently high PDI values of 1.46 and 1.31 respectively.

Table 4.5. Polymer data for acetylene terminated PCL from $Sn(Oct)_2$ (**1**).

[M] : [C] : [I]	% Conv.[a]	$M_{n,th}$[b]	$M_{n,\ GPC}$[c]	PDI[c]
10 : 0.5 : 1	98	1217	1160	1.08
20 : 0.5 : 1	96	2289	2182	1.08
30 : 0.5 : 1	92	3248	2675	1.08
40 : 0.5 : 1	89	4161	3076	1.05
50 : 0.5 :1	81	4721	3514	1.05

Polymerizations were conducted in 2 mL of toluene with 0.06 mmol of $Sn(Oct)_2$ at 70 °C for 3 hours, using 5-hexyn-1-ol as an initiator. [a] % Conv. determined by ^1H NMR spectroscopy. [b] $M_{n,th}$ = [M] × MW(ε-caprolactone) × (% conv.) + MW(5-hexyn-1-ol) [c] Determined by GPC using refractive index coupled with light scattering detectors.

In addition to these homopolymers, acetylene-terminated copolymers of PLGA were synthesized for click reactions (Table 4.6). Like the homopolymers, the PLGA copolymers showed good levels of control with PDI values low as 1.10. It is important to note that due to the high insolubility of PLGA, aggregation was required to dissolve these compounds in THF for GPC analysis. Thus, molecular weights and PDI values may not be representative of the bulk sample due to selective solubility. Conversions were obtained gravimetrically due to the insolubility of these polymers in organic media.

Table 4.6. Polymer data for acetylene terminated PLGA from $Sn(Oct)_2$ (**1**).

[M] : [C] : [I]	% Conv.[a]	$M_{n,th}$[b]	$M_{n,\ GPC}$[c]	PDI[c]
10 : 0.5 : 1	43	657	1820	1.10
20 : 0.5 : 1	21	566	1873	1.83
30 : 0.5 : 1	46	2946	4188	1.36
40 : 0.5 : 1	99	5247	2058	1.19
50 : 0.5 : 1	99	6601	2354	1.24

Polymerizations were conducted in 2 mL of toluene with 0.06 mmol of $Sn(Oct)_2$ at 70 °C for 3 hours, using 5-hexyn-1-ol as an initiator. [a] % Conv. determined by ^1H NMR spectroscopy. [b] $M_{n,th}$ = [M] × MW(ε-caprolactone) × (% conv.) + MW(5-hexyn-1-ol) [c] Determined by GPC using refractive index coupled with light scattering detectors.

4.3 Synthesis of Arm-First Polymer Stars

Recently, the concept of supramolecular click chemistry was introduced to describe self-assembling supramolecular systems.[124] Like click chemistry, it is expected that supramolecular click chemistry fulfill the conditions described by Sharpless, including that the reactions be modular, wide in scope and give high yields.[155] The advantage of supramolecular click chemistry over traditional click chemistry is the

reversible characteristics of the supramolecular system, allowing self-assembled polymer systems to switch between assembled and disassembled states by changing the temperature, pH, redox state or concentration.[124]

The synthesis of arm-first polymer stars using the arms synthesized in Section 4.2 were carried out using CuAAC conditions, similar to those reported by Schubert.[124] The copper-catalyzed cycloaddition can be conducted using aqueous conditions at room temperature, which is ideal for a greener synthetic approach to obtaining these polymer stars.[156] In addition, CuAAc is regiospecific, producing only 1,4-disubstituted triazoles.

$CuSO_4$ and sodium ascorbate ($C_6H_7NaO_6$) were chosen as the catalyst system for the click reactions. Sodium ascorbate, a mild reducing agent, combines with the copper(II) salt to generate the active copper(I) active species *in situ* leading to the formation of the triazole product. This method is commonly used in the literature and has quickly become the method of choice for the formation of 1,2,3-triazoles.[122] Using the β-CD-$(N_3)_7$ and the acetylene terminated polymers in the presence of $CuSO_4$ and sodium ascorbate, polymer stars were synthesized as described by the catalytic cycle in Scheme 4.3.

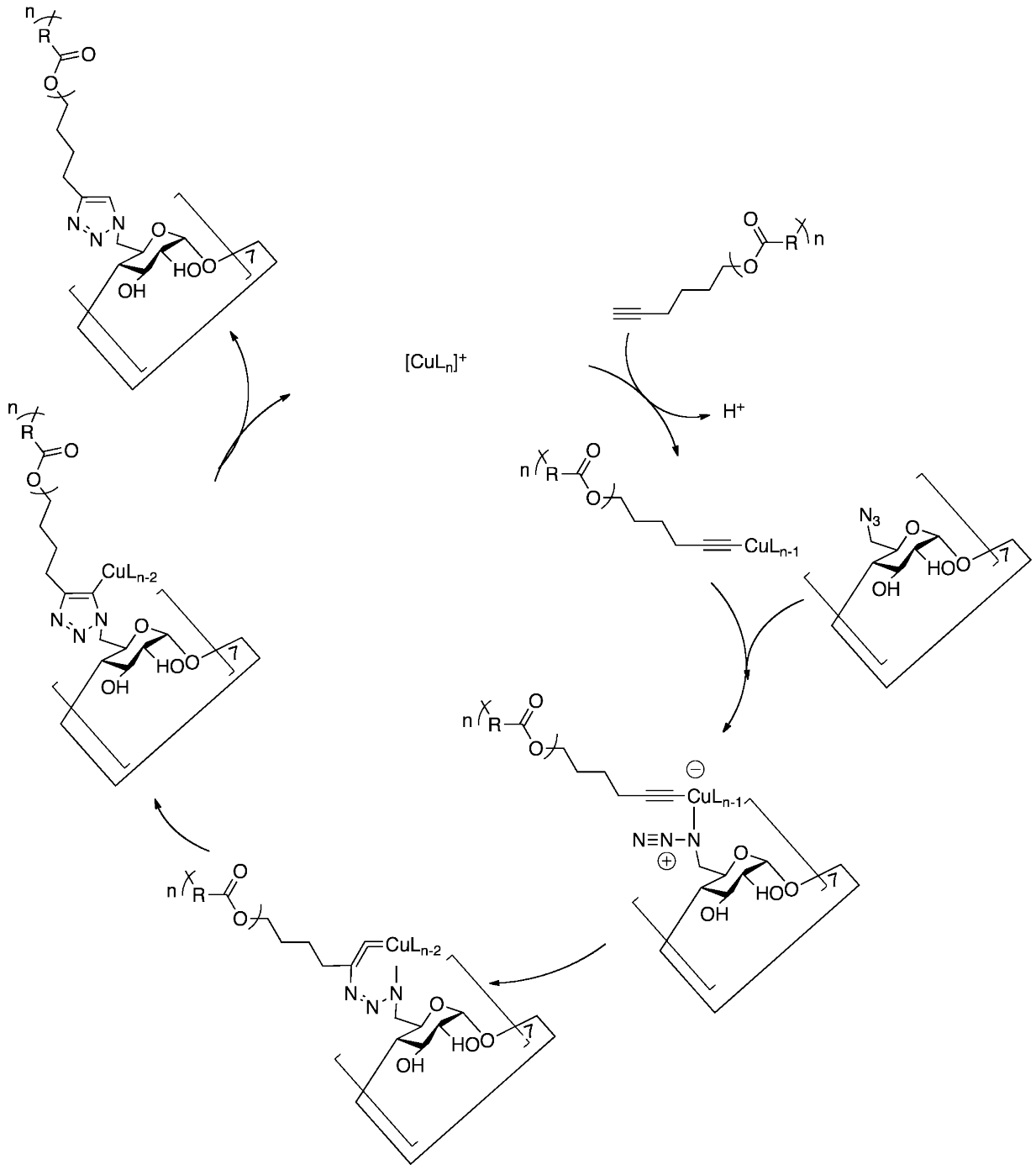

Scheme 4.3. Catalytic cycle for CuAAC for generation of arm-first polymer stars.

This mechanism for CuAAc was first proposed by Himo *et al* using density-functional theory.[157] $CuSO_4$ would coordinate to the acetylene-terminated polymers after the ascorbate abstracts the acetylene proton from the polymer end group. The β-CD-$(N_3)_7$

would then coordinate to the metal center, and at this point cyclization would take place attaching the polymer arm to the CD core through a triazole linker. Protonation would then occur, with the source of the proton being the hydrogen abstracted from the acetylene end-group. The product is formed by dissociation and the catalyst complex is regenerated. (Scheme 4.3).

CuAAc was achieved by reacting β-CD-$(N_3)_7$ with 7 eq. of the acetylene terminated *rac*-PLA in the presence of $CuSO_4$ and $C_6H_7NaO_6$. Reactions were performed in DMF, as the β-CD-$(N_3)_7$ was found to be highly insoluble in other organic solvents. Reactions were stirred at room temperature for 24 hours and it was observed that the color of the solution changed from a light green to yellow during the reaction timeframe. Polymer workup was attempted by precipitating the solution in cold methanol or pentane. However, no product could be isolated. This can be explained by the high insolubility of DMF in MeOH and pentane, as the polymer would not precipitate unless the DMF was dislodged from the polymeric matrix. In order to address this issue, water was used, as DMF has high solubility in water. Upon the addition of water to the DMF-polymer solution the polymer stars precipitated out of solution and were stirred for 30 minutes. The polymer was filtered and then dried in a vacuum oven for 24 hours at 75 °C. The product was then weighed and analyzed by ^{1}H NMR spectroscopy and GPC.

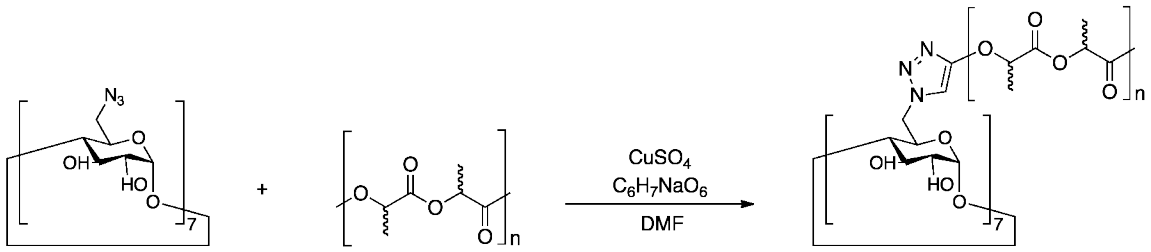

Scheme 4.4. Synthesis of *rac*-PLA arm-first stars.

Table 4.7. Polymer data for *rac*-PLA arm-first stars.

[M]/arm	% Yield[a]	$M_{n,th}$[b]	$M_{n,\ GPC}$[c]	$M_{n,\ NMR}$[d]	PDI[c]	PDI_{arm}[e]
10	40	4749	12010	14174	1.05	1.42
20	38	10774	16538	16757	1.04	1.35
30	57	23472	24680	26994	1.03	1.23
40	21	22646	23430	29229	1.04	1.31
50	48	26573	31700	35312	1.05	1.38

Polymerizations were conducted in 2 mL of DMF with 0.001 mmol of $CuSO_4$ at room temperature for 24 hours. [a] % Conv. determined by GPC. [b] $M_{n,th}$ = MW(arm) × 7(Azide Groups) + MW(core) [c] Determined by GPC using refractive index coupled with light scattering detectors. [d] Determined by ^{1}H NMR spectroscopy. [e] Calculated from the Szymanski method.

GPC analysis of these polymer stars showed excellent PDI values ranging from 1.03-1.05 and PDI_{arm} values ranging from 1.23-1.42. In addition, generally good correlation between the molecular weights obtained from GPC and ^{1}H NMR spectroscopy and theoretical molecular weights was observed for the stars synthesized. In comparison to the molecular weight correlation of the core-first stars, it can be seen that the arm-first method has better control. This indicated the absence of transesterification reactions that could occur with the arm-first synthesis, as these reactions were achieved with previously synthesized polymer arms with low PDI values (~1.10) and at room temperature. PDI values were also lower than the linear polymers, this can be explained

by the formation of a more ordered system by forming polymer stars. Deviations in molecular weights could be due to the high insolubility of the β-CD-$(N_3)_7$, resulting in some cores not initiating. As no monomer conversion was used in these reactions, percent conversions by ^{1}H NMR spectroscopy were unattainable. In addition, isolation of the polymers from DMF was difficult as precipitation in water yielded only small quantities of polymer, making gravimetric weight determination inaccurate. Interestingly, GPC analysis showed two different signals in the chromatogram as shown in Figure 4.3. The mass percent of the two peaks corresponded to the total mass of the sample. Thus, it was possible to determine conversions of the desired product by finding its peak percent from the total mass of the two peaks combined. The major peak found at a retention time of ~17 min, was determined to be the desired product by molecular weight correlation i.e. a star with all 7 arms clicked on. The smaller peak with a retention time ~18.7 min, corresponded to a second product that had formed. The molecular weight of the smaller peak was higher than that of the β-CD-$(N_3)_7$ core but significantly lower than that of the major product. Possible explanations for this second product could be β-CD-$(N_3)_7$ cores that do not have all arms clicked on or CD core molecules that do not have all 7 azide groups functionalized on the 6′ carbon. In addition, CuAAC reactions reported in the literature are often performed using microwave irradiation for short timeframes,[124] whereas these reactions were performed without irradiation for longer timeframes of 24 hours. Microwave irradiation may push these reactions to completion and eliminate any formation of a second product.

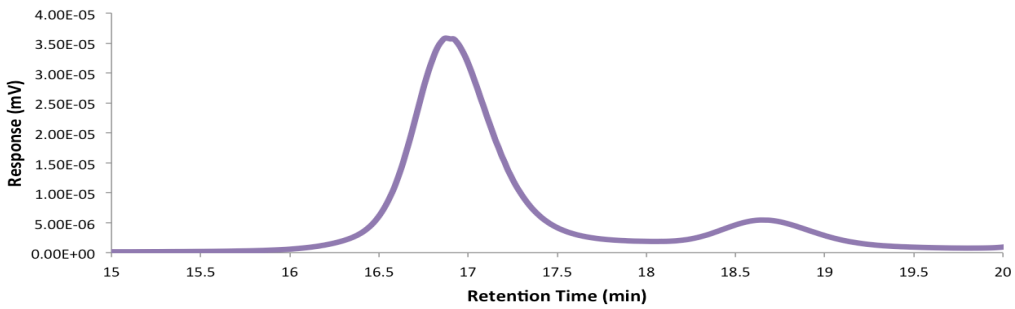

Figure 4.3. Arm-first polymer star GPC trace.

Arm-first polymer stars were also analyzed by ^{1}H NMR spectroscopy as shown in Figure 4.4. The ^{1}H NMR spectrum showed the resonances corresponding to the 3′ and 4′ protons of the β-CD-$(N_3)_7$ located at 4.11 and 4.21 ppm. In addition the 1′ and 5′ protons were found at 5.90 and 5.75 ppm, respectively.

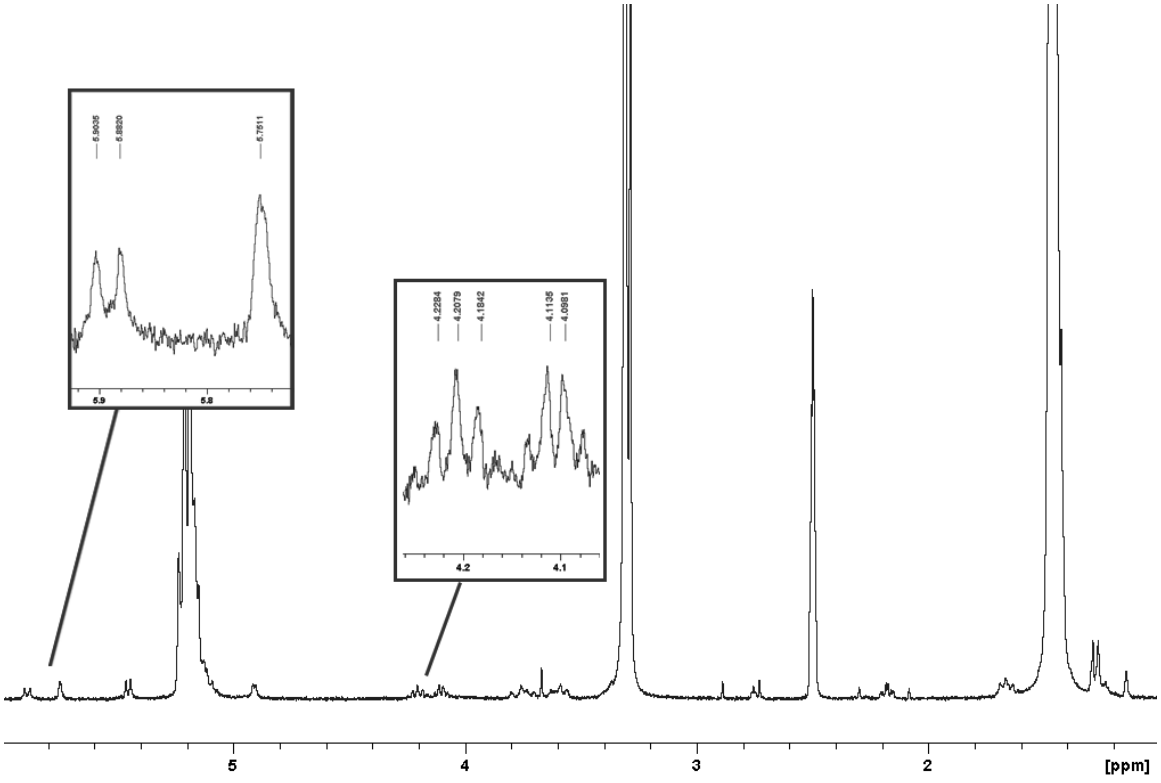

Figure 4.4. ^{1}H NMR spectrum of arm-first PLA star.

L-PLA polymer stars were also synthesized based on β-CD-$(N_3)_7$ and L-PLA acetylene terminated polymers using the same reaction conditions (Scheme 4.5). Much like the *rac*-PLA stars, the isotactic derivatives showed high correlation between theoretical and experimental molecular weights with excellent PDI (1.01-1.05) and PDI_{arm} values (1.07-1.39) as shown in Table 4.8.

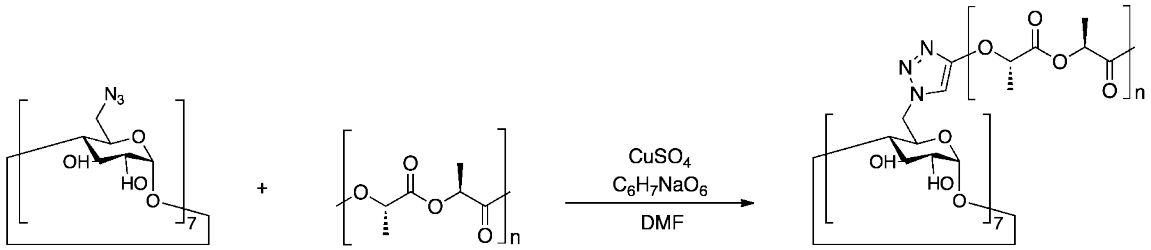

Scheme 4.5. Synthesis of L-PLA arm-first stars.

Table 4.8. Polymer data for L-PLA arm-first stars.

[M]/arm	% Yield[a]	$M_{n,th}$[b]	$M_{n,\ GPC}$[c]	$M_{n,\ NMR}$[d]	PDI[c]	PDI_{arm}[d]
10	52	11117	24470	8832	1.05	1.39
20	74	18047	23150	15867	1.02	1.15
30	75	19909	23310	21475	1.01	1.07
40	81	28838	29800	26294	1.04	1.31
50	80	29121	31650	26808	1.04	1.30

Polymerizations were conducted in 2 mL of DMF with 0.001 mmol of $CuSO_4$ at room temperature for 24 hours. [a] % Conv. determined by GPC. [b] $M_{n,th}$ = MW(arm) × 7(Azide Groups) + MW(core) [c] Determined by GPC using refractive index coupled with light scattering detectors. [d] Determined by ^{1}H NMR spectroscopy. [e] Calculated from the Szymanski method.

Stars based on PHB were also synthesized (Scheme 4.6). Isolation of these stars was challenging, as they were highly amorphous and precipitated as a green gel upon the addition of water. The water was decanted and the green gel was dissolved in dichloromethane and isolated. The product was left to air-dry followed by drying *in*

vacuo. GPC analysis of these stars gave excellent PDI values as well as moderate to high conversions. Deviations between M_n and $M_{n,th}$ can again be attributed to same reasons discussed with the PLA stars.

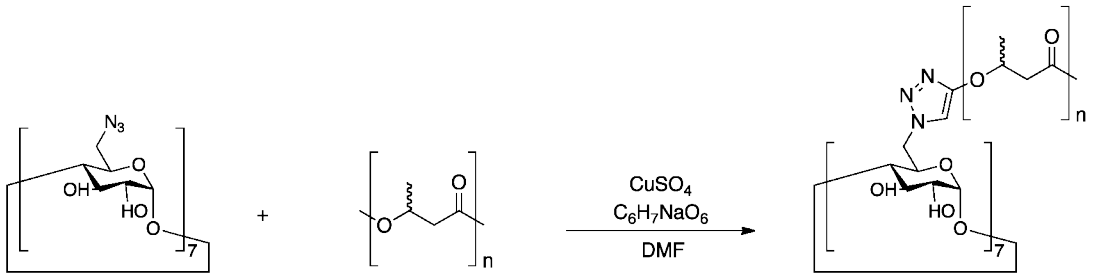

Scheme 4.6. Synthesis of PHB arm-first stars.

Table 4.9. Polymer data for PHB arm-first stars.

[M]/arm	% Yield[a]	$M_{n,th}$[b]	$M_{n,\ GPC}$[c]	$M_{n,\ NMR}$[d]	PDI[c]	PDI_{arm}[e]
10	46	5294	15260	13200	1.04	1.34
20	63	9160	14260	17713	1.02	1.17
30	86	14659	21710	19798	1.02	1.16
40	73	20763	26520	30744	1.15	2.16
50	69	23521	24470	31394	1.01	1.07

Polymerizations were conducted in 2 mL of DMF with 0.001 mmol of $CuSO_4$ at room temperature for 24 hours. [a] % Conv. determined by GPC. [b] $M_{n,th}$ = MW(arm) × 7(Azide Groups) + MW(core) [c] Determined by GPC using refractive index coupled with light scattering detectors. [d] Determined by ^{1}H NMR spectroscopy. [e] Calculated from the Szymanski method.

PCL stars similar to those reported by Schubert were synthesized and used as a reference for the modified reaction conditions that were used. Like the previous stars, excellent PDI (1.01-1.15) and PDI_{arm} (1.07-2.16) values were obtained, which were better than those reported by Schubert (PDI = 1.12), indicating that the absence of microwave irradiation possibly leads to better-defined polymers. This can be expected as high-energy

microwaves may cause polymer chains to break, therefore leading to an increase in PDI values. Molecular weights by ^{1}H NMR spectroscopy were not obtained due to the overlap of the α-methylene group of the PCL chain with that of the diagnostic resonances of the β-CD-$(N_3)_7$.

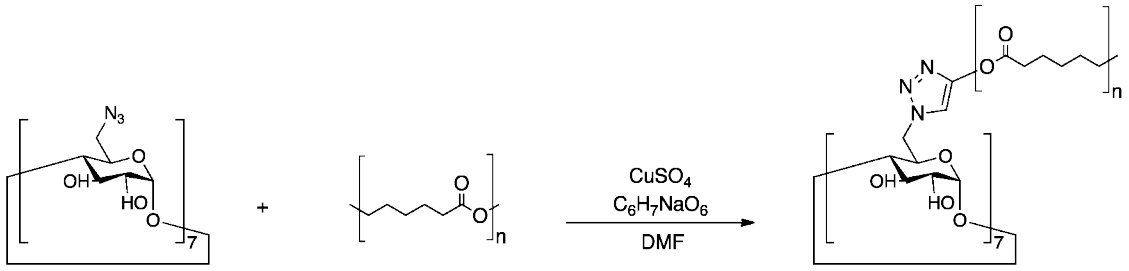

Scheme 4.7. Synthesis of PCL arm-first stars.

Table 4.10. Polymer data for PCL arm-first stars.

[M]/arm	% Yield[a]	$M_{n,th}$[b]	$M_{n,\ GPC}$[c]	PDI[c]	PDI_{arm}[e]
10	87	9430	13150	1.08	1.69
20	48	17333	19610	1.02	1.16
30	50	20665	20360	1.01	1.08
40	64	22865	26190	1.06	1.47
50	69	25908	26070	1.01	1.08

Polymerizations were conducted in 2 mL of DMF with 0.001 mmol of $CuSO_4$ at room temperature for 24 hours. [a] % Conv. determined by GPC. [b] $M_{n,th}$ = MW(arm) × 7(Azide Groups) + MW(core) [c] Determined by GPC using refractive index coupled with light scattering detectors. [d] Determined by ^{1}H NMR spectroscopy. [e] Calculated from the Szymanski method.

In addition to the homopolymers, synthesis of PLGA copolymer stars was also attempted (Scheme 4.8). The reaction conditions were identical to those used for the homopolymers. Product could be isolated however analysis of the polymer was very difficult due to solubility issues. These stars were found to be insoluble in THF, even after 24 hours. Upon filtration and GPC analysis, no clear polymer peaks could be

observed. ^{1}H NMR spectroscopic analysis also could not be performed, as the polymer would not dissolve in $CDCl_3$ or DMSO-d_6.

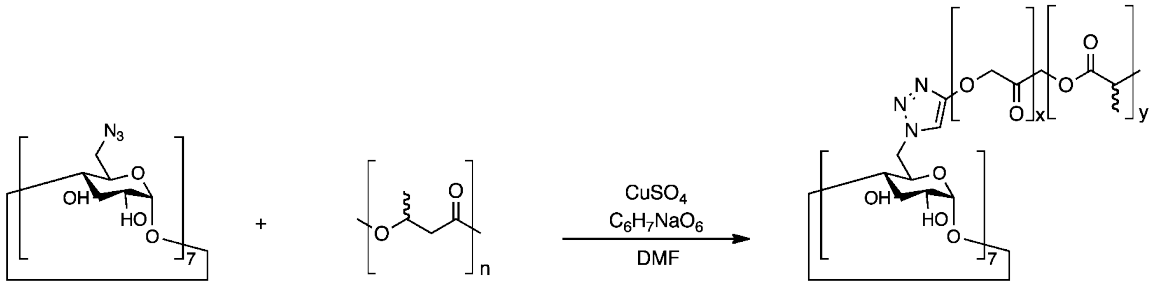

Scheme 4.8. Synthesis of PLGA arm-first stars.

4.4 Inclusion and Degradation Studies of Arm-First Polymer Stars

Inclusion of 7-MC into the polymer stars was achieved through a one-pot synthesis. Unlike the core-first stars, which required high temperature of 120 °C for inclusion, the arm-first inclusion was achieved through mixing excess 7-MC into the CuAAC reaction. After 24 hours, the product was precipitated and washed using MeOH and dried in vacuo. Analysis by ^{1}H NMR spectroscopy showed the presence of 7-MC in the polymer as shown in Figure 4.5.

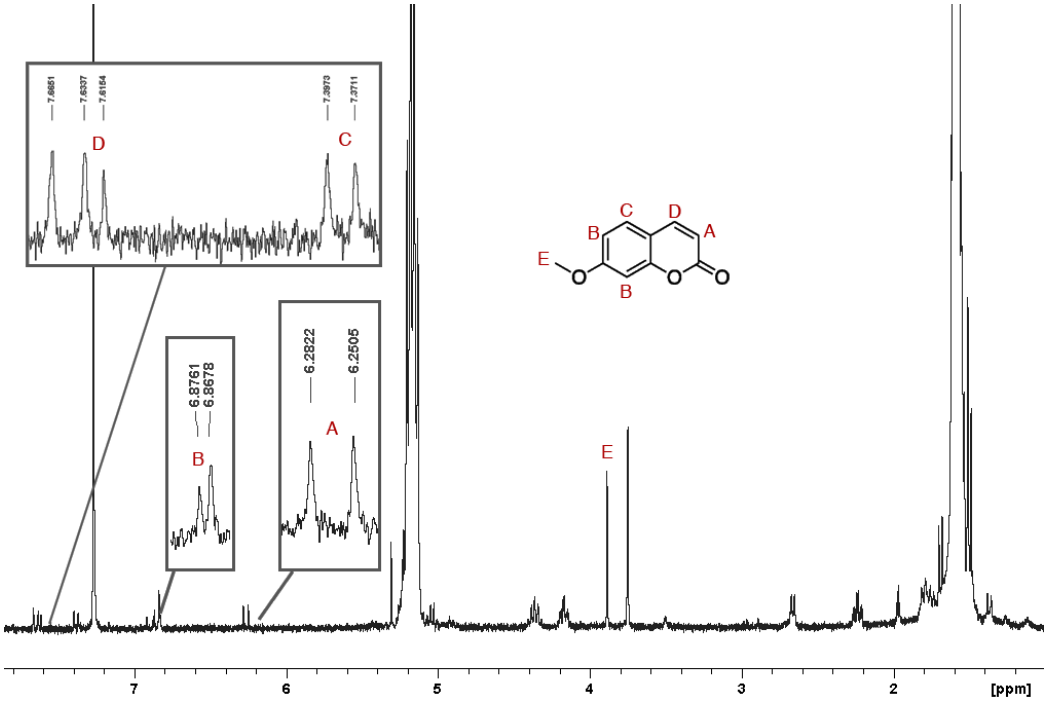

Figure 4.5. ^{1}H NMR spectrum of one-pot click reaction with 7-MC.

Resonances for the aromatic protons of the embedded 7-MC were found at δ 6.29, 6.86, 7.39 and 7.66 ppm. In addition, the methoxy protons were found at δ 3.88 ppm. The material was then tested for degradation using the same methods as the core-first stars as described in Section 3.4. Degradation was observed with PLA pellets in the presence of proteinase K over the course of 8 hours as shown in Figure 4.6. The same trend as the core-first stars was observed with an initial burst release observed from 0-1 hours followed by a slower controlled release observed from 1-8 hours.

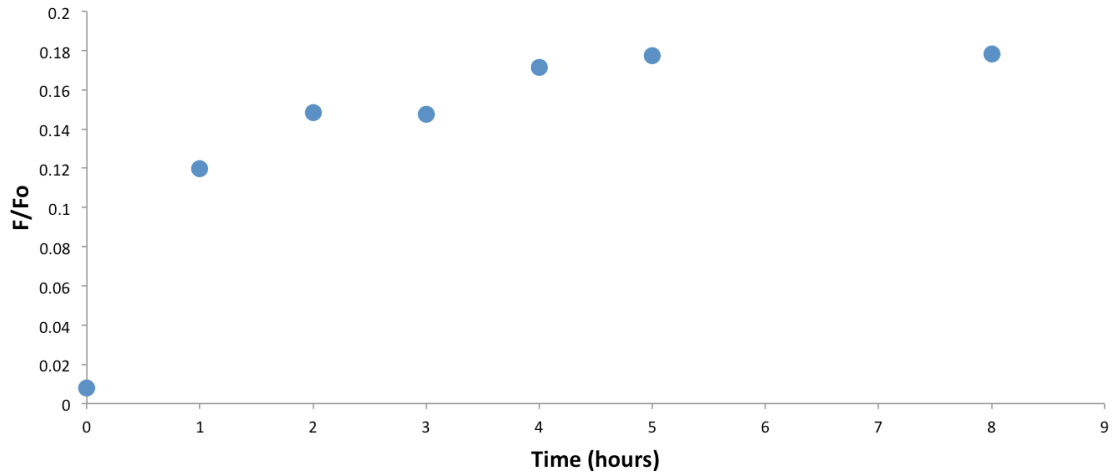

Figure 4.6. Degradation of arm-first PLA star pellet in the presence of proteinase K.

As the one-pot synthesis reaction was achieved in the presence of the 7-MC, determining the location of the fluorophore was of interest, as the location could be either inside of the CD core cavity or embedded in the polymer arms. In order to determine the 7-MC location, PLA powder with 7-MC, instead of a pellet, was immersed in a 50:50 water-methanol solution and monitored over the course of 8 hours. A high F/F_o value of 0.25 was instantly observed, indicating that a large amount of 7-MC had been released. After 1 hour the F/F_o value increased to 0.33 and plateaued there for the remainder of the timeframe. This was indication that the 7-MC was being physically compressed into the polymer network and the location of the 7-MC was likely in the polymer arms and was being released as the pellets degraded in solution.

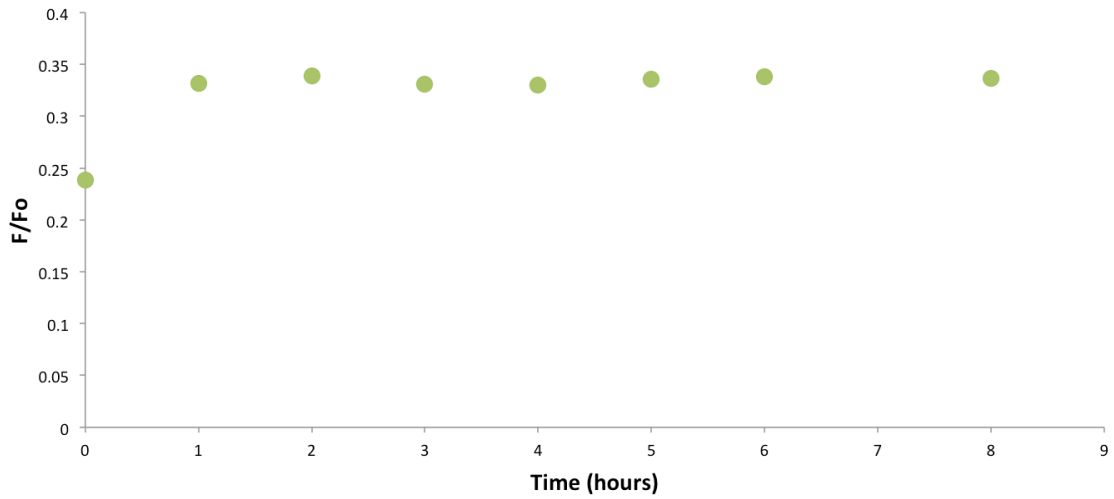

Figure 4.7. Degradation of arm-first PLA star powder in the presence of proteinase K.

Additional degradation studies in the absence of 7-MC were completed to understand the different degradation timeframes of these materials. Timed degradations were performed using polymer pellets of [30]/arm of *rac*- and L-PLA, PLGA and PCL with a solution of 1,5,7-triaza-bicyclo[4.4.0]dec-5-ene (TBD) in MeOH. The PCL pellet exhibited a very high degradation timeframe of 7 days, which was expected, as PCL is known to have longer degradation timeframes.[158] *Rac*-PLA, PLGA and L-PLA, all of which the linear arms were synthesized from $Sn(Oct)_2$, exhibited degradation timeframes of 5, 18 and 33 minutes respectively (Figure 4.8). L-PLA would be expected to have the longest degradation timeframe of 33 min due to its high crystallinity. PLGA exhibited the second highest degradation timeframe of 18 minutes, likely due to the elevated crystallinity of PGA segments in the polymer chain. The *rac*-PLA pellet exhibited the fastest degradation time of 5 minutes, due to its highly amorphous character.

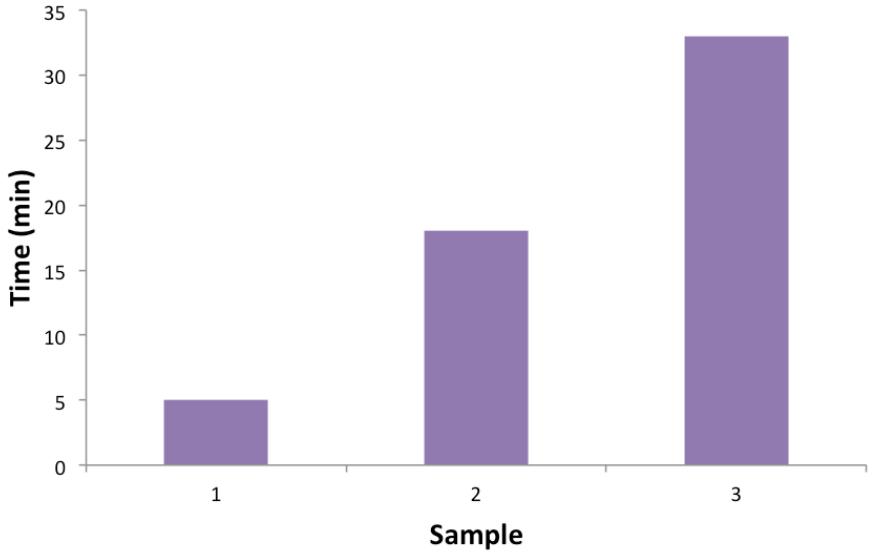

Figure 4.8. TBD-degraded polymer star timeframes. (1) *rac*-PLA, (2) PLGA and (3) L-PLA.

4.5 Thermal Analysis of Arm-First Polymer Stars

Like the core-first stars, arm-first stars were analyzed by DSC and TGA. Data for PLA stars are summarized in Table 4.11. Unlike the core-first stars, general trends were observed between the thermal transitions of the *rac*-PLA stars and their molecular weight. T_g values increased as the [M]/arm increased with 10 and 20 arm lengths giving T_g values of 33 and 27 °C, while 40 and 50 arm lengths had T_g values of 41 and 40 °C respectively. Similarly for TGA analysis, decomposition temperatures increased as the molecular weight increased. As the arm-length of the stars increase, it can be expected that longer decomposition ranges would be observed as the polymer network breaks down. As expected, the L-PLA stars exhibited higher T_g values compared to *rac*-PLA stars due to the increase in crystallinity. Similar trends were observed with L-PLA stars where the T_g values were observed to increase as the star size increased (43-57 °C). In addition the T_m also increased (96-154 °C) as the star size increased. As observed with *rac*-PLA stars,

decomposition temperatures also increased with higher molecular weights. In addition, increased crystallinity could result with longer arms, further increasing the thermal stability of larger stars. The melting enthalpies ΔH_m were also determined for the isotactic polymer stars. Generally, ΔH_m increased with higher molecular weights, indicating higher crystallinity.

Table 4.11. Thermal data for PLA arm-first stars.[a,b]

[M]/arm	Polymer	T_g (°C)	T_m (°C)	Onset (°C)	50% (°C)	T_{max} (°C)	ΔH_m (J/g)
10	*rac*-PLA	33	-	235	284	314	-
20	*rac*-PLA	27	-	225	263	317	-
30	*rac*-PLA	35	-	245	283	360	-
40	*rac*-PLA	41	-	242	306	362	-
50	*rac*-PLA	40	-	242	313	363	-
10	L-PLA	43	96	227	259	303	9.1
20	L-PLA	52	129	224	261	314	21.8
30	L-PLA	54	152	249	302	354	15.7
40	L-PLA	57	153	267	323	370	31.2
50	L-PLA	57	154	259	341	372	33.0

[a] DSC purge flow 50 mL/min N_2, heating/cooling rate 5 °C/min, heat (200 °C)/cool (0 °C) cycle employed.[b] TGA heating rate of 10 °C/min.

Thermal transitions of PHB and PLGA stars were also analyzed and the results are summarized in Table 4.12. T_g values generally increased as the PHB star size increased. However, decompositions observed from TGA analysis did not show the same trends as observed with PLA, as all stars displayed similar decomposition temperatures possibly due to the highly amorphous morphology of the PHB material. Similarly, the PLGA polymer stars did not display any significant trends in the T_g values or the

decomposition ranges as star size increased. Due to the high insolubility of PLGA, all core functionalities may not have undergone initiation, leading to a diverse range of stars of different molecular weight. Unlike the core-first PLGA stars no T_m transitions were observed in the DSC. Since the linear PLGA chains were synthesized by $Sn(Oct)_2$ as opposed to the ^{tBu}[salen]AlMe with the core-first systems, no tacticity bias was observed.

Table 4.12. Thermal data for PHB and PLGA arm-first stars. [a,b]

[M]/arm	Polymer	T_g (°C)	Onset (°C)	50% (°C)	T_{max} (°C)
10	PHB	-11	230	262	280
20	PHB	-13	235	278	296
30	PHB	-5	258	277	296
40	PHB	-2	240	266	283
50	PHB	0	241	266	285
10	PLGA	28	236	321	369
20	PLGA	33	215	275	340
30	PLGA	26	237	297	357
40	PLGA	33	225	287	354
50	PLGA	33	220	325	367

[a] DSC purge flow 50 mL/min N_2, heating/cooling rate 5 °C/min, heat (200 °C)/cool (0 °C) cycle employed.[b] TGA heating rate of 10 °C/min.

The arm-first methodology provided polymer stars with excellent PDI values as well as good correlation between molecular weights in comparison to the core-first stars. Isolation of these polymers was however challenging, resulting in low yields. The formation of a minor secondary product was indicative that further tuning to the methodology was required to obtain only the desired product. Fluorescence release trends of arm-first stars were similar to those observed with the core-first stars.

Chapter Five

5 Conclusions and Future Work

5.1 Conclusions

Exploration of the use of cyclodextrins for polymer star synthesis proved extremely useful, as novel materials were synthesized by core- and arm-first methodologies. Binding studies with the cyclodextrins and 7-MC were also used to understand the host-guest interactions of the core and guest.

Binding studies were successfully completed using β-CD and heptakis(2,6-di-O-methyl)-β-CD as hosts and 7-MC as a guest. In each study 7-MC exhibited fluorescence suppression under CD exposure. Studies on β-CD in H_2O gave a binding constant of 238 M^{-1} and an R^2 value of 0.9580. Stronger binding and a better correlation was obtained with heptakis(2,6-di-O-methyl)-β-CD in H_2O with a binding constant of 306 M^{-1} and R^2 value of 0.998. Binding in H_2O/MeOH was also tested with heptakis(2,6-di-O-methyl)-β-

CD resulting in a weaker binding constant of 120 M^{-1} and lower correlation value of 0.986 due to the decrease in bulk solution polarity.

Core-first polymer star synthesis was attempted using β-CD and $Sn(Oct)_2$ for the ROP of PLA stars, however no initiation was observed even at high temperatures and long reaction times, indicating that β-CD was not an efficient initiator for polymerization studies. Core-first *rac*- and L-PLA star synthesis using heptakis(2,6-di-O-methyl)-β-CD and $Sn(Oct)_2$ yielded poorly controlled star polymers with high PDI values and poor molecular weight correlations between theoretical molecular weights and experimental molecular weights as determined by GPC and ^1H NMR spectroscopy. Using the ^{tBu}[salen]AlMe catalyst yielded PLA stars with generally excellent PDI values of <1.1, however, poor molecular weight correlation was still observed, potentially due to the inaccuracies in conversion measurement or probable transesterification reactions. PHB and PLGA stars were also synthesized by ^{tBu}[salen]AlMe and gave good PDI values, but same trends were observed in the molecular weight correlations as for the PLA stars. Thermal analysis of these polymer stars by DSC and TGA showed variances based on the crystallinity of the polymer. No specific trend was observed based on thermal transitions and molecular weights in contrast to simple polyol stars.

Inclusion of a 7-MC fluorophore into the PLA and PLGA network was achieved by refluxing the polymer solution in the presence of excess 7-MC. Degradations of the star polymers were tested using catalyzed and uncatalyzed conditions and measured by fluorescence spectroscopy. Uncatalyzed degradations in H_2O/MeOH and pure H_2O were monitored over 135 days and showed extremely slow controlled release of the fluorophore. Enzyme catalyzed degradation using proteinase K also showed a

significantly increased rate of 7-MC release when compared to uncatalyzed reactions. In all cases, controlled release appeared to be from the arm rather than the hydrophobic core.

For arm-first polymer star synthesis, an azide-modified CD, β-CD-$(N_3)_7$, was successfully synthesized from reported procedures and characterized by ^{1}H NMR and IR spectroscopies. Binding constant studies with 7-MC were not performed using β-CD-$(N_3)_7$, as it was completely insoluble in H_2O.

Acetylene terminated linear polymers based on *rac*- and L-PLA, PHB, PCL and PLGA were synthesized using 5-hexyn-1-ol as an initiator and $Sn(Oct)_2$ as a catalyst. ^{1}H NMR spectroscopy was used to determine polymer end-functionalization. GPC analysis confirmed excellent PDI values and good correlation between theoretical and actual molecular weights.

CuAAC reactions were carried out using β-CD-$(N_3)_7$ and 7 eq. of the acetylene terminated polymer in the presence of copper(II) sulfate and sodium ascorbate. CuAAC reactions yielded polymer stars that were superior to the core-first method, with excellent PDI values of <1.1 and good molecular weight correlation determined by GPC and ^{1}H NMR spectroscopy. Thermal analysis by DSC and TGA showed increased thermal stability based on crystallinity and molecular weights.

Inclusion of 7-MC into the polymer network was achieved by adding excess 7-MC to the CuAAC reaction in a one-pot synthesis. Degradations were performed using the same methods as the core-first polymers and showed similar 7-MC release profile as the core-first stars.

Both core- and arm-first methodologies showed advantages and disadvantages. The core-first method allowed the synthesis of a diverse library of polymer with excellent

PDI values using high temperatures. However, poor molecular weight correlation was indicated that all heptakis(2,6-di-O-methyl)-β-CD cores did not initiate possibly due to poor solubility. The arm-first methodology was used to synthesize polymer stars with excellent PDI values and good molecular weight correlation at room temperature. Some deviations in the molecular weights can be explained by the high insolubility of the β-CD-$(N_3)_7$ core. Yields of these stars were low due to the difficulty in isolating these polymers from DMF. GPC analysis showed the presence of an undesired minor second product, indicating further modifications to the process would be required to ensure only formation of the desired product formed.

Fluorescence was useful in observing the release profiles of both core- and arm-first stars. Location of the 7-MC fluorophore was determined to be in the polymer arms, rather than the hydrophobic core. However, physically compressing 7-MC into the polymer network allowed controlled release to be observed in catalyzed and uncatalyzed degradation mediums.

The different synthetic methodologies and controlled release characteristics of these materials have laid a foundation for the exploration of new materials based on cyclodextrin cores used for controlled release.

5.2 Future Work

Further tuning of the novel core-first stars based on heptakis(2,6-di-O-methyl)-β-CD could be achieved by exploring different catalyst systems other than $Sn(Oct)_2$ and ^{tBu}[salen]AlMe. This could useful in obtaining polymers that have more uniform molecular weight distributions as well as better correlation between the theoretical and actual molecular weights. Recent work in our group suggests toluene-based

polymerizations of cyclic esters catalyzed by [salen]Al complexes at 80 °C offers better control and limited transesterification.

The arm-first synthesis gave excellent polymer stars, however exploring different CuAAC catalyst systems other than copper(II) sulfate and sodium ascorbate may enhance polymer yields. Another interesting prospect would be to use ruthenium catalysis (RuAAC) to form a 1,5-triazole linker as opposed to 1,4 observed with CuAAC. Expanding the monomer scope would be attractive in developing new polymer stars. Exploring other copolymers such as PLA-PHB and PEG-PLA that have recently been studied in our group could be used to develop new materials.

For this project, only 7-MC was used for binding constant, correlation and degradation studies. Degradations using acid-or base catalysis could not be used as 7-MC was quenched in the presence of acid or base. Using another fluorophore that exhibits fluorescence suppression and is less susceptible to acid or base could allow for complete pellet degradation to be observed. Increased degradation rates could also be explored with the use of base such as TBD. It would also be possible to see release trends once the pellet reaches complete degradation, i.e. burst release upon complete degradation of the polymer arms.

Other than embedding a fluorophore into the network, a bioactive molecule would be of interest as it could be embedded into these core-first and arm-first stars and observe the controlled release profiles through NMR spectroscopy as opposed to fluorescence. This would be the next step in the exploration of these novel materials as controlled release vectors.

Chapter Six

6 Experimental

6.1 Materials

HPLC-grade toluene, dichloromethane and methanol were purchased from Fisher Scientific. Deuterated chloroform and dimethyl sulfoxide were purchased from Cambridge Isotopes. Spectroscopic-grade dimethylformamide was obtained from Sigma Aldrich. Anhydrous toluene was obtained by passing the solvent through an Innovative Technologies solvent purification system consisting of columns of alumina and a copper catalyst and was degassed prior to use. Chemicals for catalyst synthesis including trimethylaluminum (2.0M solution in hexanes), 3,5-di-tert-butyl-2-hydroxybenzaldehyde, 1,3-diaminopropane and paraformaldehyde were purchased from Aldrich Chemicals and used as received. Tin(II) ethylhexanoate was purchased from Aldrich Chemicals and distilled under reduced pressure prior to use. β-Cyclodextrin and heptakis(2,6-di-O-methyl)-β-cyclodextrin were purchased from Aldrich Chemicals. The monomers *rac*- and

L-lactide were purchased from PURAC Biomaterials and were purified by three successive vacuum sublimations prior to use. Glycolide was purchased from Aldrich Chemicals and was used as received. β-Butyrolactone and ε-caprolactone was purchased from Aldrich Chemicals, dried over CaH_2 and distilled under reduced pressure before use. Aluminum catalyst ^{tBu}[salen]AlMe, where ^{tBu}[salen] is N,N'-bis(3,5-di-*tert*-butylsalicylidene)-1,3-propanediamine, was synthesized according to previously reported procedures.[78] 5-Hexyn-1-ol was purchased from Aldrich chemicals and was distilled under vacuum at 80 °C prior to use. Copper(II) sulfate was purchased from Aldrich Chemicals and sodium ascorbate from Alfa Aesar. Heptakis-azido-β-cyclodextrin was synthesized according to a previously reported literature procedure.[152]

6.2 General Considerations

All experiments involving moisture and air-sensitive compounds were performed under a nitrogen atmosphere using an MBraun LABmaster sp glovebox system equipped with a -35 °C freezer and [H_2O] and [O_2] analyzers. All GPC analyses were performed in THF (flow rate: 1 mL min^{-1}) at 50 °C with a Polymer Laboratories PL-GPC 50 Plus integrated GPC system with two 300 × 7.8 mm Jordi Gel DVB mixed bed columns coupled to a Wyatt miniDAWN Treos Light Scattering system using dn/dc values for lactide, butyrolactone, lactide + glycolide and ε-caprolactone of 0.0558, 0.0670, 0.0540 and 0.0650 respectively.[159-162] Sonication was performed using a Branson 200 ultrasonic cleaner. All UV-Vis absorption measurements were performed using a Cary 50 Bio UV-visible spectrophotometer. All fluorescence experiments were performed using a Photon Technology International RF-M2004 luminescence spectrophotometer equipped with a PTI LPS-220 lamp power supply, a xenon 75 watt arc lamp, a PTI-610 photomultiplier

tube detector, and a PTI MD-5020 motor driver. All samples were excited at 320 nm and the emission was scanned from 330-630 nm using a step size of 1 nm and integration time of one second. ^{1}H NMR spectra were recorded with a Bruker Avance Spectrophotometer (300 MHz) in $CDCl_3$. IR spectra were recorded with a Bruker Alpha ATR FTIR. Thermogravimetic analysis was performed on a TA instruments TGA Q500 in air with a flow rate of 60 mL min^{-1} and a heating rate of 10 °C min^{-1}. DSC was performed on a TA instruments DSC Q100 using a heating rate of 10 °C min^{-1}.

6.3 Fluorescence Titrations

A 3.0×10^{-5} M solution of 7-MC was prepared by dissolving 0.0005 g (0.003 mmol) in 100 mL of nano-pure H_2O. The solution was sonicated until all 7-MC crystals went into solution. Similarly, a 1.5×10^{-5} M solution of 7-MC was prepared by dissolving 0.0002 (0.002 mmol) in a 100 mL solution containing a 1:1 mixture of spectroscopic grade MeOH and nano-pure H_2O.

All absorption measurements were performed using ultraviolet-visible spectroscopy. 3 mL each solution were placed in a 1 cm^2 quartz cuvette and places into the spectrophotometer sample chamber and scanned from 200-500 nm using a medium scan rate. The baseline was corrected for each sample depending on the solvent system by scanning the solvent in the same wavelength range before running each solution. This ensured that the absorbance measured was from 7-MC only.

The spectra were then analyzed to determine their absorbance at 320 nm. 320 nm was selected because it is located near the maximum absorbance of the 7-MC absorption peaks and this makes for an ideal excitation wavelength for fluorescence titration experiments. The absorbance of the solution was ensured not to pass 0.40 as in such a

case the excitation light might be completely absorbed in the first few millimeters of the cuvette, and therefore the fluorescence intensity coming from the middle of the cuvette would decrease.

These solutions were used to create host-guest solutions by adding different masses of the cyclodextrin of interest to 3.00 mL aliquots of the 7-MC solution. The specified amount of cyclodextrin was dissolved into the 7-MC solution to give a desired millimolar solution of cyclodextrin in the presence of 7-MC. The solution was sonicated to ensure the cyclodextrin was completely dissolved. 3 mL of the host-guest solution was then placed into a 1 cm^2 quartz cuvette, and placed into a fluorescence spectrometer and the emission of the solution was scanned from 330-630 nm. The monochromator slits were adjusted by hand to ensure the counts per second did not exceed 2×10^6 for the highest intensity solution for each trial, as such intensity could be damaging to the photomultiplier tube. The spectrum was analyzed by obtaining the total area under the fluorescence peak using the Felix analysis software. This data was then used to determine the F/F_o and R^2 values for the host-guest complexes.

6.4 Core-First Polymer Stars

All polymerization experiments were performed in sealed ampules under an inert nitrogen atmosphere at 120 °C in toluene using a varying monomer ratio (70, 140, 210, 280 and 350 eq.) and an core:catalyst ratio of 1:0.5 for $Sn(Oct)_2$ and 1:1 for ^{tBu}[salen]AlMe. Monomers used were *rac*-lactide, L-lactide, β-butyrolactone and glycolide, with heptakis(2,6-di-O-methyl)-β-cyclodextrin as the initiator. The reactions were carried out for 3 hours and then quenched with a 10:1 v/v mixture of CH_2Cl_2/MeOH

solution and stirred for 30 minutes. The resulting mixture was precipitated into cold pentane, filtered and dried *in vacuo* prior to analysis.

Synthesis of PLA heptakis(2,6-di-O-methyl)-β-CD stars using $Sn(Oct)_2$ or ^{tBu}[salen]AlMe

The same procedure was followed for all PLA stars with varying molecular weights. For example in the case of stars with 30 monomer length arms, *rac*- or L-lactide (0.500 g, 3.5 mmol), heptakis(2,6-di-O-methyl)-β-cyclodextrin (0.022 g, 0.02 mmol), $Sn(Oct)_2$ (0.005 g, 0.01 mmol) or ^{tBu}[salen]AlMe (0.010 g, 0.02 mmol) and toluene were added to an ampule equipped with a magnetic stir bar in the glovebox. The ampule was sealed and placed into an oil bath at 120 °C for 3 hours. The ampule was then removed from the oil bath and cooled to room temperature. The vessel was opened to the atmosphere and quenched with 5 mL of a 10:1 v/v mixture of CH_2Cl_2 and MeOH. The resulting solution was stirred for 30 minutes and then precipitated by dropwise addition into 100 mL of cold pentane. The polymer was then filtered and dried *in vacuo* for 24 hours. Percent conversion was determined by gravimetric analysis or ^{1}H-NMR spectroscopy and was calculated to be 72%. ^{1}H NMR (300 MHz, $CDCl_3$, 25°C) δ: 5.16 (m, PLA-C*H*), 3.63 (s, 21H, OCH_3), 3.40 (s, 21H, OCH_3), 1.53 (m, PLA-CH_3).

Synthesis of PHB heptakis(2,6-di-O-methyl)-β-CD stars using ^{tBu}[salen]AlMe

The same procedure as reported above was used in the synthesis of PHB stars, except using β-butyrolactone (0.500 g, 5.8 mmol), heptakis(2,6-di-O-methyl)-β-cyclodextrin (0.036 g, 0.03 mmol) and ^{tBu}[salen]AlMe (0.015 g, 0.03 mmol). Monomer conversion by ^{1}H NMR analysis of the crude reaction mixture was determined to be 94%.

^{1}H NMR (300 MHz, $CDCl_3$, 25°C) δ: 5.31 (m, PHB-C*H*), 3.61 (s, 21H, OCH_3), 3.39 (s, 21H, OCH_3), 2.51 (m, PHB-CH_2). 1.35 (m, PHB-CH_3).

Synthesis of PLGA heptakis(2,6-di-O-methyl)-β-CD stars using ^{tBu}[salen]AlMe

The same procedure as reported above was used in the synthesis of PLGA stars except using *rac*-lactide (0.250 g, 1.7 mmol), glycolide (0.202 g, 1.7 mmol), heptakis(2,6-di-O-methyl)-β-cyclodextrin (0.022 g, 0.02 mmol) and ^{tBu}[salen]AlMe (0.010 g, 0.02 mmol). Percent conversion by gravimetric analysis was determined to be 41%. ^{1}H NMR (300 MHz, $CDCl_3$, 25°C) δ: 5.18 (m, PLA-C*H*), 4.95 (m, PGA-CH_2), 3.62 (s, 21H, OCH_3), 3.42 (s, 21H, OCH_3), 1.55 (m, PLA-CH_3).

6.5 Arm-First Polymer Stars

6.5.1 Synthesis of β-CD-$(N_3)_7$

Synthesis of β-CD-$(I)_7$ precursor

Ph_3P (18.405 g, 70.2 mmol) was dissolved in 100 mL of dried DMF in a oven dried schlenk under a nitrogen atmosphere. To this solution, I_2 (17.949 g, 70.8 mmol) was added over the course of 15 minutes. The solution was then heated to 50 °C. Freshly dried β-CD (5.737 g, 5.1 mmol) was then added to dark brown solution. The solution was then heated to 70 °C and mixed for 24 hours. The mixture was then partially concentrated under reduced pressure and a 3.0 M solution of sodium methoxide was added drop-wise over the course of 5 minutes. Upon addition of the NaOMe, the solution changed to a deep red color and a white solid suspension had formed. The solution was then placed into an ice bath and further formation of precipitate was observed. The mixture was then precipitated by 800 mL of methanol to yield a yellow solid. The product was then dried *in vacuo* and then washed with MeOH in a Soxhlet extractor. The β-CD-$(I)_7$ was then

dried in a vacuum oven for 24 hours. Percent conversion was determined by gravimetric analysis to 50%. ^{1}H NMR (300 MHz, CD_3SOCD_3, 25°C) δ 6.03 (d, C*H*O, *J* = 7 Hz, 7H), 5.92 (d, C*H*O, *J* = 2 Hz, 7H), 5.00 (d, C*H*OH, *J* = 7 Hz, 7H), 3.80 (d, C*H* *J* = 9 Hz, 7H), 3.54-3.68 (m, O*H*, 14H), 3.34-3.48 (m, CH_2I, 14H), 3.28 (t, C*H*OH, *J* = 9 Hz, 7H).

Synthesis of β-CD-$(N_3)_7$.

β-CD-$(I)_7$ (3.881 g, 2.0 mmol) was dissolved in 40 mL of dried DMF in a schlenk flask under a nitrogen atmosphere. NaN_3 (1.387 g, 21.3 mmol) was then added to the solution and it was observed that a solid suspension had formed and the solution turned yellow. The solution was then heated to 70 °C and stirred for 24 hours. The solution was removed from the heat, cooled to room temperature and an excess of H_2O was added to flask, which resulted in the formation a white precipitate. The precipitate was filtered under vacuum and then dried in a vacuum oven for 24 hours at 70 °C. Percent conversion was determined by gravimetric analysis to 95%. ^{1}H NMR (300 MHz, CD_3SOCD_3, 25°C) δ 5.91 (d, C*H*O, *J* = 7 Hz, 7H), 5.74 (d, C*H*, *J* = 2 Hz, 7H), 4.91 (d, C*H*OH *J* = 2 Hz, 7H), 3.69-3.79 (m, C*H*, 14H), 3.54-3.62 (m, C*H*, 14H), 3.30-3.40 (m, CH_2N_3, 14H).

6.5.2 Acetylene-Terminated Polymers

Acetylene-Terminated PLA

The same procedure was followed for all PLA chains with varying arm lengths. For example, in the synthesis of polymer chains 30 monomer units in arm length, *rac*- or L-lactide (0.500 g, 3.5 mmol), 5-hexyn-1-ol (0.011 g, 0.12 mmol), $Sn(Oct)_2$ (0.025 g, 0.06 mmol) and in toluene (2 mL) were added to an ampule under an N_2 atmosphere. The ampule was then placed heated to 70 °C in an oil bath and the reaction was set to stir for 3 hours. The reaction was then quenched with 5 mL of a 10:1 v/v mixture of CH_2Cl_2 and

MeOH. The resulting solution was stirred for 30 minutes and then precipitated by dropwise addition into 100 mL of cold pentane. The polymer was then filtered and dried *in vacuo* for 24 hours. Percent conversion was done by ^{1}H-NMR spectroscopy and was determined to be 99%. ^{1}H NMR (300 MHz, $CDCl_3$, 25°C) δ: 5.19 (m, PLA-C*H*), 3.75 (t, *J* = 2 Hz, 2H CH_2OH), 1.97 (t, *J* = 3 Hz, 1H, *H*CC), 1.55 (m, PLA-CH_3).

Acetylene-Terminated PHB

The same procedure as reported above was used in the synthesis of acetylene terminated PHB except using β-butyrolactone (0.250 g, 2.9 mmol), 5-hexyn-1-ol (0.011 g, 0.12 mmol) and ^{tBu}[salen]AlMe (0.042 g, 0.06 mmol). Monomer conversion by ^{1}H NMR analysis of the crude reaction mixture was determined to be >99%. ^{1}H NMR (300 MHz, $CDCl_3$, 25°C) δ: 5.33 (m, PHB-C*H*), 3.75 (t, *J* = 2 Hz, 2H CH_2OH), 2.52 (m, PHB-CH_2), 1.97 (t, *J* = 3 Hz, 1H, *H*CC), 1.39 (m, PHB-CH_3).

Acetylene-Terminated PCL

The same procedure as reported above was used in the synthesis of acetylene terminated PCL except using ε-caprolactone (0.405 g, 3.5 mmol), 5-hexyn-1-ol (0.011 g, 0.12 mmol) and $Sn(Oct)_2$ (0.023 g, 0.06 mmol) Monomer conversion by ^{1}H NMR analysis of the crude reaction mixture was determined to be 92%. ^{1}H NMR (300 MHz, $CDCl_3$, 25°C) δ: 4.09 (m, PCL-CH_2), 3.75 (t, *J* = 2 Hz, 2H CH_2OH), 2.33 (m, PCL-CH_2), 1.97 (t, *J* = 3 Hz, 1H, *H*CC), 1.72 (m, PCL-CH_2), 1.33 (m, PCL-CH_2).

Acetylene-Terminated PLGA

The same procedure as reported above was used in the synthesis of acetylene terminated PLGA except using *rac*-lactide (0.256 g, 1.8 mmol), glycolide (0.201 g, 1.8 mmol), 5-hexyn-1-ol (0.011 g, 0.12 mmol) and $Sn(Oct)_2$ (0.023 g, 0.06 mmol) Monomer

conversion by analysis of the crude reaction mixture was determined to be 46%. ^{1}H NMR (300 MHz, $CDCl_3$, 25°C) %. δ: 5.16 (m, PLA-C*H*), 4.97 (m, PGA-CH_2), 3.77 (t, *J* = 2 Hz, 2H CH_2OH), 3.42 (s, 21H, OCH_3), 1.97 (t, *J* = 3 Hz, 1H, *H*CC), 1.55 (m, PLA-CH_3).

6.5.3 CuAAC Click Stars

PLA CuAAC Star

Same procedure was followed for all PLA stars with varying arm lengths. PLA (0.187 g, 0.07 mmol), β-CD-$(N_3)_7$ (0.013, 0.01 mmol), $CuSO_4$ (0.002 g, 1.2×10^{-3} mmol) and sodium ascorbate (0.010 g, 0.05 mmol) were dissolved in DMF (2 mL) The reaction mixture was stirred for 24 hours at room temperature. The reaction was then precipitated into 50 mL of deionized H_2O, filtered and dried at 70 °C in a vacuum oven. Percent conversion by GPC was determined to be 57%. ^{1}H NMR (300 MHz, $CDCl_3$, 25°C) δ: 5.90 (br, 7H, β-CD-$(N_3)_7$), 5.75 (br, 7H, , β-CD-$(N_3)_7$), 5.22 (m, PLA-C*H*), 4.21 (m, 7H, β-CD-$(N_3)_7$), 4.11 (m, 7H, β-CD-$(N_3)_7$), 1.55 (m, PLA-CH_3).

PHB CuAAC Star

The same procedure as above was used in the synthesis of PHB stars except using PHB (0.136 g, 0.07 mmol), β-CD-$(N_3)_7$ (0.013, 0.01 mmol), $CuSO_4$ (0.003 g, 1.2×10^{-3} mmol) and sodium ascorbate (0.011 g, 0.05 mmol). ^{1}H NMR (300 MHz, $CDCl_3$, 25°C) δ: 5.89 (br, 7H, β-CD-$(N_3)_7$), 5.73 (br, 7H, , β-CD-$(N_3)_7$), 5.32 (m, PHB-C*H*), 4.20 (m, 7H, β-CD-$(N_3)_7$), 4.09 (m, 7H, β-CD-$(N_3)_7$), 2.51 (m, PHB-CH_2). 1.35 (m, PHB-CH_3).

PCL CuAAC Star

The same procedure as above was used in the synthesis of PCL stars except using PCL (0.180 g, 0.07 mmol), β-CD-$(N_3)_7$ (0.013, 0.01 mmol), $CuSO_4$ (0.002 g, 1.2×10^{-3} mmol) and sodium ascorbate (0.012 g, 0.05 mmol). ^{1}H NMR (300 MHz, $CDCl_3$, 25°C) δ:

5.90 (br, 7H, β-CD-$(N_3)_7$), 5.72 (br, 7H, β-CD-$(N_3)_7$), 4.20 (m, 7H, β-CD-$(N_3)_7$), 4.10 (m, PCL-CH_2), 2.34 (m, PCL-CH_2), 1.71 (m, PCL-CH_2), 1.34 (m, PCL-CH_2).

PLGA CuAAC Star

The same procedure as above was used in the synthesis of PLGA stars except using PLGA (0.148 g, 0.07 mmol), β-CD-$(N_3)_7$ (0.013, 0.01 mmol), $CuSO_4$ (0.002 g, 1.2×10^{-3} mmol) and sodium ascorbate (0.012 g, 0.05 mmol).

6.6 Inclusion and Degradation Studies.

7-MC Inclusion

For the core-first polymer stars polymer was dissolved in DCM and an excess (10 eq) of 7-MC was added to the solution. The solution was then refluxed for 24 hours at 70 °C and then precipitated into MeOH and then dried *in vacuo*. For core-first inclusion, CuAAC reactions were performed in the presence of 10 eq. of 7-MC and worked up in the same procedures as discussed above.

Polymer Degradation

All degradation experiments were performed at room temperature. The polymer samples (100.0 mg) were pressed at 2000 psi into thin pellets. 3.0×10^{-5} M^{-1} and 1.5×10^{-5} M^{-1} stock solutions of 7MC were prepared by dissolving 0.20 mg or 0.10 mg of 7MC in 100mL of a 1:1 solution of H_2O/MeOH and 100 mL of H_2O respectively. The uncatalyzed pellets were then placed in 20 mL of a 1:1 mixture of H_2O and MeOH or pure H_2O in order for hydrolytic degradation to occur. For enzymatic degradation a 1:1 8 mL solution of H_2O/MeOH containing 16 mg (2 mg/mL) of proteinase K with about 5 mg of $CaCl_2$ was used. The degradation was followed at desired times by agitating the

solution and then measuring the fluorescence spectrum of a 3 mL aliquot of the solution compared to standard stock solutions as well as blank solutions.

For timed degradation studies a pellets were exposed to a solution of 1,5,7-triazabicyclo[4.4.0]dec-5-ene (TBD) in methanol at a concentration of 4.34×10^{-2} M at 23 °C. The samples were monitored at 23°C until all polymer had degraded in solution.

References

(1) Hoffman, A. S. *J. Controlled Release* **2008**, *132*, 153.

(2) Chaudhary, H.; Kohli, K.; Amin, S.; Rathee, P.; Kumar, V. *J. Pharm. Sci.* **2011**, *100*, 580.

(3) Farokhzad, O. C.; Langer, R. *ACS Nano* **2009**, *3*, 16.

(4) Patri, A. K.; Majoros, I. J.; Baker Jr, J. R. *Curr. Opin. Chem. Biol.* **2002**, *6*, 466.

(5) Brannon-Peppas, L. *Int. J. Pharm.* **1995**, *116*, 1.

(6) Aprahamian, M.; Michel, C.; Humbert, W.; Devissaguet, J. P.; Damge, C. *Biol. Cell* **1987**, *61*, 69.

(7) Hans, M. L.; Lowman, A. M. *Curr. Opin. Solid State Mater. Sci.* **2002**, *6*, 319.

(8) Shi, J.; Votruba, A. R.; Farokhzad, O. C.; Langer, R. *Nano Lett.* **2010**, *10*, 3223.

(9) Nair, L. S.; Laurencin, C. T. *Prog. Polym. Sci.* **2007**, *32*, 762.

(10) van der Giessen, W. J.; Lincoff, A. M.; Schwartz, R. S.; van Beusekom, H. M. M.; Serruys, P. W.; Holmes, D. R.; Ellis, S. G.; Topol, E. J. *Circulation* **1996**, *94*, 1690.

(11) Lanza, R.; Langer, R.; Vacanti, J. P. *Principles of Tissue Engineering*; Elsevier Science, 2000.

(12) Lendlein, A.; Sisson, A. *Handbook of Biodegradable Polymers*; Wiley, 2011.

(13) Allan, B. *Br. J. Ophthalmol.* **1999**, *83*, 1235.

(14) Lewis, O. G.; Fabisiak, W. *Kirk-Othmer Encyclopedia of Chemical Technology* **2000**.

(15) Jendrossek, D.; Knoke, I.; Habibian, R.; Steinbüchel, A.; Schlegel, H. *J. Environ. Polymer Degradation* **1993**, *1*, 53.

(16) Albertsson, A. C.; Varma, I. K. *Biomacromolecules* **2003**, *4*, 1466.

(17) Liu, C.; Gu, Y. C.; Qian, Z.; Fan, L. Y.; Li, J.; Chao, G. T.; Tu, M. J.; Jia, W. J. *Journal of Biomedical Materials Research Part A* **2005**, *75*, 465.

(18) Davachi, S. M.; Kaffashi, B.; Roushandeh, J. M. *Polym. Adv. Technol.* **2012**, *23*, 565.

(19) Deng, F.; Gross, R. A. *Int. J. Biol. Macromol.* **1999**, *25*, 153.

(20) El-Gewely, R. *Biotechnology Annual Review*; Elsevier, 2006.

(21) Foucher, D. A.; Tang, B. Z.; Manners, I. *J. Am. Chem. Soc.* **1992**, *114*, 6246.

(22) Thomas, C. M. *Chem. Soc. Rev.* **2010**, *39*, 165.

(23) Lim, L.-T.; Cink, K.; Vanyo, T. In *Poly(Lactic Acid)*; John Wiley & Sons, Inc.: 2010, p 189.

(24) Nederberg, F.; Connor, E. F.; Möller, M.; Glauser, T.; Hedrick, J. L. *Angew. Chem. Int. Ed.* **2001**, *40*, 2712.

(25) Kricheldorf, H. R. *Chemosphere* **2001**, *43*, 49.

(26) Mecerreyes, D.; Jérôme, R.; Dubois, P. *Macromolecular Architectures* **1999**, 1.

(27) Rasal, R. M.; Janorkar, A. V.; Hirt, D. E. *Prog. Polym. Sci.* **2010**, *35*, 338.

(28) Garlotta, D. *J. Polym. Environ.* **2001**, *9*, 63.

(29) Rasal, R. M.; Janorkar, A. V.; Hirt, D. E. *Prog. Polym. Sci.* **2010**, *35*, 338.

(30) Stanford, M. J.; Dove, A. P. *Chem. Soc. Rev.* **2010**, *39*, 486.

(31) Vink, E. T. H.; Rábago, K. R.; Glassner, D. A.; Gruber, P. R. *Polym. Degrad. Stab.* **2003**, *80*, 403.

(32) Okada, H.; Toguchi, H. *Crit. Rev. Ther. Drug Carrier Syst.* **1995**, *12*, 1.

(33) Jérôme, C.; Lecomte, P. *Adv. Drug Del. Rev.* **2008**, *60*, 1056.

(34) Törmälä, P.; Pohjonen, T.; Rokkanen, P. *Proceedings of the Institution of Mechanical Engineers, Part H: Journal of Engineering in Medicine* **1998**, *212*, 101.

(35) Makadia, H. K.; Siegel, S. J. *Polymers* **2011**, *3*, 1377.

(36) Graham, P.; Brodbeck, K.; McHugh, A. *J. Controlled Release* **1999**, *58*, 233.

(37) Woo, B. H.; Jiang, G.; Jo, Y. W.; DeLuca, P. P. *Pharm. Res.* **2001**, *18*, 1600.

(38) Luo, D.; Saltzman, W. M. *Nat. Biotechnol.* **2000**, *18*, 33.

(39) Nafee, N.; Taetz, S.; Schneider, M.; Schaefer, U. F.; Lehr, C. M. *Nanomed. Nanotechnol. Biol. Med.* **2007**, *3*, 173.

(40) Takeuchi, H.; Yamamoto, H.; Kawashima, Y. *Adv. Drug Del. Rev.* **2001**, *47*, 39.

(41) Sinha, V. R.; Khosla, L. *Drug Dev. Ind. Pharm.* **1998**, *24*, 1129.

(42) Thomson, R. C.; Mikos, A. G.; Beahm, E.; Lemon, J. C.; Satterfield, W. C.; Aufdemorte, T. B.; Miller, M. J. *Biomaterials* **1999**, *20*, 2007.

(43) Alexis, F. *Polym. Int.* **2004**, *54*, 36.

(44) Leja, K.; Lewandowicz, G. *Polish J. Environ. Stud* **2010**, *19*, 255.

(45) Choi, J.; Lee, S. Y. *Bioprocess Biosystems Eng.* **1997**, *17*, 335.

(46) Borah, B.; Thakur, P.; Nigam, J. *J. Appl. Microbiol.* **2002**, *92*, 776.

(47) Jaffredo, C. G.; Carpentier, J.-F.; Guillaume, S. M. *Macromol. Rapid Commun.* **2012**, *33*, 1938.

(48) Ajellal, N.; Bouyahyi, M.; Amgoune, A.; Thomas, C. M.; Bondon, A.; Pillin, I.; Grohens, Y.; Carpentier, J.-F. o. *Macromolecules* **2009**, *42*, 987.

(49) Carpentier, J.-F. *Macromol. Rapid Commun.* **2010**, *31*, 1696.

(50) Labet, M.; Thielemans, W. *Chem. Soc. Rev.* **2009**, *38*, 3484.

(51) Bordes, C.; Fréville, V.; Ruffin, E.; Marote, P.; Gauvrit, J.; Briançon, S.; Lantéri, P. *Int. J. Pharm.* **2010**, *383*, 236.

(52) Aubin, M.; Prud'Homme, R. E. *Macromolecules* **1980**, *13*, 365.

(53) Fields, R.; Rodriguez, F.; Finn, R. *J. Appl. Polym. Sci.* **1974**, *18*, 3571.

(54) Sun, H.; Mei, L.; Song, C.; Cui, X.; Wang, P. *Biomaterials* **2006**, *27*, 1735.

(55) Kweon, H. Y.; Yoo, M. K.; Park, I. K.; Kim, T. H.; Lee, H. C.; Lee, H. S.; Oh, J. S.; Akaike, T.; Cho, C. S. *Biomaterials* **2003**, *24*, 801.

(56) Armani, D. K.; Liu, C. In *Micro Electro Mechanical Systems, 2000. MEMS 2000. The Thirteenth Annual International Conference on*; IEEE: 2000, p 294.

(57) Wong, S. C.; Baji, A.; Gent, A. N. *Compos. Part A-Appl. S.* **2008**, *39*, 579.

(58) Plackett, D. V.; Holm, V. K.; Johansen, P.; Ndoni, S.; Nielsen, P. V.; Sipilainen‐Malm, T.; Södergård, A.; Verstichel, S. *Packag. Technol. Sci.* **2005**, *19*, 1.

(59) Pitt, G.; Gratzl, M.; Kimmel, G.; Surles, J.; Sohindler, A. *Biomaterials* **1981**, *2*, 215.

(60) Wang, C.; Li, H.; Zhao, X. *Biomaterials* **2004**, *25*, 5797.

(61) Dittrich, V.; Schultz, R. *Angew. Makromol. Chem* **1971**, *15*, 109.

(62) Kricheldorf, H. R.; Berl, M.; Scharnagl, N. *Macromolecules* **1988**, *21*, 286.

(63) Dubois, P.; Jérŏme, R.; Teyssie, P. In *Makromolekulare Chemie. Macromolecular Symposia*; Wiley Online Library: 1991; Vol. 42, p 103.

(64) Lindblad, M.; Liu, Y.; Albertsson, A.-C.; Ranucci, E.; Karlsson, S. *Degradable Aliphatic Polyesters* **2002**, 139.

(65) Kowalski, A.; Duda, A.; Penczek, S. *Macromolecules* **2000**, *33*, 7359.

(66) Kowalski, A.; Libiszowski, J.; Duda, A.; Penczek, S. *Macromolecules* **2000**, *33*, 1964.

(67) Chisholm, M. H.; Delbridge, E. E. *Chem. Commun.* **2001**, 1308.

(68) von Schenck, H.; Ryner, M.; Albertsson, A. C.; Svensson, M. *Macromolecules* **2002**, *35*, 1556.

(69) Hormnirun, P.; Marshall, E. L.; Gibson, V. C.; White, A. J. P.; Williams, D. J. *J. Am. Chem. Soc.* **2004**, *126*, 2688.

(70) Cross, E. D.; Allan, L. E. N.; Decken, A.; Shaver, M. P. *J. Polym. Sci., Part A: Polym. Chem.* **2012**, 1137.

(71) Nomura, N.; Akita, A.; Ishii, R.; Mizuno, M. *J. Am. Chem. Soc.* **2010**, *132*, 1750.

(72) Le Borgne, A.; Vincens, V.; Jouglard, M.; Spassky, N. In *Makromolekulare Chemie. Macromolecular Symposia*; Wiley Online Library: 1993; Vol. 73, p 37.

(73) Wisniewski, M.; Borgne, A. L.; Spassky, N. *Macromol. Chem. Phys.* **1997**, *198*, 1227.

(74) Ovitt, T. M.; Coates, G. W. *J. Am. Chem. Soc.* **2002**, *124*, 1316.

(75) Zhong, Z.; Dijkstra, P. J.; Feijen, J. *J. Am. Chem. Soc.* **2003**, *125*, 11291.

(76) Nomura, N.; Ishii, R.; Akakura, M.; Aoi, K. *J. Am. Chem. Soc.* **2002**, *124*, 5938.

(77) Tang, Z.; Chen, X.; Yang, Y.; Pang, X.; Sun, J.; Zhang, X.; Jing, X. *J. Polym. Sci., Part A: Polym. Chem.* **2004**, *42*, 5974.

(78) Hormnirun, P.; Marshall, E. L.; Gibson, V. C.; Pugh, R. I.; White, A. J. P. *Proceedings of the National Academy of Sciences* **2006**, *103*, 15343.

(79) Cameron, P. A.; Jhurry, D.; Gibson, V. C.; White, A. J.; Williams, D. J.; Williams, S. *Macromol. Rapid Commun.* **1999**, *20*, 616.

(80) Bhaw-Luximon, A.; Jhurry, D.; Spassky, N. *Polym. Bull.* **2000**, *44*, 31.

(81) Cameron, D. J. A.; Shaver, M. P. *Chem. Soc. Rev.* **2011**, *40*, 1761.

(82) Stoddart, J. F. *Angew. Chem. Int. Ed.* **1992**, *31*, 846.

(83) Liu, L.; Guo, Q.-X. *J. Inclusion Phenom. Macrocyclic Chem.* **2002**, *42*, 1.

(84) Schalley, C. A. *Int. J. Mass spectrom.* **2000**, *194*, 11.

(85) Lehn, J.-M. *Angew. Chem. Int. Ed.* **1988**, *27*, 89.

(86) Kuhn, R.; Stoecklin, F.; Erni, F. *Chromatographia* **1992**, *33*, 32.

(87) Das, S.; Thomas, K. G.; George, M. V.; Kamat, P. V. *J. Chem. Soc., Faraday Trans.* **1992**, *88*, 3419.

(88) Harada, A. *Acc. Chem. Res.* **2001**, *34*, 456.

(89) Reuter, H. *Angew. Chem. Int. Ed.* **1992**, *31*, 1185.

(90) Mohanty, J.; Bhasikuttan, A. C.; Nau, W. M.; Pal, H. *J. Phys. Chem. B* **2006**, *110*, 5132.

(91) Mandolini, L.; Cacciapaglia, R.; Di Stefano, S. In *Molecular Encapsulation*; John Wiley & Sons, Ltd: 2010, p 201.

(92) Buschmann, H. J.; Jansen, K.; Schollmeyer, E. *Thermochim. Acta* **2000**, *346*, 33.

(93) Reetz, M. T.; Niemeyer, C. M.; Harms, K. *Angew. Chem. Int. Ed.* **1991**, *30*, 1472.

(94) Diederich, F. *Angew. Chem. Int. Ed.* **1988**, *27*, 362.

(95) Irwin, J. L.; Sherburn, M. S. *Org. Lett.* **2000**, *3*, 225.

(96) Tunstad, L. M.; Tucker, J. A.; Dalcanale, E.; Weiser, J.; Bryant, J. A.; Sherman, J. C.; Helgeson, R. C.; Knobler, C. B.; Cram, D. J. *J. Org. Chem.* **1989**, *54*, 1305.

(97) Brian, D. W. *Current Analytical Chemistry* **2007**, *3*, 183.

(98) Astray, G.; Gonzalez-Barreiro, C.; Mejuto, J. C.; Rial-Otero, R.; Simal-Gándara, J. *Food Hydrocolloids* **2009**, *23*, 1631.

(99) Clarke, R. J.; Coates, J. H.; Lincoln, S. F. In *Adv. Carbohydr. Chem. Biochem.*; Tipson, R. S., Derek, H., Eds.; Academic Press: 1988; Vol. Volume 46, p 205.

(100) Loftsson, T.; Brewster, M. E. *J. Pharm. Sci.* **1996**, *85*, 1017.

(101) Baglole, K. N.; Boland, P. G.; Wagner, B. D. *J. Photochem. Photobiol. A: Chem.* **2005**, *173*, 230.

(102) Laza-Knoerr, A.; Gref, R.; Couvreur, P. *J. Drug Targeting* **2010**, *18*, 645.

(103) Loftsson, T.; Duchêne, D. *Int. J. Pharm.* **2007**, *329*, 1.

(104) Belikov, V. G.; Kompantseva, E. V.; Botezat-Belyi, Y. K. *Pharm. Chem. J.* **1986**, *20*, 299.

(105) Wagner, B.; Fitzpatrick, S. *J. Inclusion Phenom. Macrocyclic Chem.* **2000**, *38*, 467.

(106) Wenz, G. *Angew. Chem. Int. Ed.* **1994**, *33*, 803.

(107) Manunza, B.; Deiana, S.; Pintore, M.; Gessa, C. *J. Mol. Struc-Theochem.* **1997**, *419*, 133.

(108) Del Valle, E. M. M. *Process Biochem.* **2004**, *39*, 1033.

(109) Ohno, K.; Wong, B.; Haddleton, D. M. *J. Polym. Sci., Part A: Polym. Chem.* **2001**, *39*, 2206.

(110) Stenzel, M. H.; Davis, T. P. *J. Polym. Sci., Part A: Polym. Chem.* **2002**, *40*, 4498.

(111) Miura, Y.; Narumi, A.; Matsuya, S.; Satoh, T.; Duan, Q.; Kaga, H.; Kakuchi, T. *J. Polym. Sci., Part A: Polym. Chem.* **2005**, *43*, 4271.

(112) Li, J.; Loh, X. J. *Adv. Drug Del. Rev.* **2008**, *60*, 1000.

(113) Yhaya, F.; Gregory, A. M.; Stenzel, M. H. *Aust. J. Chem.* **2010**, *63*, 195.

(114) Xu, F.; Zhang, Z.; Ping, Y.; Li, J.; Kang, E.; Neoh, K. *Biomacromolecules* **2009**, *10*, 285.

(115) Miura, Y.; Narumi, A.; Matsuya, S.; Satoh, T.; Duan, Q.; Kaga, H.; Kakuchi, T. *J. Polym. Sci., Part A: Polym. Chem.* **2005**, *43*, 4271.

(116) Stenzel-Rosenbaum, M. H.; Davis, T. P.; Chen, V.; Fane, A. G. *Macromolecules* **2001**, *34*, 5433.

(117) Ge, Z.; Xu, J.; Hu, J.; Zhang, Y.; Liu, S. *Soft Matter* **2009**, *5*, 3932.

(118) Adeli, M.; Zarnegar, Z.; Kabiri, R. *Eur. Polym. J.* **2008**, *44*, 1921.

(119) Gou, P. F.; Zhu, W. P.; Xu, N.; Shen, Z. Q. *J. Polym. Sci., Part A: Polym. Chem.* **2008**, *46*, 6455.

(120) Gao, H.; Matyjaszewski, K. *Prog. Polym. Sci.* **2009**, *34*, 317.

(121) Barner, L.; Barner-Kowollik, C.; Davis, T. P.; Stenzel, M. H. *Aust. J. Chem.* **2004**, *57*, 19.

(122) Hein, J. E.; Fokin, V. V. *Chem. Soc. Rev.* **2010**, *39*, 1302.

(123) Xu, J.; Liu, S. *J. Polym. Sci., Part A: Polym. Chem.* **2009**, *47*, 404.

(124) Hoogenboom, R.; Moore, B. C.; Schubert, U. S. *Chem. Commun.* **2006**, 4010.

(125) Bünzli, J.-C. G. *Chem. Rev.* **2010**, *110*, 2729.

(126) Valeur, B. *Molecular fluorescence: principles and applications*; Wiley-Vch, 2012.

(127) Lakowicz, J. R. *Principles of fluorescence spectroscopy*; Springer, 2006; Vol. 1.

(128) Itoh, T. *Chem. Rev.* **2012**, *112*, 4541.

(129) Nau, W. M.; Zhang, X. *JACS* **1999**, *121*, 8022.

(130) Horspool, W. M.; Lenci, F. *CRC Handbookof Organic Photochemistry and Photobiology, Volumes 1 & 2*; CRC, 2003.

(131) Wagner, B.; Fitzpatrick, S.; McManus, G. *J. Inclusion Phenom. Macrocyclic Chem.* **2003**, *47*, 187.

(132) Surpateanu, G. G.; Becuwe, M.; Lungu, N. C.; Dron, P. I.; Fourmentin, S.; Landy, D.; Surpateanu, G. *J. Photochem. Photobiol. A: Chem.* **2007**, *185*, 312.

(133) Nalwa, H. S. *Handbook of Photochemistry and Photobiology: Supramolecular photochemistry*; American Scientific Publishers, 2003.

(134) Wagner, B. D. *Molecules* **2009**, *14*, 210.

(135) Peña, A. M.; Salanas, F.; Gómez, M. J.; Acedo, M. I.; Peña, M. S. *J. Inclusion Phenom. Mol. Recognit. Chem.* **1993**, *15*, 131.

(136) Wagner, B. D.; Stojanovic, N.; Day, A. I.; Blanch, R. J. *J. Phys. Chem. B* **2003**, *107*, 10741.

(137) Wagner, B. D.; MacDonald, P. J. *J. Photochem. Photobiol. A: Chem.* **1998**, *114*, 151.

(138) Frankewich, R. P.; Thimmaiah, K.; Hinze, W. L. *Anal. Chem.* **1991**, *63*, 2924.

(139) Reeuwijk, H.; Irth, H.; Tjaden, U.; Merkus, F.; Van der Greef, J. *J. Chrom. B Biomed. Sci. Appl.* **1993**, *614*, 95.

(140) Shaver, M. P.; Cameron, D. J. A. *Biomacromolecules* **2010**, *11*, 3673.

(141) Matyjaszewski, K. *Polym. Int.* **2003**, *52*, 1559.

(142) Qian, F.; Huang, J.; Hussain, M. A. *J. Pharm. Sci.* **2010**, *99*, 2941.

(143) Zhong, Z.; Dijkstra, P. J.; Feijen, J. *Angew. Chem.* **2002**, *114*, 4692.

(144) Tang, H. Y.; Chen, H. Y.; Huang, J. H.; Lin, C. C. *Macromolecules* **2007**, *40*, 8855.

(145) Chrissafis, K.; Pavlidou, E.; Paraskevopoulos, K.; Beslikas, T.; Nianias, N.; Bikiaris, D. *J. Therm. Anal. Calorim.* **2011**, *105*, 313.

(146) Barham, P.; Keller, A.; Otun, E.; Holmes, P. *J. Mat. Sci.* **1984**, *19*, 2781.

(147) Jose, M. V.; Thomas, V.; Johnson, K. T.; Dean, D. R.; Nyairo, E. *Acta Biomater.* **2009**, *5*, 305.

(148) Grizzi, I.; Garreau, H.; Li, S.; Vert, M. *Biomaterials* **1995**, *16*, 305.

(149) Lenglet, S.; Li, S.; Vert, M. *Polym. Degrad. Stab.* **2009**, *94*, 688.

(150) Park, T. G. *Biomaterials* **1995**, *16*, 1123.

(151) Gadelle, A.; Defaye, J. *Angew. Chem. Int. Ed.* **1991**, *30*, 78.

(152) Ashton, P. R.; Königer, R.; Stoddart, J. F.; Alker, D.; Harding, V. D. *J. Org. Chem.* **1996**, *61*, 903.

(153) Helms, B.; Mynar, J. L.; Hawker, C. J.; Fréchet, J. M. J. *J. Am. Chem. Soc.* **2004**, *126*, 15020.

(154) Opsteen, J. A.; van Hest, J. C. M. *Chem. Commun.* **2005**, *0*, 57.

(155) Kolb, H. C.; Finn, M. G.; Sharpless, K. B. *Angew. Chem. Int. Ed.* **2001**, *40*, 2004.

(156) Hein, J. E.; Fokin, V. V. *Chem. Soc. Rev.* **2010**, *39*, 1302.

(157) Himo, F.; Lovell, T.; Hilgraf, R.; Rostovtsev, V. V.; Noodleman, L.; Sharpless, K. B.; Fokin, V. V. *J. Am. Chem. Soc.* **2005**, *127*, 210.

(158) Sung, H.-J.; Meredith, C.; Johnson, C.; Galis, Z. S. *Biomaterials* **2004**, *25*, 5735.

(159) Yu, I.; Acosta-Ramirez, A.; Mehrkhodavandi, P. *J. Am. Chem. Soc.* **2012**.

(160) Mehrkhodavandi, P.; Xu, C.; Yu, I. *Chem. Commun.* **2012**.

(161) Körber, M. *Pharm. Res.* **2010**, *27*, 2414.

(162) Corbin, P. S.; Webb, M. P.; McAlvin, J. E.; Fraser, C. L. *Biomacromolecules* **2001**, *2*, 223.